

NOVEL REGULATORY PATHWAYS OF PROTEIN CHANNELS

by

Sheenah Lynn Bryant

A dissertation

submitted in partial fulfillment

of the requirements for the degree of

Doctor of Philosophy in Biomolecular Sciences

Boise State University

December 2018

© 2018

Sheenah Lynn Bryant

ALL RIGHTS RESERVED

BOISE STATE UNIVERSITY GRADUATE COLLEGE

DEFENSE COMMITTEE AND FINAL READING APPROVALS

of the dissertation submitted by

Sheenah Lynn Bryant

Dissertation Title: Novel Regulatory Pathways of Protein Channels

Date of Final Oral Examination: 10 August 2018

The following individuals read and discussed the dissertation submitted by student Sheenah Lynn Bryant, and they evaluated the student's presentation and response to questions during the final oral examination. They found that the student passed the final oral examination.

Daniel Fologea, Ph.D.	Chair, Supervisory Committee
Julia Thom Oxford, Ph.D.	Member, Supervisory Committee
Kenneth A. Cornell, Ph.D.	Member, Supervisory Committee
Denise G. Wingett, Ph.D.	Member, Supervisory Committee

The final reading approval of the dissertation was granted by Daniel Fologea, Ph.D., Chair of the Supervisory Committee. The dissertation was approved by the Graduate College.

DEDICATION

To my most patient and loving children.

ACKNOWLEDGMENTS

Many mentors, colleagues, and friends supported the completion of this dissertation. Foremost, I would like to acknowledge my primary advisor, Dr. Daniel Fologea, who pushed me to learn academically and professionally every day, and who supported and encouraged my pursuit of opportunities beyond the requirements of my doctoral degree. He is a tireless, inspirational mentor and citizen who is selflessly motivated by scientific discovery. He is an example of self-efficacy, which I will remember forever. I would also like to thank Dr. Julia Oxford, a member of my committee, for her support throughout my Ph.D. endeavor. She provided critical technical information during the preparation of my graduate fellowship proposal, continued to support me logistically with cell culture training and materials, and became a source of confidence for me as I developed into a professional scientist. She and my other committee members, Dr. Ken Cornell and Dr. Denise Wingett, have provided expert advice, instruction and encouragement throughout my doctorate. My graduate training was comprehensive and interdisciplinary because of the great efforts of many other instructors, from many departments, who taught me within the Biomolecular Sciences Graduate Program.

I am grateful to the Boise State University Department of Physics for their support throughout my undergraduate and graduate training. My deepest and sincerest thanks to Dr. Charles Hanna, Chair, for shaping my future by introducing me to research and thermal physics.

I would also like to thank the Biomolecular Sciences Graduate Program for providing me with a graduate fellowship during the first year of the program. I would also like to acknowledge the director of the BMOL program, Dr. Denise Wingett, who has advocated for my success from my very first day as a graduate student to the very last. Thank you to Elizabeth Gee, the program coordinator, who managed all of the funding accounts, advised me academically, and encouraged me to succeed. I would also like to thank the Biomolecular Research Center for their training and financial support. I am immensely grateful to the National Aeronautics and Space Administration (NASA) Office of Education for their generously awarded full graduate fellowship.

The NASA Graduate Fellowship also allowed me to train under the most knowledgeable and experienced space biology scientists in the world at NASA Ames Research Center. Dr. Ruth Globus, my technical advisor, is an inspirational scientist who expanded the direction and scope of my graduate research. I would like to thank Dr. Candice Tahimic, Dr. Josh Alwood, and Dr. Ann-Sofie Schreurs for their technical advice, as well as their friendship, during my three years of fellowship.

Many graduate and undergraduate students have supported my research and academic success; Dr. Nisha Shrestha, Josh Eixenburger, Stephanie Tuft, Dr. Jonathan Reeck, Christopher Alex Thomas, Paul Carnig, Samuel Kosydar, Daniel Prather, Lizzie Leung, Colleen Calzacorta, and Andrew Bogard.

I would also like to acknowledge my parents, Becky and Tracey Bryant, who emotionally and logistically supported me throughout my education at Boise State University.

ABSTRACT

Since the proposal of the fluid mosaic model of a cell membrane, substantial scientific evidence has shown that the cell membrane is not simply an inert structure with the sole role of separating two chemically different environments. The cell membrane dynamically satisfies basic needs, such as water, ion and nutrient transport, without which the cell could not survive. It is a structure which actively participates in a great variety of physiological functions. The activity of the cell membrane is responsible for the contraction of our muscles and information processing in our brain. In order to participate in such a wide range of biological processes, the cell membrane incorporates an extensive variety of protein transporters in its structure. These transporters are highly regulated and contribute to the selective barrier function of the membrane.

It is this regulation that enables certain complex physiological functions. The mechanisms of regulation of membrane transporters are obvious in the case of ion channels, which are transmembrane protein transporters facilitating controlled transport of specific ions across the membrane. Their regulation is mediated by specific physical or chemical stimuli, of which voltage, ligands, temperature, light and pressure are most common. However, recent reports indicate that regulation of such transporters may also be achieved by other environmental factors which are not easy to identify in the complex biochemical environment of the cell. Understanding these novel environmental factors and how they modulate the transport across membranes may be a crucial step to better understand the functionality of transmembrane transporters in health and disease.

In this respect, the work presented here employs a highly regulated transmembrane transporter, lysenin, which is a pore-forming toxin extracted from red earthworms. Lysenin shares many of the fundamental features of ion channels, such as voltage and ligand regulation. In addition to these features, lysenin accumulates in lipid rafts (which are ubiquitous in animal cells). This model transporter offers opportunities to investigate novel regulatory pathways that are otherwise very difficult to identify in a living cell. In the work presented in this dissertation, I investigated how specific physical and chemical determinants of the membrane and surrounding solution, as well as the gating mechanism itself, may contribute to the emergence of unexpected cellular functionalities.

In this endeavor, I showed that increasing the local density of lysenin channels in a target membrane substantially changed the voltage-induced regulation, and that this density can be simply manipulated by altering the membrane's lipid composition. Next, I demonstrated that the macroergic molecule ATP plays an important role in adjusting the conductance of pore-forming transporters and modulates their biological activity. These observations expand the well-established role of ATP as a signaling molecule, which has been proposed and well-studied for the last several decades. Finally, based on experimental observations that lysenin is endowed with molecular memory, I hypothesized a gating mechanism capable of explaining such a novel and unexpected feature. For these investigations, I focused my work on understanding the influence of multivalent cations on lysenin, which are capable of modulating the voltage-induced gating by electrostatic screening of the voltage domain sensor. The proposed gating mechanism, in which the voltage domain sensor moves into the hydrophobic core of the

membrane upon gating, is supported by experimental evidence showing that anion binding to the channel lumen presents qualitative and quantitative differences in voltage regulation, as opposed to binding to the voltage domain sensor.

Therefore, the work presented here advances our knowledge with respect to how transmembrane transporters are influenced by frequently overlooked environmental factors, and how this may significantly contribute to the achievement of novel physiological functions. This level of understanding may prove crucial for determining potential connections between metabolic pathways and channelopathies that are commonly attributed to genetic defects of ion channels.

TABLE OF CONTENTS

DEDICATION	iv
ACKNOWLEDGMENTS	v
ABSTRACT	vii
LIST OF FIGURES	xiii
LIST OF ABBREVIATIONS	xix
CHAPTER ONE: MOTIVATION AND BACKGROUND.....	1
References	10
CHAPTER TWO: INTRAMEMBRANE CONGESTION EFFECTS ON LYSENIN CHANNEL VOLTAGE-INDUCED GATING	18
Abstract	19
Introduction	20
Materials and Methods.....	22
Results and Discussion.....	23
Acknowledgments.....	35
References	35
Electronic Supplementary Material	40
CHAPTER THREE: PURINERGIC CONTROL OF LYSENIN'S TRANSPORT AND VOLTAGE-GATING PROPERTIES	43
Abstract	44
Introduction	45

Materials and Methods	48
Results	50
ATP Reversibly Reduces the Macroscopic Conductance of Lysenin Channels Via a Non-gating Mechanism	50
ATP, ADP, and AMP Inhibit the Macroscopic Conductance of Lysenin Channels In a Charge-dependent Manner by Partially Occluding the Conducting Pathway upon Cooperative Binding	54
Ionic Screening Reduces ATP's Inhibition Efficiency.....	58
ATP and AMP Affect the Voltage-induced Gating	60
dATP Inhibits the Macroscopic Conductance of Lysenin Channels.....	63
Discussion.....	64
Acknowledgments.....	70
References	70
Electronic Supplementary Material	77
CHAPTER FOUR: INSIGHTS INTO THE VOLTAGE REGULATION MECHANISM OF THE PORE-FORMING TOXIN LYSENIN	79
Abstract	80
Introduction	82
Results and Discussions	86
2.1. Monovalent Metal Cations Modulate the Voltage-Induced Gating of Lysenin Channels During Inactivation, while Minimally Influencing the Reactivation Pathway	86
2.2. Multivalent Metal Cations Influence the Voltage Regulation of Lysenin Channels Similarly to Monovalent Ions.....	91
2.3. ATP Binding to Lysenin Channels Modulates the Voltage-Induced Gating and Affects Both the Inactivation and Reactivation Pathways.....	95
Materials and Methods.....	100

Acknowledgements.....	103
References	104

LIST OF FIGURES

Chapter One

- Fig. 1. General properties of the lysenin channel. (a) Profile of the channel radius. (b) Side view of the electrostatic surface (red used for negative potential and blue used for positive). (c) The distribution of Threonine (blue-red) and Serine (yellow-red) residues throughout the pore. (d) Overhead view of the electrostatic surface (colors are as in b). (e) Hydrophobic residue distribution (green). (f) Relative fractional uptake measured by HDX-MS mapped to the surface of lysenin pore. Left: top view, right: side view. Adapted from Podobnik, M.; *et al. Nature Communications* 2016, 7, 11598 [17]. Available under Creative Common License.4

Chapter Two

- Fig. 1. The number of lysenin channels inserted into a planar lipid membrane containing 50% SM affects the I-V characteristics (a) and induces a rightward shift of the experimental open probability P_{open} (b). Each I-V and P_{open} plot is the average of three individual recordings for the same experimental setup and all data points in the graphs are experimental values with standard errors < 5%.25
- Fig. 2. (a) The I-V plots for increasing numbers of lysenin channels inserted into planar lipid membranes containing 10% SM. (b) A more significant rightward shift in the open probability is observed for the reduced SM concentration compared to the 50% SM condition shown in Fig. 1. Each I-V and P_{open} plot is the average of three individual recordings for the same experimental setup and all data points are experimental values with standard errors < 5%.29
- Fig. 3. The half-activation voltage $V_{0.5}$ (mean \pm SD, n=3) as a function of the number of lysenin channels inserted into similar-size planar lipid membranes undergoes more pronounced changes for bilayers containing 10% SM (open squares), 20% SM (open triangles), and 50% SM (open circles).....31
- Fig. 4. The half-activation voltage $V_{0.5}$ undergoes negligible changes for low number of lysenin channels inserted into 50% SM lipid membranes. Each

$V_{0.5}$ was determined from independent parallel experiments and the data are reported as mean \pm SD, n=3-10.34

Fig. 5 Low ionic concentration does not affect the functionality of lysenin channels. (a) Insertion of identical lysenin channels in a lipid membrane containing 50% sphingomyelin (weight ratio relative to the amount of asolectin) and bathed by 50 mM KCl is indicated by the stepwise increase of the open current. (b) The current distribution of the open current indicates a unitary conductance increase of $\sim 0.391 \pm 0.025$ nS/channel. (c) The I-V plot recorded at 0.2mV/s indicates the voltage-induced gating at positive transmembrane potentials and demonstrates the functionality of lysenin channels in low ionic concentration conditions.40

Fig. 6 Sphingomyelin depletion does not affect the functionality of lysenin channels. (a) Insertion of identical lysenin channels in a bilayer containing 10% sphingomyelin (weight ratio relative to asolectin) and bathed by 50 mM KCl. (b) The current distribution of the open current indicates a unitary conductance increase of $\sim 0.394 \pm 0.025$ nS/channel. (c) The I-V plot recorded at 0.2mV/s indicates the voltage-induced gating at positive transmembrane potentials and demonstrates the functionality of lysenin channels in sphingomyelin-depleted conditions.41

Fig. 7 Consecutive addition of lysenin for achieving increased number of inserted channels into the target lipid membrane. a) Channel insertion after addition of lysenin to a pristine membrane biased by - 60 mV is indicated by changes in ionic current. The completion of insertion is indicated by a steady state is achieved in ~ 40 minutes. b) After recording the I-V plots, a new lysenin addition promotes further insertion and leads to an increased number of channels in the membrane.42

Chapter Three

Fig. 1 ATP inhibits the macroscopic currents through lysenin channels inserted into planar BLMs. Addition of ATP to the electrolyte solutions bathing the lysenin channels yielded a significant decrease of the ionic currents in a concentration-dependent manner. The experiment was recorded at -60 mV transmembrane potential at a sampling rate of 1s, with a 1 kHz hardware filter and a 0.1 kHz software filter. Each ATP addition (indicated by *arrows*) increased the ATP concentration into the bulk by 1 mM.51

Fig. 2 Changes in macroscopic conductance induced by ATP addition are reversible. Addition of 20 mM ATP to the ground reservoir decreased the ionic current by ~ 80 %. Buffer exchange quickly reinstated the macroscopic conductance and demonstrated reversibility.52

Fig. 3	The mechanism of ATP-induced conductance inhibition does not imply ligand-induced gating. a The insertion of two lysenin channels in the BLM was observed from the unitary step-wise variation of the open current produced upon each insertion. b ATP addition to the ground reservoir yielded a slow and monotonic decrease of the ionic current by ~60 %. The absence of transient changes in the open current upon ATP addition suggests that gating is not a valid mechanism for explaining ATP's inhibitory action.54
Fig. 4	Changes in relative conductance induced by the addition of ATP, ADP, or AMP. The relative macroscopic conductance G_r indicates that ATP (a) and ADP (b) were more efficient inhibitors compared to AMP (c). The relative conductance values represented by <i>symbols</i> in the plots are reported as mean \pm SD from three independent experiments. The conductance data, fitted to the Hill equation (<i>full line</i>), yielded the following parameters: (i) ATP: $IC_{50} = 4.53 \pm 0.07$ mM, and $n = 4.15 \pm 0.2$, (ii) ADP: $IC_{50} = 8.92 \pm 0.07$ mM, and $n = 3.43 \pm 0.16$, and (iii) AMP: $IC_{50} = 13.43 \pm 0.08$ mM and $n = 1.62 \pm 0.17$56
Fig. 5	Ionic screening reduces ATP inhibitory effects. The relative conductance indicates that ionic screening elicited by the addition of KCl affected the conductance changes induced by ATP addition. The lowest KCl concentration (50 mM) promoted electrostatic interactions, increased binding, and enhanced the ATP-induced inhibition. Increased KCl concentrations (135 mM and 500 mM, respectively) diminished the ATP-induced inhibition by weakening the electrostatic interactions and the binding affinity. The experimental conductance data (<i>symbols</i>) are presented as mean \pm SD from six traces recorded for each of the experiments. The average conductance data fitted to the Hill equation (<i>full lines</i>) yielded the next parameters: (i) 50 mM KCl: $IC_{50} = 3.83 \pm 0.05$ mM, $n = 4.11 \pm 0.16$; (ii) 135mM KCl: $IC_{50} = 4.36 \pm 0.07$ mM, $n = 4.14 \pm 0.2$; and (iii) 500 mM KCl: $IC_{50} = 6.94 \pm 0.07$ mM, $n = 4.1 \pm 0.14$59
Fig. 6	ATP and AMP alter the voltage-induced gating of lysenin in a concentration-dependent manner, simultaneous with conductance inhibition. ATP addition induced a rightward shift of the voltage-induced gating, which was observed in the I-V (a) and P_{open} (c) plots. The changes induced by AMP (b I-V curves, and d P_{open}) were minimal. All data points are experimental values, with the <i>symbols</i> added solely to aid in discriminating between different experimental conditions.61
Fig. 7	dATP inhibits the macroscopic currents through lysenin channels inserted into planar BLMs. Addition of 1 mM dATP to the electrolyte solutions bathing the lysenin channels yielded a significant yet slow decrease of the ionic currents. The <i>inset</i> shows step-wise variations of the open current, suggesting a possible gating mechanism. The experiment was recorded at -

60 mV transmembrane potential at a sampling rate of 1s, with a 1 kHz hardware filter and a 0.1 kHz software filter.64

Fig. 8 The experimental setup consisted of a custom-made planar bilayer lipid membrane chamber, which was comprised of two PTFE reservoirs, each capable of accommodating ~1 mL electrolyte solution. The two reservoirs were separated by a thin PTFE film (~120 μm thickness) in which a small central hole of ~60 μm diameter was produced by an electric spark. The agarose/Ag/AgCl electrodes immersed into the electrolyte solutions were connected through flexible wires to the electrophysiology amplifier.77

Fig. 9 ATP inhibits the macroscopic currents through lysenin channels inserted into planar lipid membranes irrespective of the addition side. Addition of ATP to the headstage-wired solution yielded a significant decrease of the ionic currents in a concentration-dependent manner, similar to what was observed after ATP addition to the ground side (see the main text). The experiment was recorded at -60 mV transmembrane potential at a sampling rate of 1s, with a 1 kHz hardware filter and a 0.1 kHz software filter. Each ATP addition (indicated by arrows) increased the ATP concentration by the amount indicated in the figure.78

Chapter Four

Fig. 1 Effects of KCl addition on the I–V characteristics of a population of lysenin channels. (a) The I–V plots recorded during ascending voltage ramps indicated changes of the macroscopic conductance (I/V) and voltage required to initiate gating. (b) The I–V plots corresponding to descending voltage ramps showed similar changes in the macroscopic conductance of open channels but less dependence of the close-open transition on the ionic concentration, along with hysteresis in macroscopic conductance. Each trace in the panels represents a single, typical run for each particular concentration. All the points in the plots are experimental points; the symbols have been added as a visual aid to discriminate between ionic concentrations.88

Fig. 2 KCl influence on lysenin channels' experimental open probability. (a) The open probability of lysenin channels as a function of voltage underwent a substantial rightward shift for the ascending voltage ramps as the KCl concentration increased. (b) In contrast, negligible changes of the open probability occurred during channel reactivation (descending voltage ramps), irrespective of the bulk KCl concentration. Each plot represents a typical curve of the experimental open probability calculated for each particular concentration. All the points in the plots are experimental points, with the symbols added to allow identification of the ionic conditions.89

- Fig. 3 Variation of the midway voltage of activation $V_{0.5}$ and number of elementary gating charges n as a function of KCl concentration. (a) The experimental values of $V_{0.5}$ calculated for ascending voltage ramps presented a significant increase with added KCl, while only a weak influence was encountered for descending voltage ramps. (b) The values of n calculated from the fit of the Boltzmann distribution equation, for each KCl concentration, suggested strong electrostatic screening of the voltage domain sensor for channel inactivation; only minor changes were estimated for channel reactivation. Each experimental point is represented as mean \pm SD from three independent experiments.90
- Fig. 4 LaCl_3 influence on the I–V characteristics of lysenin channels. (a) The I–V plots recorded for ascending voltage ramps indicated LaCl_3 induced changes of the voltage required to initiate gating. (b) The I–V plots corresponding to descending voltage ramps indicated a minimal influence from the multivalent cations. Each trace in the plots for both panels represents experimental points, with the symbols added as a visual aid. ..93
- Fig. 5 Changes of the experimental open probability (P_{open}) of lysenin channels induced by addition of LaCl_3 . (a) The voltage-dependent open probability of the lysenin channels shifted substantially rightward for the ascending voltage ramps as the LaCl_3 concentration increased. (b) Conversely, and as with addition of KCl, minor changes were observed during descending voltage ramps. Each trace was constructed from experimental points, with the symbols added for better discrimination between ionic conditions.94
- Fig. 6 The dependence of $V_{0.5}$ and n on the bulk LaCl_3 concentration. (a) Addition of LaCl_3 induced significant increases of the $V_{0.5}$ calculated for ascending voltage ramps, while having yielded little change for the descending voltage ramps. (b) The total number of elementary charges indicated effective electrostatic screening of the voltage domain sensor upon addition of LaCl_3 during channel inactivation, while insignificant changes occurred during reactivation. Each experimental point is represented as mean \pm SD from three independent experiments.95
- Fig. 7 ATP affects the I–V characteristics of lysenin channels in a concentration dependent manner. (a) The I–V plots recorded during ascending voltage ramps showed that ATP addition modulated the macroscopic conductance and voltage-induced gating of lysenin channels. (b) Opposite to metal cations, ATP induced similar significant changes during descending voltage ramps. Each trace in the panels of the plots represents experimental points, and the symbols have been added to allow easy identification of experimental concentrations.97
- Fig. 8 Increased ATP concentration shifted the voltage-dependent open probability of lysenin channels. Addition of ATP induced a rightward shift

of the experimental open probability during both (a) ascending and (b) descending voltage ramps. Each plot represents a typical curve of the experimental open probability calculated for each particular concentration. All the points in the plots are experimental points, and the symbols have been added to allow easy identification of the ATP concentrations. For representation, the P_{open} curves have been smoothed with the Savitsky–Golay protocol (23 smoothing points).....98

Fig. 9

ATP addition alters $V_{0.5}$ and n for both inactivation and reactivation voltage ramps. For the ascending and descending voltage ramps, both $V_{0.5}$ (a) and n (b) varied with the concentration of ATP. Each experimental point is represented as mean \pm SD from three independent experiments..99

LIST OF ABBREVIATIONS

ATP	Adenosine 5' Triphosphate
ADP	Adenosine Diphosphate
AMP	Adenosine Monophosphate
AFM	Atomic Force Microscopy
Aso	Asolectine
BLM	Bilayer lipid membrane
Chol	Cholesterol
dATP	Deoxyadenosine Triphosphate
F	Faraday's number
G_0	Conductance measured in the absence of inhibitor
G	Conductance
G_{\min} and G_{\max}	Maximal and minimal relative conductance measured in the absence of inhibitor
HEPES	4-(2-hydroxyethyl)-1-piperazineethanesulfonic acid
I	Current at each voltage in IV curve
IC_{50}	Concentration of an inhibitor where the binding or response is reduced by half
I-V	Current voltage
I_{\max}	Theoretical maximum current
k_B	Boltzmann constant

K	Equilibrium constant of open-close transition
$P_{\text{open}} = I/I_{\text{max}}$	Open Probability
PTFE	Polytetrafluoroethylene
PFT	Pore-Forming Toxin
q	Gating charge
R	Universal gas constant
SM	Sphingomyelin
T	Absolute temperature
$V_{0.5}$	Midway voltage of activation
ΔG	Difference in free energy between open and closed state

CHAPTER ONE: MOTIVATION AND BACKGROUND

Transmembrane transporters are crucial elements of the cellular machinery responsible for paramount cellular functionalities. Water, ions, molecules and nutrient transport, creation and maintenance of electrochemical gradients, communication, and information transmission are essential cellular functions that are achieved through membrane transport [1-6]. There is little doubt that alterations of transmembrane transport may result in serious cell malfunction, potentially culminating in life-threatening diseases [7]. The importance of transmembrane transporters is well reflected in the resources dedicated to their synthesis. Up to half of the bacterial genome encodes genetic information for transmembrane transporters, and these large numbers are typical of all living cells [8].

Since all of life's fundamental processes require controlled transport across membranes, all transporters are regulated by simple or complex physical and chemical determinants. The determinants of controlled transport are most obvious for ion channels, which are protein channel transporters specializing in the diffusion of ions across the membrane down electrochemical gradients [9]. The correct functionality of excitable cells such as neurons or muscle cells is predominantly determined by the precise physiology of ion channels. In fact, the utilization of transmembrane transporters is a ubiquitous cellular necessity for ensuring homeostasis and other essential functions. All known ion channels share three fundamental features [3, 6]; high transport rate (essential for swift response to environmental changes), selectivity (required for specialized

transport of particular solutes), and regulation (which provides control of transport activities, and is a major focus of my research).

Regulation is paramount for the correct functionality of transmembrane transporters. In select cases, a simple concentration gradient may trigger directed transport, while in many others, more specific physical and chemical stimuli are required to elicit a response. In simple terms, 'regulation' means that the transport is controlled by specific modulators. Such complex regulation is necessary because the cell membrane separates two environments characterized by very different chemical compositions. For example, unregulated ion channels would allow uncontrolled, free diffusion of ions, with catastrophic consequences for the cell. Therefore, ion channels are structurally and functionally endowed with gating mechanisms that allow passage of ions only under well-determined conditions. Mechanistically, gating involves a conformational change of the channel between a high-conducting state (open) and a low-conducting state (closed) [6]. This toggle between states is modulated by physical and chemical stimuli such as voltage, temperature, pressure, light, or ligands. The scientific community has dedicated decades to understanding the mechanisms of gating and their physiological implications. In spite of tremendous progress in this field, we typically lack structural data which might elucidate the biophysical aspects of gating. Consequently, there is still much that is not understood about transporter regulation. Although the patch-clamp technique introduces an innovative approach for studying ion channels [10], the simultaneous exposure to very complex chemical and physical environments presents convoluted interactions, which may obscure the response to distinct stimuli. Therefore, it is largely recognized that a

bottom-up approach, which reduces confounding variables, may be more fruitful for better understanding the biophysical mechanisms of regulation.

Such an approach requires a simplified model system, devoid of all the complex interactions occurring in a natural cellular environment. Transporter reconstitution into artificial bilayer membranes is an appropriate approach for deciphering distinct gating mechanisms, yet its application to ion channels (or other transporters) is severely limited. Most ion channels are not commercially available in pure form. The few that have been made available by genetic engineering often have poor stability. Further, reconstitution in artificial membrane systems is problematic and technically difficult. These drawbacks seriously limit not only the characterization of classic gating mechanisms, but also the discovery of novel mechanisms that have been either neglected or difficult to identify in complex biological and biochemical systems.

To alleviate these major roadblocks, scientists look towards the use of other protein channels that share many features of ion channels for revealing the details of regulation and potential physiological implications. In the quest for the discovery of novel regulatory mechanisms, we exploited one such alternative model channel transporter: lysenin. Lysenin is a pore-forming protein consisting of 297 amino acids, extracted from the coelomic fluid of a common red earthworm, *Eisenia fetida*. Lysenin is strongly hemolytic and cytolytic, and therefore is classified as a pore-forming toxin (PFT) [11]. To exert lytic activity, lysenin self-oligomerizes as a nonameric pore in natural and artificial membranes containing sphingomyelin [12-14]. Recent structural data reveals a long β -barrel channel of ~ 3 nm diameter and ~ 11 nm length (Fig. 1) [15-17].

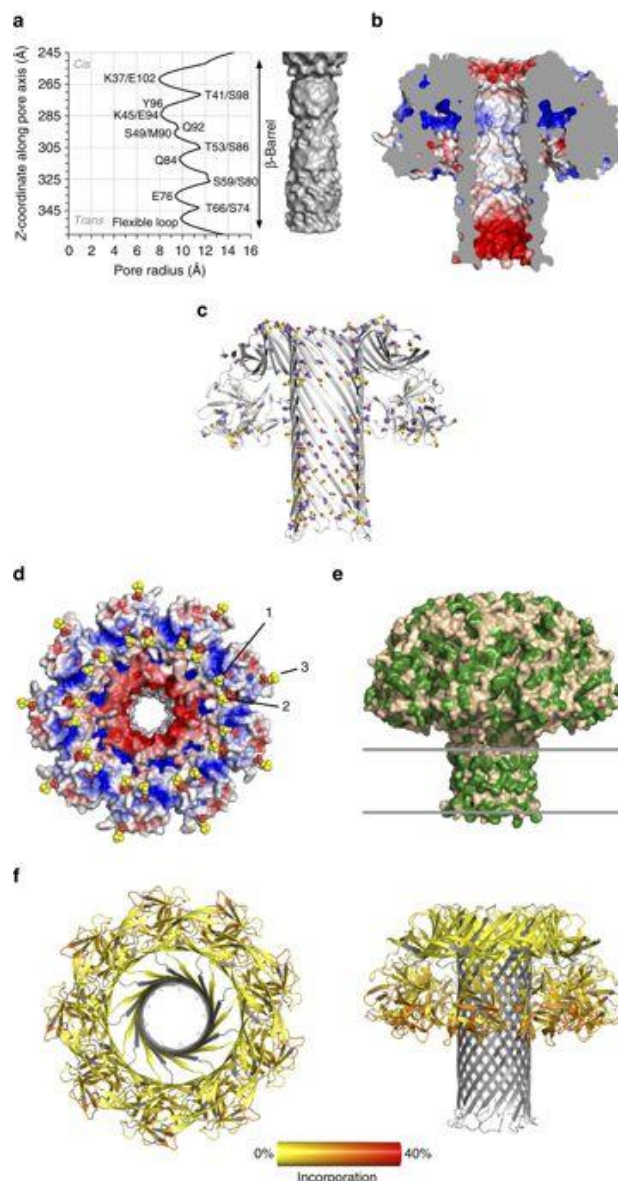


Fig. 1. General properties of the lysenin channel. (a) Profile of the channel radius. (b) Side view of the electrostatic surface (red used for negative potential and blue used for positive). (c) The distribution of Threonine (blue-red) and Serine (yellow-red) residues throughout the pore. (d) Overhead view of the electrostatic surface (colors are as in b). (e) Hydrophobic residue distribution (green). (f) Relative fractional uptake measured by HDX-MS mapped to the surface of lysenin pore. Left: top view, right: side view. Adapted from Podobnik, M.; *et al. Nature Communications* 2016, 7, 11598 [17]. Available under Creative Common License.

Lysenin channels are able to self-insert into membranes with consistent orientation, so that the direction of the external electric field is identical for all channels. Lysenin's large conductance yield large ionic currents that are easier to measure

experimentally. Additionally, lysenin channels are very stable within a lipid membrane, remaining functional for days [18, 19]. Each of these characteristics qualifies lysenin as an excellent model for studying high-rate and stable channel transporters reconstituted in artificial membrane systems. Moreover, lysenin possesses complex regulatory functions, which are unique among known PFTs [20, 21]. As one such unique feature, lysenin channels strongly and asymmetrically gate in response to voltage changes [22, 23] upon insertion into artificial lipid membranes composed of asolectin, cholesterol, and sphingomyelin. This voltage-induced gating manifests at transmembrane voltages well within physiological ranges. In typical electrophysiology experiments, when inserted from the ground side, a population of lysenin channels shows a linear, ohmic I-V characteristic for a large range of negative transmembrane voltages (i.e., -100 mV : - 0 mV). This linearity is maintained through low positive-voltages, indicative of fully open channels. However, as membrane polarization progresses over ~10 mV, significant changes in linearity occur. The I-V characteristic shows a decrease of the current at large positive voltages, indicative of a diminished macroscopic conductance. The transition between high and low conducting states is realized through a dynamic negative conductance region [20].

Analysis of the voltage response using single channels has shown that membrane depolarization elicits sudden, stepwise changes of the ionic currents, indicating conformational changes and gating [20, 23]. The voltage-induced gating process is well described by considering a Boltzmann distribution of the conformational states within a two-state model (i.e., open – close) [20], which is similarly used for ion channel gating behavior [4, 6]. This biophysical feature clearly indicates the usefulness of lysenin as a

model voltage-gated channel that shares basic structural and functional traits of ion channels. Additionally, studies have shown that lysenin channels are ligand-gated [21, 24], which is another fundamental regulatory feature of ion channels with critical physiological implications. Lysenin channels also present a strong hysteresis in conductance [18], which may constitute a source of molecular memory in many cells, an essential feature that may explain memory functions in the absence of a brain. These fundamental regulatory properties of lysenin are completed by the experimental observations that the voltage-induced gating manifests only for particular membrane compositions, requiring anionic lipids in the target membrane [20, 21, 23]. When replaced with electrically neutral lipids, the voltage induced gating is abrogated and the channels remain in the open conformation for a large range of hyperpolarizing and depolarizing bias voltages [20, 21, 23], indicating a role for the lipid composition of the membrane as a regulator of lysenin's voltage-induced gating.

Given the complex behavior of lysenin channels, we undertook this work in an attempt to use this model transporter for investigating how novel regulatory mechanisms, hidden in the complex biochemical milieu of biological systems, may modulate transmembrane transport and potentially influence cell functionality. We focused on: i) understanding how self-congestion of transporters in the membrane may modulate their activity by non-specific crowding effects (Chapter 2), ii) demonstrating the role of purines as channel conductance modulators by electrostatic binding to specific sites within the conducting pathway of transporters (Chapter 3), and iii) further developing models of voltage-induced gating that explain novel functions such as hysteretic conductance and memory (Chapter 4).

Chapter 2 investigates how the voltage regulation of lysenin channels reconstituted in artificial membrane systems is strongly affected by crowding, which is a fundamental feature of any biological environment [25-32]. Both the cytosol and membrane are fully packed with molecules that may be chemically inert for a specific chemical interaction yet occupy physical space in the local environment [25, 27, 28, 32]. Excluded volume plays an important role in modulating essential physical interactions and biochemical reactions. This was successfully demonstrated by an *in vitro* replication of crowded cellular environments [25, 32-37]. However, the impact of such environmental factors on membrane protein activity is not well understood due to the difficulty of precisely controlling experimental conditions designed to reveal excluded surface effects [31, 38-43]. Fortunately, lysenin presents several crucial features that make it an ideal candidate for such explorations. Self-insertion of lysenin in an artificial membrane system facilitates control of the number of channels within the membrane (i.e. the density of channels), and constitutes an appropriate platform for experimentally determining the effects of congestion on transporter activity. More importantly, lysenin has been shown to target sphingomyelin-rich lipid rafts [11, 12, 44-47], which is common for many ion channels expressed in biological membranes [48, 49]. Using this controllable setup, we show that self-congestion of lysenin within a target membrane significantly modulates the transport properties by altering the voltage-induced gating. In addition, we show that the membrane's lipid composition may facilitate self-congestion by influencing lipid raft formation. Therefore, we successfully relate channel function and regulation to both chemical composition and self-organization of the membrane.

In Chapter 3, we focus on the regulation of lysenin conductance by purinergic signaling. Purines are best known as macroergic molecules and nucleic acid substrates. The study of their role as signaling molecules has slowly gained momentum, despite high initial skepticism [50, 51]. Currently, purinergic signaling is recognized as one of the most ubiquitous and potentially earliest intercellular signaling mechanisms [52, 53]. The majority of the work dedicated to understanding such an important signaling mechanism focuses on purines acting as ligands for their receptors (i.e. the purinergic receptors) [54-56]. Recent studies have expanded the role of purines by showing that the hemolytic function of some exogenous PFTs is dependent on autocrine signaling upon release of Adenosine 5'-triphosphate (ATP) directly through the toxin pore [57-62]. Similar to purinergic regulation of ion channel receptors, there may be a more direct regulatory mechanism in which purines act as ligands of PFTs. The work presented here demonstrates that purines can directly regulate lysenin, and possibly other PFTs, by binding to a specific site on the protein structure. The binding process is cooperative, strongly influenced by the net charge of the binder molecules, and affected by electrostatic screening. Further, this binding induces changes in the transport properties of lysenin channels by reversibly modulating their macroscopic conductance and voltage-gating profile.

In Chapter 4, our work focuses on understanding how voltage-regulated channels may achieve novel biological functions through a particular gating mechanism. In brief, we investigate conductance hysteresis, bi-stability, and molecular memory of lysenin channels and expand the findings into a gating model capable of explaining such unique features.

Customarily, bi-stability in response to oscillatory voltage stimuli is considered a dynamic consequence of a characteristic relaxation time (i.e., the time required by the channels to achieve equilibrium at a given voltage) unmatched to the period of the driving voltage [63-67]. The general mathematical model developed for a qualitative description of the hysteresis in conductance predicts bi-stability that vanishes for two limiting cases of the oscillatory voltage: very fast and very slow [67]. Previous work performed by our group identified a dynamic hysteresis in conductance, dependent on the speed at which the driving voltage changes, and vanishing at high speeds [18]. However, lysenin channels also show a static hysteresis in conductance, which persists for periods of the voltage oscillations extending to several hours [18] which greatly exceeds the channel's relaxation time. Apparently, the source of hysteresis in bi-stability stems from a particular mechanism of voltage-induced gating, characterized by an invariant reactivation pathway (channel reopening after complete closure by external voltages) [18]. Prompted by this unusual behavior, we hypothesized that the voltage domain sensor, upon exposure to external electric fields, moves from the ionic, aqueous environment into the hydrophobic core of the membrane, which excludes bound ions and water molecules. We present experimental evidence in support of this hypothesis by investigating the voltage-induced gating of lysenin channels exposed to solutions of monovalent or multivalent metal cations of increasing ionic strengths. For both cases, electrostatic screening of the voltage domain sensor induces a substantial rightward shift of the open probability when the driving voltage closes the channel, as predicted by the biophysical model. Voltage sweeps generated to reactivate (reopen) the previously closed channels (i.e., from large positive transmembrane voltages to zero) show an invariant

reactivation pathway, which suffers only negligible changes in the open probability, irrespective of the ionic strength of the bulk solution. To further demonstrate the role played by ionic screening of the voltage domain sensor in the gating mechanism, we analyzed how ATP, which does not bind to the voltage domain sensor but rather to a different site in the channel lumen [68], adjusts the open probability as a function of voltage for open-close and close-open transitions. In support of the central hypothesis, we found that ATP addition, unlike metal cations, obliterates the invariant reactivation pathway of lysenin channels and induces significant changes of the open probability for both directions of the voltage sweeps, while still presenting hysteretic conductance.

In conclusion, the presented work exploits the regulatory biophysical features of lysenin channels for a better understanding of how overlooked or difficult to isolate environmental factors may contribute to the regulation of transmembrane transporters. This work sheds more light on the intricate regulation of lysenin channels, which may help decipher their obscure physiological role, and may be easily extrapolated to other pore-forming proteins possessing regulatory mechanisms. The great functional and mechanistic similarities between lysenin and ion channels warrant its use as a functional model, capable of revealing unexpected connections between novel biological functionalities and environmental factors not yet accounted for.

References

1. Ackerman, M.J. and D.E. Clapham, *Ion channels - basic Science and clinical disease*. The New England Journal of Medicine, 1997. **336**(22): p. 1575-1586.
2. Agre, P., *The Aquaporin Water Channels*. Proc. Am. Thorac. Soc., 2006. **3**(1): p. 5-13.

3. Aidley, D.J. and P.R. Stanfield, *Ion Channels. Molecules in Action*. 1996, Cambridge: Cambridge University Press.
4. Andersen, O.S., H.I. Ingolfsson, and J.A. Lundbaek, *Ion Channels*. Wiley Encyclopedia of Chemical Biology, 2008: p. 1-14.
5. Baruscotti, M., G. Thiel, and A. Moroni, *Ion Transport in Biological Membranes*, in *Encyclopedia of Condensed Matter Physics*, G. Bassani, G. Liedl, and P. Wyder, Editors. 2005, Elsevier.
6. Bezanilla, F., *Voltage-Gated Ion Channels*. IEEE Transactions on Nanobioscience, 2005. **4**(1): p. 34-48.
7. Ashcroft, F.M., *Ion Channels and Disease*. 1999, San Diego, CA, USA: Academic Press.
8. Ren, Q. and I.T. Paulsen, Comparative analyses of fundamental differences in membrane transport capabilities in prokaryotes and eukaryotes. *PLoS Computational Biology*, 2005. **1**(3): p. 27.
9. Yu, F., et al., Overview of molecular relationships in the voltage-gated ion channel superfamily. *Pharmacological Reviews*, 2005. **57**(4): p. 387-395.
10. Sakmann, B. and E. Neher, *Patch Clamp Techniques for Studying Ionic Channels in Excitable Membranes*. *Annual Review of Physiology*, 1984. **46**(1): p. 455-472.
11. Yamaji, A., et al., *Lysenin, a novel sphingomyelin-specific binding protein*. *Journal of Biological Chemistry*, 1998. **273**(9): p. 5300-5306.
12. Yamaji-Hasegawa, A., et al., *Oligomerization and pore formation of a sphingomyelin-specific toxin, lysenin*. *Journal of Biological Chemistry*, 2003. **278**(25): p. 22762-22770.
13. Kwiatkowska, K., et al., Lysenin-His, a sphingomyelin-recognizing toxin, requires tryptophan 20 for cation-selective channel assembly but not for membrane binding. *Molecular Membrane Biology*, 2007. **24**(2): p. 121-34.

14. Hereć, M., et al., *Secondary structure and orientation of the pore-forming toxin lysenin in a sphingomyelin-containing membrane*. *Biochimica et Biophysica Acta (BBA) - Biomembranes*, 2008. **1778**(4): p. 872-879.
15. Bokori-Brown, M., et al., *Cryo-EM structure of lysenin pore elucidates membrane insertion by an aerolysin family protein*. *Nature Communications*, 2016. **7**: p. 11293.
16. De Colibus, L., et al., *Structures of Lysenin Reveal a Shared Evolutionary Origin for Pore-Forming Proteins And Its Mode of Sphingomyelin Recognition*. *Structure*(London, England:1993), 2012. **20**(9-3): p. 1498-1507.
17. Podobnik, M., et al., *Crystal structure of an invertebrate cytolysin pore reveals unique properties and mechanism of assembly*. *Nature Communications*, 2016. **7**: p. 11598.
18. Fologea, D., et al., *Bi-stability, hysteresis, and memory of voltage-gated lysenin channels*. *Biochimica et Biophysica Acta (BBA) - Biomembranes*, 2011. **1808**(12): p. 2933-2939.
19. Shrestha, N., et al., *Stochastic sensing of Angiotensin II with lysenin channels*. *Scientific Reports*, 2017. **7**(1): p. 2448.
20. Fologea, D., et al., *Controlled gating of lysenin pores*. *Biophysical Chemistry*, 2010. **146**(1): p. 25-9.
21. Fologea, D., et al., *Multivalent ions control the transport through lysenin channels*. *Biophysical Chemistry*, 2010. **152**(1-3): p. 40-45.
22. Ishitsuka, R. and T. Kobayashi, *Lysenin: a new tool for investigating membrane lipid organization*. *Anatomical Science International*, 2004. **79**(4): p. 184-90.
23. Ide, T., et al., *Lysenin forms a voltage-dependent channel in artificial lipid bilayer membranes*. *Biochemical and Biophysical Research Communications*, 2006. **346**(1): p. 288-292.

24. Fologea, D., et al., *Potential analytical applications of lysenin channels for detection of multivalent ions*. Analytical and Bioanalytical Chemistry, 2011. **401**(6): p. 1871-9.
25. Bancaud, A., et al., Molecular crowding affects diffusion and binding of nuclear proteins in heterochromatin and reveals the fractal organization of chromatin. The EMBO Journal, 2009. **28**(24): p. 3785-3798.
26. Berg, B.v.d., R.J. Ellis, and C.M. Dobson, *Effects of macromolecular crowding on protein folding and aggregation*. The EMBO Journal, 1999. **18**(24): p. 6927-6933.
27. Chebotareva, N.A., B.I. Kurganov, and N.B. Livanova, *Biochemical Effects of Molecular Crowding*. Biochemistry (Moscow), 2004. **69**(11): p. 1522-1536.
28. Minton, A.P., *Implications of macromolecular crowding for protein assembly*. Current Opinion in Structural Biology, 2000. **10**: p. 34-39.
29. Minton, A.P., G.C. Colclasure, and J.C. Parker, *Model for the role of macromolecular crowding in regulation of cellular volume*. Proceedings of the National Academy of Sciences of the United States of America, 1992. **89**: p. 10504-10506.
30. Spitzer, J. and B. Poolman, The role of biomacromolecular crowding, ionic strength, and physicochemical gradients in the complexity of life's emergence. Microbiology and Molecular Biology Reviews, 2009. **73**(2): p. 371-388.
31. Zhou, H.X., *Crowding effects of membrane proteins*. Physical Chemistry B, 2009. **113**(23): p. 7995-8005.
32. Zimmerman, S.B. and A.P. Minton, *Macromolecular Crowding: Biochemical, Biophysical, and Physiological Consequences*. Annual Review of Biophysics and Biomolecular Structure, 1993. **22**: p. 27-65.
33. Beg, Q.K., et al., Intracellular crowding defines the mode and sequence of substrate uptake by Escherichia coli and constrains its metabolic activity. Proceedings of the National Academy of Sciences, 2007. **104**: p. 12663-12668.

34. Ralston, G.B., *Effects of "Crowding" in Protein Solutions*. Journal of Chemical Education, 1990. **67**(10): p. 857-859.
35. Satyam, A., et al., *Macromolecular Crowding Meets Tissue Engineering by Self-Assembly: A Paradigm Shift in Regenerative Medicine*. Advanced Materials, 2014. **26**: p. 3024-3034.
36. Zeiger, A.S., et al., *Macromolecular Crowding Directs Extracellular Matrix Organization and Mesenchymal Stem Cell Behavior*. PLoS ONE, 2012. **7**(5): p. e37904.
37. Zhou, H.-X., G. Rivas, and A.P. Minton, *Macromolecular Crowding and Confinement : Biochemical, Biophysical, and Potential Physiological Consequences*. Annual Review of Biophysics, 2008. **37**: p. 375-397.
38. Phillips, R., et al., *Emerging roles for lipids in shaping membrane-protein function*. Nature, 2009. **459**(7245): p. 379-385.
39. Ursell, T., et al., *Cooperative gating and spatial organization of membrane proteins through elastic interactions*. Public Library of Science Computational Biology, 2007. **3**(5): p. 81.
40. de Planque, M.R. and J.A. Killian, *Protein-lipid interactions studied with designed transmembrane peptides: role of hydrophobic matching and interfacial anchoring*. Molecular Membrane Biology, 2003. **20**(4): p. 271-84.
41. Dekker, J.P. and G. Yellen, *Cooperative gating between single HCN pacemaker channels*. The Journal of General Physiology, 2006. **128**(5): p. 561-567.
42. Erdem, R. and E. Aydiner, *Monte Carlo simulation for statistical mechanics model of ion-channel cooperativity in cell membranes*. Physical Review, 2009. **79**: p. 031919.
43. Aisenbrey, C., G. Bechinger B Fau - Grobner, and G. Grobner, *Macromolecular crowding at membrane interfaces: adsorption and alignment of membrane peptides*. Journal of Molecular Biology, 2008. **375**(2): p. 376-385.

44. Abe, M. and T. Kobayashi, *Imaging local sphingomyelin-rich domains in the plasma membrane using specific probes and advanced microscopy*. *Biochimica et Biophysica Acta (BBA) - Molecular and Cell Biology of Lipids*, 2014. **1841**(5): p. 720-726.
45. Kulma, M., et al., *Sphingomyelin-rich domains are sites of lysenin oligomerization: implications for raft studies*. *Biochimica et Biophysica Acta*, 2010. **1798**(3): p. 47-81.
46. Yilmaz, N., et al., *Real-time visualization of assembling of a sphingomyelin-specific toxin on planar lipid membranes*. *Biophysical Journal*, 2013. **105**(6): p. 1397-1405.
47. Yilmaz, N. and T. Kobayashi, *Visualization of Lipid Membrane Reorganization Induced by a Pore-Forming Toxin Using High-Speed Atomic Force Microscopy*. *ACS Nano*, 2015. **9**(8): p. 7960-7967.
48. Dietrich, C., et al., *Partitioning of Thy-1, GM1, and cross-linked phospholipid analogs into lipid rafts reconstituted in supported model membrane monolayers*. *Proceedings of the National Academy of Sciences of the United States of America*, 2001. **98**(19): p. 10642-10647.
49. Lingwood, D. and K. Simons, *Lipid rafts as a membrane-organizing principle*. *Science*, 2010. **327**(5961): p. 46-50.
50. Burnstock, G., *Purinergic signalling--an overview*. *Novartis Found symposium*, 2006. **276**: p. 26-48.
51. Burnstock, G., *Purinergic signalling: past, present and future*. *Brazilian Journal of Medical and Biological Research*, 2009. **42**(1): p. 3-8.
52. Burnstock, G. and A. Verkhatsky, *Evolutionary origins of the purinergic signalling system*. *Acta Physiologica*, 2009. **195**(4): p. 415-447.
53. Chatterjee, C. and D.L. Sparks, *P2X receptors regulate adenosine diphosphate release from hepatic cells*. *Purinergic Signalling*, 2014. **10**(4): p. 587-93.

54. Hattori, M. and E. Gouaux, *Molecular mechanism of ATP binding and ion channel activation in P2X receptors*. Nature, 2012. **485**(7397): p. 207-212.
55. Vial, C., R.J. Roberts Ja Fau - Evans, and R.J. Evans, *Molecular properties of ATP-gated P2X receptor ion channels*. Trends in Pharmacological Sciences, 2004. **25**(9): p. 487-93.
56. Takai, E., et al., *Autocrine signaling via release of ATP and activation of P2X7 receptor influences motile activity of human lung cancer cells*. Purinergic Signalling, 2014. **10**(3): p. 487-97.
57. Skals, M., et al., *Alpha-hemolysin from Escherichia coli uses endogenous amplification through P2X receptor activation to induce hemolysis*. Proceedings of the National Academy of Sciences of the United States of America, 2009. **106**(10): p. 4030-4035.
58. Skals, M., et al., *Bacterial RTX toxins allow acute ATP release from human erythrocytes directly through the toxin pore*. The Journal of Biological Chemistry, 2014. **289**(27): p. 19098-109.
59. Skals, M., et al., *Escherichia coli alpha-hemolysin triggers shrinkage of erythrocytes via K(Ca)3.1 and TMEM16A channels with subsequent phosphatidylserine exposure*. The Journal of Biological Chemistry, 2010. **285**(20): p. 15557-65.
60. Skals, M., H.A. Leipziger J Fau - Praetorius, and H.A. Praetorius, *Haemolysis induced by alpha-toxin from Staphylococcus aureus requires P2X receptor activation*. Pflugers Archiv : European Journal of Physiology, 2011. **462**(5): p. 669-79.
61. Larsen, C.K., et al., *Python erythrocytes are resistant to alpha-hemolysin from Escherichia coli*. Journal of Membrane Biology, 2011. **244**(3): p. 131-40.
62. Masin, J., et al., *Differences in purinergic amplification of osmotic cell lysis by the pore-forming RTX toxins Bordetella pertussis CyaA and Actinobacillus pleuropneumoniae ApxIA: the role of pore size*. Infection and Immunity, 2013. **81**(12): p. 4571-82.

63. Zhu, H., S. Dong, and J.M. Liu, *Hysteresis loop area of the Ising model*. Physical Review B, 2004. **70**(13): p. 132403.
64. Kaestner, L., et al., *The non-selective voltage-activated cation channel in the human red blood cell membrane: reconciliation between two conflicting reports and further characterisation*. Bioelectrochemistry, 2000. **52**(2): p. 117-25.
65. Nowak, L.M. and J.M. Wright, *Slow voltage-dependent changes in channel open-state probability underlie hysteresis of NMDA responses in Mg²⁺-free solutions*. Neuron, 1992. **8**(1): p. 181-187.
66. Andersson, T., *Exploring voltage-dependent ion channels in silico by hysteretic conductance*. Mathematical Biosciences, 2010. **226**(1): p. 16-27.
67. Pustovoit, M.A., A.M. Berezhkovskii, and S.M. Bezrukov, *Analytical theory of hysteresis in ion channels: Two state model*. Journal of Chemical Physics, 2006. **125**: p. 194907(8).
68. Bryant, S., et al., *Purinergic control of lysenin's transport and voltage-gating properties*. Purinergic Signalling, 2016. **12**(3): p. 549-559.

CHAPTER TWO: INTRAMEMBRANE CONGESTION EFFECTS ON LYSENIN
CHANNEL VOLTAGE-INDUCED GATING

Eric Krueger, Sheenah Bryant, Nisha Shrestha, Tyler Clark, Charles Hanna,

¹David Pink, *Daniel Fologea

Department of Physics, Boise State University, Boise, Idaho 83725, United States

¹Department of Physics, St. Francis Xavier University, Antigonish, Nova Scotia

B2G 2W5, Canada

Corresponding Author

*Email: DanielFologea@boisestate.edu, Phone: +1 208 426 2664, Fax: +1 208

426 4330

Reprinted with permission from Copyright Clearance Center: Springer Nature,
European Biophysical Journal, Intramembrane congestion effects on lysenin channel
voltage-induced gating, Krueger and Bryant *et al*, (2015).

<https://doi.org/10.1007/s00249-015-1104-z>

https://static-content.springer.com/esm/art%3A10.1007%2Fs00249-015-1104-z/MediaObjects/249_2015_1104_MOESM1_ESM.doc

Abstract

All cell membranes are packed with proteins. The ability to investigate the regulatory mechanisms of protein channels in experimental conditions mimicking their congested native environment is crucial for understanding the environmental physicochemical cues that may fundamentally contribute to their functionality in natural membranes. Here we report on investigations of the voltage-induced gating of lysenin channels in congested conditions experimentally achieved by increasing the number of channels inserted into planar lipid membranes. Typical electrophysiology measurements reveal congestion-induced changes to the voltage-induced gating, manifested as a significant reduction of the response to external voltage stimuli. Furthermore, we demonstrate a similar diminished voltage sensitivity for smaller populations of channels by reducing the amount of sphingomyelin in the membrane. Given lysenin's preference for targeting lipid rafts, this result indicates the potential role of the heterogeneous organization of the membrane in modulating channel functionality. Our work indicates that local congestion within membranes may alter the energy landscape and the kinetics of conformational changes of lysenin channels in response to voltage stimuli. This level of understanding may be extended to better characterize the role of the specific membrane environment in modulating the biological functionality of protein channels in health and disease.

Keywords; lysenin; crowding; lipid rafts; sphingomyelin; open probability; voltage gating

Introduction

The conformational changes by which protein channels exercise precise control over membrane permeability are central to life-sustaining processes. The basic science of membranes has demonstrated relationships between protein channel functionality and multiple environmental cues unrelated to variations in their primary structure. All cell membranes are packed with proteins, which may occupy up to 50% of the membrane surface area [11, 25, 39]. This congested environment may promote specific and non-specific interactions originating from molecular crowding (excluded-surface effects) and confinement [39], changes to membrane elasticity [30, 34], hydrophobic mismatch [8], membrane bending [30] or direct interactions between membrane species [7, 9, 12]. The two-dimensional configuration of the membrane further restricts spatial arrangements, promoting congestion and self-congestion of identical molecular species [2, 39]. The heterogeneous organization of the membrane into lipid rafts [10, 26, 29] adds another level of complexity since many membrane components, including protein channels, have specificity for accumulation into lipid rafts [3, 6, 20, 22, 27], consequently promoting local congestion with fewer molecules.

Excluded surface effects, electrostatic, and membrane-elasticity mediated interactions each has a dependency on local channel density, ultimately determining the distance between protein channels and allowing short or long-range interactions to manifest [12, 30, 39]. Although a synergetic contribution from all of these environmental cues is expected to influence channel functionality, previous reports have limited their investigative scope to individual factors. Nonetheless, the common denominator of congestion is the change of the free energy of the system, which in turn may be

experimentally observable as changes in the kinetics of the protein channel conformational transitions [9, 12, 21, 25, 34, 39]. The scarcity of experimental reports on the behavior of protein channels in congested conditions originates from the lack of an adequate experimental platform to control channel population densities. Ion channels are not readily available and are not easily reconstituted in artificial systems in controlled-density conditions. Pore-forming toxins may provide a better *in vitro* platform for experimental realization of congestion conditions. However, they often lack regulation and their biological activity is not necessarily determined by a specific response to external stimuli that induce conformational changes observable as alterations of their functionality. In this line of inquiries, we focused our investigations on the effects of congestion within a membrane by analyzing changes in the gating behavior of lysenin channels inserted into artificial planar bilayer lipid membranes (BLMs). Lysenin is a 297 amino acid pore-forming protein extracted from the coelomic fluid of *Eisenia fetida* that self-inserts to form ~3 nm diameter channels in membranes containing sphingomyelin (SM) [13, 17, 18, 36]. Although lysenin is not an ion channel, it constitutes an excellent experimental model for studying the effects of congestion on regulated protein channels irrespective of their structure and biological function. Lysenin channels exhibit salient features of ion channels such as high transport rate and regulation by voltage [13, 17]. Their response to voltage stimuli has been well characterized within a two-state (open-close) model, and changes in the energy landscape can be identified through established relationships between channel gating and Boltzmann statistics [13] similar to ion channels [5, 16, 24]. Lysenin's ability to self-insert stable channels into artificial membranes facilitates establishing congested conditions by successively increasing the

number of channels inserted into the BLM, which is expected to influence the voltage-induced gating. In addition, lysenin has been shown to favor insertion into SM-rich lipid rafts [1, 22, 35-38], which facilitates further self-congestion conditions by manipulating the surface area of the rafts through changes in the SM amount in the membrane [1, 20, 28].

Materials and Methods

Dry asolectin (Aso) from soy bean (Sigma-Aldrich), powder brain SM (Avanti Polar Lipids), and powder cholesterol (Chol) from Sigma-Aldrich were dissolved in n-decane in a 10:1:5 weight ratio for the 10% SM solution, and a 10:5:5 weight ratio for the 50% SM solution. The percentage indicates SM weight relative to Aso. Lyophilized lysenin (Sigma-Aldrich) was prepared as a 0.3 μM stock solution by dissolving it in a solution containing 100 mM KCl, 20 mM HEPES (pH 7) and 50% glycerol and used without further purification.

The experimental setup consisted of two 1 ml PTFE reservoirs separated by a thin PTFE film with a ~ 70 μm diameter aperture acting as a hydrophobic frame for BLM formation. Each reservoir was filled with buffered electrolyte (50 mM KCl, 20 mM HEPES, pH 7.2) and a planar BLM was formed by painting small amounts of one of the lipid mixtures over the aperture. The electrical connections were established via two Ag/AgCl electrodes embedded in the electrolyte solution on each side of the BLM, and connected to the headstage of an Axopatch 200B amplifier (Molecular Devices). The data was digitized and recorded through a DigiData 1440A Digitizer (Molecular Devices), and further analyzed by using Clampfit 10.2 (Molecular Devices) and Origin 8.5.1 (OriginLab) software packages. After a stable BLM was achieved, small amounts of

lysenin (~0.3 nM final concentration in the reservoir) were added to the ground side of the BLM under continuous stirring with a low-noise magnetic stirrer (Dual Dipole Stirplate, Warner Instruments). Channel insertion was monitored by measuring the ionic currents through the BLM in voltage clamp conditions at negative transmembrane potentials and a 1 kHz low-pass hardware filter (Electronic Supplementary Material Fig. S1 and Fig. S2). Successive addition of increased amounts of lysenin to the ground side of the BLM provided additional channels to facilitate congested conditions (Electronic Supplementary Material Fig. S3), and ensured consistent channel orientation [13]. After each lysenin addition, the system was monitored to ensure completion of channel insertion before each data measurement, as indicated by a steady-state open current usually achievable in less than 1 hour (Electronic Supplementary Material Fig. S3) [15]. All of the experiments were performed at room temperature ($22.5 \pm 0.5^\circ \text{C}$).

Results and Discussion

We hypothesized that experimental congestion conditions may be achieved by increasing the number of lysenin channels inserted into planar BLMs. However, large channel populations in this study were expected to yield ionic currents exceeding the 200 nA limit of the instrumentation at practical transmembrane voltages. To circumvent this limitation, we decreased the conductance of the support electrolyte by using 50 mM KCl and characterized the insertion and functionality of individual lysenin channels to ensure consistent behavior among experimental conditions. Using BLMs comprised of 50% SM weight ratio relative to Aso, the addition of lysenin to the ground reservoir at -30 mV transmembrane potential produced discrete changes in the open current (Electronic Supplementary Material Fig. S1) indicative of individual channel insertions [17]. The

stepwise open current distribution for four inserted channels yielded a unitary conductance of 0.391 ± 0.025 nS/channel, consistent with previous reports [14, 17, 23]. The I-V curves recorded in response to voltage ramps ranging from -100 to 100 mV at 0.2 mV/s demonstrated the linear behavior in the negative voltage region (hence absence of conformational changes and a constant conductance in the negative voltage range), followed by voltage induced gating at positive potentials [15, 17] (Electronic Supplementary Material Fig. S1). Therefore, we concluded that the low ionic concentration did not affect the insertion, the transport capabilities, and the voltage regulation of lysenin channels.

After the insertion of lysenin channels into the 50% SM BLMs, the gating behavior was assessed by measuring the ionic current in response to a slow voltage ramp (0.16 mV/s) ranging from 0 mV to 100 mV. Incorporating more lysenin from the stock into the grounded bathing solution facilitated additional channel insertions into the BLM, increasing the density of channels within the membrane (Electronic Supplementary Material Fig. S3). The number of channels in the population was approximated from the ratio of the total membrane conductance determined from the ionic current measured at -60 mV (when all of the channels were open) to the unitary single channel conductance measured during the initial insertion events (~ 0.39 nS/channel). Effects due to the increased population were identified from the analysis of the I-V curves recorded for different numbers of inserted channels. As shown in Fig. 1a, the I-V curves revealed a significant increase in the voltage required for the channels to gate as the number of inserted channels increased. Each I-V plot shown in Fig. 1 is the average of three consecutive runs for the same experimental setup. Although multiple parallel experiments

indicated an identical behavior (i.e., increase of voltage required to initiate gating), assuring identical experimental conditions by exact control of the number of inserted channels was elusive.

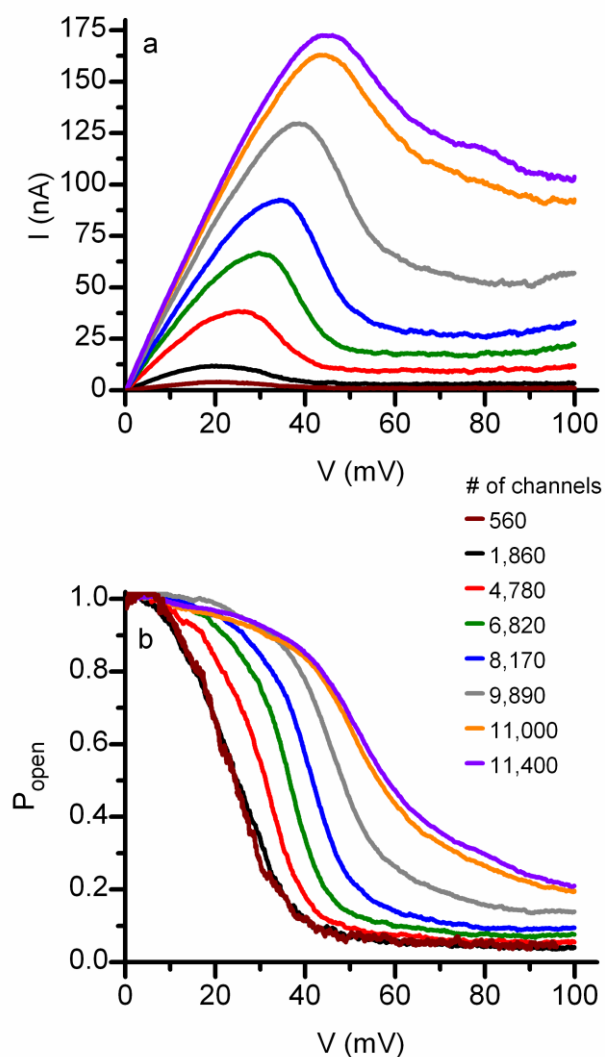


Fig. 1. The number of lysenin channels inserted into a planar lipid membrane containing 50% SM affects the I-V characteristics (a) and induces a rightward shift of the experimental open probability P_{open} (b). Each I-V and P_{open} plot is the average of three individual recordings for the same experimental setup and all data points in the graphs are experimental values with standard errors < 5%.

To further analyze the gating behavior, linear fits of the I-V curves in the low positive voltage range (when all of the channels were in the open state [15]) were used to

determine a theoretical maximum current I_{\max} for each voltage as if channel gating was not observed, and the probability of finding a channel in open state (P_{open}) was determined from [4, 33]:

$$P_{\text{open}} = \frac{I}{I_{\max}} \quad (1)$$

where I is the actual measured current at each voltage in the I-V curve. The plot of the open probabilities, shown in Fig. 1b, demonstrated the rightward shift of P_{open} with increased channel population. Ionic currents larger than the instrument's limit recorded for increased channel populations consequently limited the maximum number of channels that could be investigated. Analysis of the I-V curves shown in Fig. 1a indicated that subsequent increases to the channel population would yield currents outside of the measurable range of the instrument, making the open probability calculations unfeasible.

One may argue that the actual transmembrane voltage decreased for large channel populations due to the increased voltage drop across the serial resistance of the bulk electrolyte. Each reservoir can be approximated as a cube of 1 cm side length, and the measured electrolyte solution was 6.5 mS/cm thus yielding a total conductance for the two reservoirs of ~13 mS. Since each channel contributes to the membrane conductance by ~ 0.39 nS, the total conductance of 10,000 inserted channels of ~3.9 μS is ~3300 times smaller than the electrolyte conductance. Therefore, any change in the actual transmembrane voltage due to increased voltage drop on the serial resistance of the electrolyte is negligible. Hence, we attribute the changes observed in the voltage response of lysenin channels to the increased population in the target membrane. Given the approximate surface area occupied by one channel [36] ($\sim 10^{-4} \mu\text{m}^2$) and the relatively large area of the BLM ($\sim 1,900 \mu\text{m}^2$ for a 25 μm radius) it is difficult to link the observed

shift in gating to excluded-surface effects [39] even for a population of 10,000 inserted channels. In addition, the average inter-channel distance for a uniform distribution of channels within the membrane (roughly estimated at ~ 400 nm for 10,000 channels inserted into a $1,900 \mu\text{m}^2$ membrane) may be sufficiently large to prevent manifestation of any specific interactions between channels. However, lysenin channels prefer insertion into lipid rafts [18, 22], which promote localized accumulation and increased local channel density. Lysin clustering into SM-rich domains and formation of 2-D arrays in supported lipid membranes has been clearly demonstrated by using high-speed Atomic Force Microscopy [37, 38] and these studies revealed that rafts are the first target for oligomerization. However, at very high lysenin concentration, pore assembly has been shown to gradually expand into the disordered phase following exclusion of SM and Chol from the SM-rich domain. Nonetheless, our experiments comprised much lower amounts of lysenin added to the solutions and, implicitly, a significantly reduced number of inserted channels. Therefore, we may assume that our experimental conditions describe the functionality of lysenin channels located into lipid rafts. Since SM is a major component of the lipid rafts and SM depletion may modulate the lipid raft size and distribution [1, 20, 28], we expanded our investigations to a BLM with a lower SM concentration (10% weight ratio relative to Aso) in the same ionic conditions. Given the importance of SM for the lysenin pore formation and insertion [17], we questioned if the reduced SM concentration affects the functionality of individual lysenin channels. Similar to the 50% SM conditions, the open current recorded after addition of lysenin to the ground reservoir changed in discrete steps (Electronic Supplementary Material Fig. S2), and the stepwise distribution of the open current for the four inserted channels

yielded a unitary conductance of $\sim 0.394 \pm 0.015$ nS, comparable to the 50% SM conditions. The I-V plot recorded in response to voltage ramps from -100 to 100 mV also exhibited the familiar linear behavior in the negative voltage region, followed by voltage induced gating at positive potentials [15] (Electronic Supplementary Material Fig. S2). Therefore, we concluded that the reduced SM concentration did not affect the insertion, the conductance properties or the voltage regulation of lysenin channels.

We then introduced additional lysenin from the stock into the grounded bathing solution, which permitted further channel insertions into the BLM, consequently increasing the density of channels within the membrane. Experimentally, the conditions and methods were identical to the higher SM concentration BLMs, and the open probability was calculated in the same manner. The I-V curves and the open probability for increasing numbers of channels in the lower SM concentration membranes are shown in Fig. 2a and 2b, respectively.

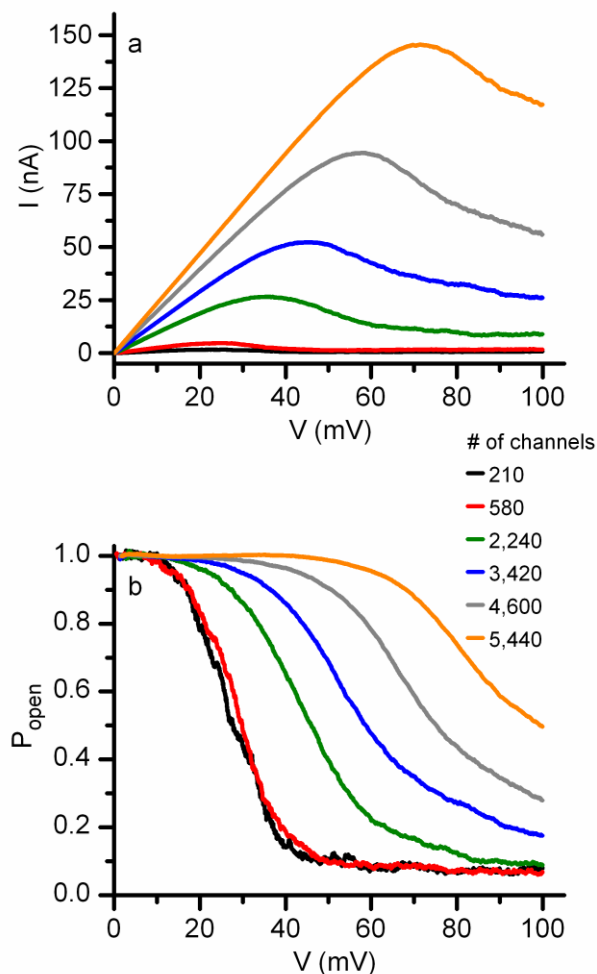


Fig. 2. (a) The I-V plots for increasing numbers of lysenin channels inserted into planar lipid membranes containing 10% SM. (b) A more significant rightward shift in the open probability is observed for the reduced SM concentration compared to the 50% SM condition shown in Fig. 1. Each I-V and P_{open} plot is the average of three individual recordings for the same experimental setup and all data points are experimental values with standard errors $< 5\%$.

As with the higher SM concentration membranes, increases in channel population shifted the gating toward higher voltages. However, the shift was more significant for the 10% SM conditions compared with the 50% SM conditions. To gain further insight into the effect of SM ratio, we considered a simple biophysical model of gating. The conformational changes of lysenin channels in response to transmembrane voltages are considered transitions between two conduction states, i.e open and close [13].

Accordingly, the theoretical probability of finding a channel in the open state at equilibrium is described by Boltzmann statistics as [24, 30]:

$$P_{open} = \frac{1}{1 + K} = \frac{1}{1 + e^{\frac{-\Delta G}{k_B T}}} = \frac{1}{1 + e^{\frac{-q}{k_B T}(V - V_{0.5})}} \quad (2)$$

where K is the equilibrium constant of the open-close transition, ΔG is the difference in free energy between the open and closed state, q is the gating charge, k_B is the Boltzmann constant, T is the absolute temperature, and $V_{0.5}$ is the half-activation voltage, i.e. the voltage where $P_{open} = 0.5$ [32, 33]. Equation (2) establishes the relationship between kinetics and free energy; the changes in P_{open} reflect changes in kinetics which are indicative of changes in the free energy due to all of the specific and non-specific interactions arising from local congestion, which may include excluded surface effects originating in crowding, electrostatic interactions, or changes in the mechanical properties of the membrane [12, 30, 32, 39]. Next, our analysis focused on the changes of the half-activation voltage, indicative of the balance between the energy supplied by the external electric field and all the other energies in the system [32]. The experimental $V_{0.5}$ values for 50% SM BLMs increased by ~ 30 mV over the approximately 20-fold increase in channel population (Fig. 3). The smaller populations of channels (less than 2,000 channels) exhibited negligible changes of the $V_{0.5}$ values, and indicated that smaller numbers of channels did not establish a congested environment to significantly alter channel functionality. The shift toward higher voltages for the increasing population of channels suggested that the congested conditions make the channels less sensitive to voltage.

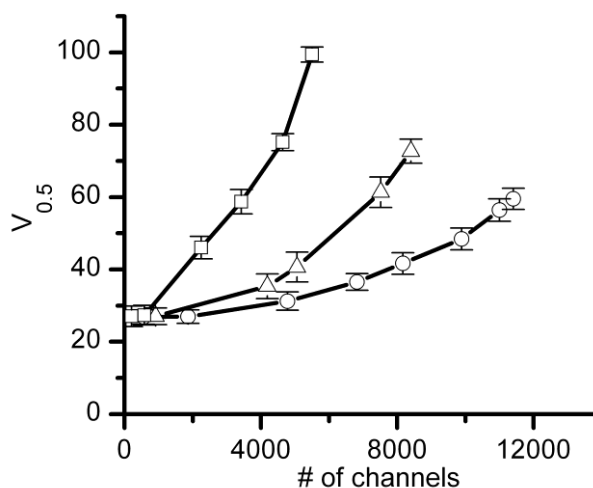


Fig. 3. The half-activation voltage $V_{0.5}$ (mean \pm SD, $n=3$) as a function of the number of lysenin channels inserted into similar-size planar lipid membranes undergoes more pronounced changes for bilayers containing 10% SM (open squares), 20% SM (open triangles), and 50% SM (open circles).

For 10% SM, the values of $V_{0.5}$ induced by an approximately 25-fold increase in channel population shifted by ~ 72 mV (Fig. 3). Again, smaller populations of channels (~ 210 and ~ 580) did not exhibit significant changes in the $V_{0.5}$ values of the open probability, indicating that small numbers of channels did not constitute a congested environment in which significant changes in functionality manifest. Consistent with these observations, a parallel experiment comprising lysenin channels inserted into BLMs containing 20% SM (weight ratio relative to the amount of Aso) shows that for similar number of inserted channels the $V_{0.5}$ values are situated between the extreme values determined for the 10% SM and 50% SM (Fig. 3). A reasonable explanation for such behavior may consider the role played by lipid rafts as a target for lysenin channel insertion [1, 18, 19, 22]. A BLM containing a smaller concentration of SM was theorized to create smaller lipid rafts where lysenin channels will insert. This, therefore, led to a greater local density of channels from the decreased raft area. Comparing the lower-concentration to the higher-concentration SM membranes, we observed that for a given

number of channels, the bilayers containing the lower SM concentration yielded greater values of $V_{0.5}$. However, for low numbers of channels, $V_{0.5}$ was approximately the same for both concentrations. As the number of channels in the populations increased, the BLMs containing a lower concentration of SM exhibited a more significant increase in $V_{0.5}$. Once again, the higher density of channels, presumed to originate in the reduced surface area of the lipid rafts, produced a prominent congestion effect manifested as a significant change in the voltage gating.

The behavioral changes for channels in congested conditions, observed as changes in the voltage gating profile, indicates an altered kinetics of the conformational transitions. Our analysis implies that the measured open probability was independent of time, thus was estimated from open currents measured at equilibrium. However, the slow equilibration of lysenin channels in response to transmembrane voltages [15] may prevent accurate estimations of the open probability as a representative of the steady state for each of the experimental conditions. For small populations of inserted channels, the low voltage ramp rate used to plot the I-V characteristics (0.16 mV/s) suffices to approximate each current as descriptive of a true steady state [15]. A more thorough analysis would require either using extremely slow voltage rates [15] or determining the time evolution of the ionic currents in response to step voltages. Neither of these approaches is feasible owing to membrane lifetime and technical limitations. Irrespective of the steady-state approximation, our results suggest that high density conditions alter channel functionality by changing the free energy landscape of conformational transitions.

The open probabilities of the small populations show the presence of a minimum threshold in the number of channels required to initiate observable changes in gating, consistent with congestion effects dependent on inter-channel distance. We also observed that low SM ratio conditions exhibit a more abrupt relationship between $V_{0.5}$ and the number of channels, providing further evidence that the behavioral effects could be attributed to the more congested conditions. Since only minor changes in gating were observed for low numbers of channels irrespective of SM concentration, this suggests that the congested conditions were dependent on the local density of the channels in the BLM. We assumed that as the channels were inserted into the membrane, smaller rafts produced more noticeable effects on the gating than when the channels were allowed to spread out in the higher SM concentration membrane. To further analyze the behavior of lysenin channels at low densities, we estimated $V_{0.5}$ for populations ranging from 3 to 943 channels inserted into 50% SM BLMs (Fig. 4). Although each $V_{0.5}$ represents the average value determined for a particular number of inserted channels, each point was determined from an independent experiment. Very low number of inserted channels (< 20) yielded a spurious signal owing to the large contribution to the open current of individual closing events. In order to avoid the large experimental errors achievable in such conditions, at least ten I-V plots were averaged for each analysis, while for larger number of channels the average was calculated from at least three I-V plots. We found no change in the values of $V_{0.5}$ (within the errors) for the channel populations in this range, reinforcing our assertion that suggests a minimum inter-channel distance is required to manifest changes in the energy landscape.

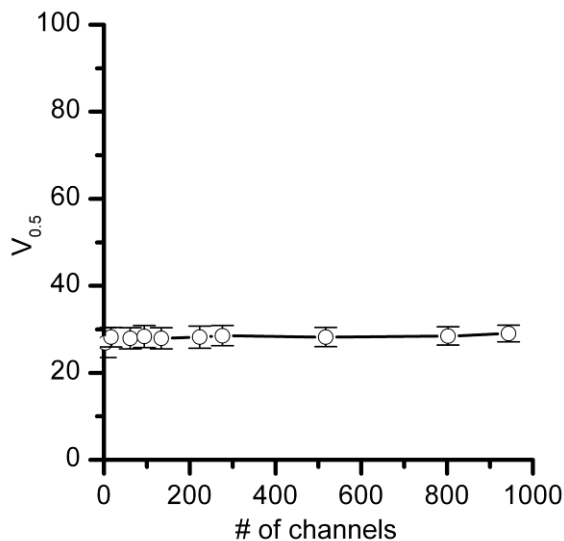


Fig. 4. The half-activation voltage $V_{0.5}$ undergoes negligible changes for low number of lysenin channels inserted into 50% SM lipid membranes. Each $V_{0.5}$ was determined from independent parallel experiments and the data are reported as mean \pm SD, n=3-10.

A better analysis of the experimental results should include the average distance between channels, instead of number of inserted channels. However, such calculations are seriously impeded by the current lack of knowledge with regards to the size of the rafts as a function of lipid composition. Lipid rafts are not exclusively composed of SM therefore the area occupied by rafts for a given SM concentration may not be accurately determined. It is estimated that only 20-30% of the SM is actually included into lipid rafts [22, 31], which may significantly contribute to a reduced raft area, higher channel density and shorter inter-channel distance.

We reported on changes in lysenin channel voltage-induced gating exclusively prompted by congestion effects within a planar BLM. The origins of these effects are hypothesized to stem from changes in the energy landscape, which resulted in modified channel-state kinetics and/or equilibrium. Our work illustrates how congested conditions typical of cell membranes influence the performance and behavior of voltage-gated

channels. Although the precise physiological role of lysenin remains unknown, our work revealed functional relationships between micro-environmental conditions and regulated protein channels. Lysenin is not an ion channel but its response to external voltage stimuli is satisfactorily described by two-state models commonly used for ion channels. This mechanistic similarity may prove crucial for deeper insights into ion channel physiology since all ion channels are crowded proteins in their native environments and many are known to have specificity for accumulation in lipid rafts [3, 6, 20, 27]. This extra layer of complexity and the connection between biological functionality and local environment may be expanded to explain the biological activity of porins, malfunctioning of ion channels, impaired signaling, or the development of serious diseases [20, 28].

Acknowledgments

Research reported in this publication was partially supported by the National Institute of General Medical Sciences of the National Institutes of Health under Award Number P20GM109095. The content is solely the responsibility of the authors and does not necessarily represent the official views of the National Institute of Health. EK and SB equally contributed to this article.

Conflict of Interest: The authors declare that they have no conflict of interest.

References

1. Abe M, Kobayashi T (2014) Imaging local sphingomyelin-rich domains in the plasma membrane using specific probes and advanced microscopy. *BBA-Mol Cell Biol L* 1841:720-726
2. Aisenbrey C, Bechinger B, Grobner G (2008) Macromolecular crowding at membrane interfaces: adsorption and alignment of membrane peptides. *J Mol Biol* 375:376-385

3. Barfod ET, Moore AL, Roe MW, Lidofsky SD (2007) Ca^{2+} -activated IK_1 Channels Associate with Lipid Rafts upon Cell Swelling and Mediate Volume Recovery. *J Biol Chem* 282:8984-8993
4. Bezanilla F (2005) Voltage-gated ion channels. *IEEE T Nanobiosci* 4:34-48
5. Bezanilla F (2008) Ion Channels: From Conductance to Structure. *Neuron* 60:456-468
6. Brady JD, Rich TC, Le X, Stafford K, Fowler CJ, Lynch L, Karpen JW, Brown RL, Martens JR (2004) Functional Role of Lipid Raft Microdomains in Cyclic Nucleotide-Gated Channel Activation. *Mol Pharmacol* 65:503-511
7. Dan N, Pincus P, Safran SA (1993) Membrane-Induced Interactions between Inclusions. *Langmuir* 9:2766-2771
8. de Pianque MRR, Killian JA (2003) Protein-lipid interactions studied with designed transmembrane peptides: role of hydrophobic matching and interfacial anchoring. *Mol Membr Biol* 20:271
9. Dekker JP, Yellen G (2006) Cooperative Gating between Single HCN Pacemaker Channels. *J Gen Physiol* 128:561-567
10. Dietrich C, Volovyk ZN, Levi M, Thompson NL, Jacobson K (2001) Partitioning of Thy-1, GM1, and cross-linked phospholipid analogs into lipid rafts reconstituted in supported model membrane monolayers. *P Natl Acad Sci USA* 98:10642-10647
11. Dupuy AD, Engelman DM (2008) Protein area occupancy at the center of the red blood cell membrane. *P Natl Acad Sci USA* 105:2848-2852
12. Erdem R, Aydiner E (2009) Monte Carlo simulation for statistical mechanics model of ion-channel cooperativity in cell membranes. *Phys Rev E* 79:031919
13. Fologea D, Al Faori R, Krueger E, Mazur YI, Kern M, Williams M, Mortazavi A, Henry R, Salamo GJ (2011a) Potential analytical applications of lysenin channels for detection of multivalent ions. *Anal Bioanal Chem* 401:1871-1879

14. Fologea D, Krueger E, Lee R, Naglak M, Mazur Y, Henry R, Salamo G (2010) Controlled Gating of Lysenin Pores. *Biophys Chem* 146:25-29
15. Fologea D, Krueger E, Mazur YI, Stith C, Yui O, Henry R, Salamo GJ (2011b) Bi-stability, hysteresis, and memory of voltage-gated lysenin channels. *BBA-Biomembranes* 1808:2933-2939
16. Hille B (2001) *Ion channels of excitable membranes*. 3rd edn. Sinauer Associates, Inc., Sunderland, MA
17. Ide T, Aoki T, Takeuchi Y, Yanagida T (2006) Lysenin forms a voltage-dependent channel in artificial lipid bilayer membranes. *Biochem Biophys Res Commun* 346:288-292
18. Ishitsuka R, Kobayashi T (2004) Lysenin: a new tool for investigating membrane lipid organization. *Anat Sci Int* 79:184-190
19. Ishitsuka R, Kobayashi T (2007) Cholesterol and Lipid/Protein ratio Control the Oligomerization of a Sphingomyelin-Specific Toxin, Lysenin. *Biochemistry* 46:1495-1502
20. Jin Z-X, Huang C-R, Dong L, Goda S, Kawanami T, Sawaki T, Sakai T, Tong X-P, Masaki Y, Fukushima T, Tanaka M, Mimori T, Tojo H, Bloom ET, Okazaki T, Umehara H (2008) Impaired TCR signaling through dysfunction of lipid rafts in sphingomyelin synthase 1 (SMS1)-knockdown T cells. *Int Immunol* 20:1427-1437
21. Keleshian AM, Edeson RO, Liu G-J, Madsen BW (2000) Evidence for Cooperativity Between Nicotinic Acetylcholine Receptors in Patch Clamp Records. *Biophys J* 78:1-12
22. Kulma M, Herec M, Grudzinski W, Anderluh G, Gruszecki WI, Kwiatkowska K, Sobota A (2010) Sphingomyelin-rich domains are sites of lysenin oligomerization: Implications for raft studies. *BBA-Biomembranes* 1798:471-481
23. Kwiatkowska K, Hordejuk R, Szymczyk P, Kulma M, Abdel-Shakor A-B, Plucienniczak A, Dolowy K, Szewczyk A, Sobota A (2007) Lysenin-His, a

- sphingomyelin-recognizing toxin, requires tryptophan 20 for cation-selective channel assembly but not for membrane binding. *Mol Membr Biol* 24:121-134
24. Latorre R, Vargas G, Orta G, Brauchi S (2007) Voltage and Temperature Gating of ThermoTRP Channels. In: Liedtke WB, Heller S (eds) *TRP Ion Channel Function in Sensory Transduction and Cellular Signaling Cascades*. CRC Press, New York
 25. Linden M, Sens P, Phillips R (2012) Entropic tension in crowded membranes. *PLoS Comput Biol* 8:e1002431
 26. Lingwood D, Simons K (2010) Lipid Rafts As a Membrane-Organizing Principle. *Science* 327:46-50
 27. Maguy A, Hebert TE, Nattel S (2006) Involvement of lipid rafts and caveolae in cardiac ion channel function. *Cardiovasc Res* 69:798-807
 28. Mitsutake S, Zama K, Yokota H, Yoshida T, Tanaka M, Mitsui M, Ikawa M, Okabe M, Tanaka Y, Yamashita T, Takemoto H, Okasaki T, Watanabe K, Igarashi Y (2011) Dynamic modification of Sphingomyelin in Lipid Microdomains Controls Development of Obesity, Fatty Liver, and Type 2 Diabetes. *J Biol Chem* 286:28544-28555
 29. Munro S (2003) Lipid Rafts: Elusive or Illusive? *Cell* 115:377-388
 30. Phillips R, Ursell T, Wiggins P, Sens P (2009) Emerging roles for lipids in shaping membrane-protein function. *Nature* 459:379-385
 31. Pike LJ, Han X, Chung KN, Gross RW (2002) Lipid Rafts are enriched in arachidonic acid and plasmenylethanolamine and their composition is independent of caveolin-1 expression; a quantitative electrospray ionization/mass spectrometric analysis. *Biochemistry* 41:2075-2088
 32. Reeves D, Ursell T, Sens P, Kondev J, Phillips R (2008) Membrane mechanics as a probe of ion-channel gating mechanisms. *Phys Rev E* 78:041901
 33. Tao X, Lee A, Limapichat W, Dougherty DA, MacKinnon R (2010) A gating charge transfer center in voltage sensors. *Science* 328:67-73

34. Ursell T, Huang KC, Peterson E, Phillips R (2007) Cooperative Gating and Spatial Organization of Membrane Proteins through Elastic Interactions. *PLoS Comput Biol* 3:e81
35. Yamaji-Hasegawa A, Makino A, Baba T, Senoh Y, Kimura-Suda H, Sato S, Terada N, Ohno S, Kiyokawa E, Umeda M, Kobayashi T (2003) Oligomerization and pore formation of a sphingomyelin-specific toxin, lysenin. *J Biol Chem* 278:22762-22770
36. Yamaji A, Sekizawa Y, Emoto K, Sakuraba H, Inoue K, Kobayashi H, Umeda M (1998) Lysenin, a novel sphingomyelin-specific binding protein. *J Biol Chem* 273:5300-5306
37. Yilmaz N, Kobayashi T (2015) Visualization of Lipid membrane Reorganization Induced by a Pore-Forming Toxin Using High-Speed Atomic Force Microscopy. *ACS Nano* 9:7960-7967
38. Yilmaz N, Yamada T, Greimel P, Uchihashi T, Ando T, Kobayashi T (2013) Real-Time Visualization of Assembling of a Sphingomyelin-Specific Toxin on Planar Lipid Membranes. *Biophys J* 105:1397-1405
39. Zhou H-X (2009) Crowding effects of membrane proteins. *J Phys Chem B* 113:7995-8005

Electronic Supplementary Material

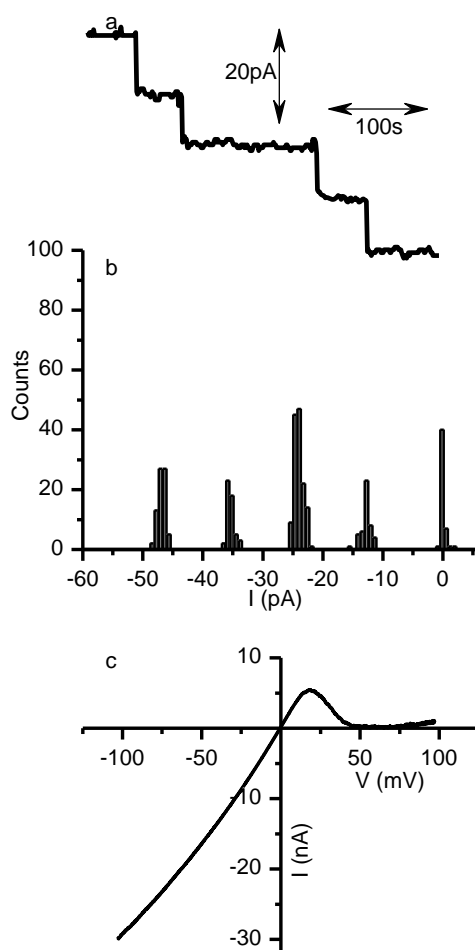


Fig. 5 Low ionic concentration does not affect the functionality of lysenin channels. (a) Insertion of identical lysenin channels in a lipid membrane containing 50% sphingomyelin (weight ratio relative to the amount of asolectin) and bathed by 50 mM KCl is indicated by the stepwise increase of the open current. (b) The current distribution of the open current indicates a unitary conductance increase of $\sim 0.391 \pm 0.025$ nS/channel. (c) The I-V plot recorded at 0.2mV/s indicates the voltage-induced gating at positive transmembrane potentials and demonstrates the functionality of lysenin channels in low ionic concentration conditions.

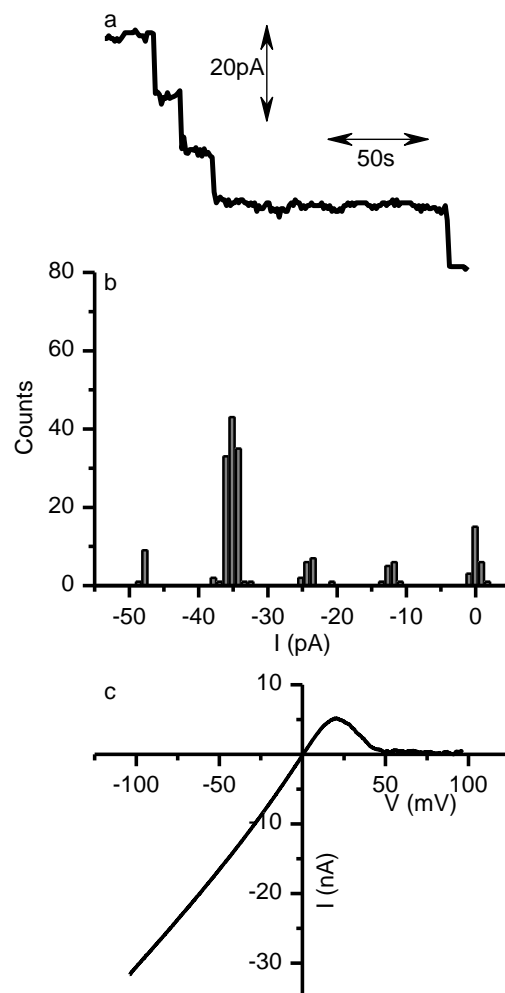


Fig. 6 Sphingomyelin depletion does not affect the functionality of lysenin channels. (a) Insertion of identical lysenin channels in a bilayer containing 10% sphingomyelin (weight ratio relative to asolectin) and bathed by 50 mM KCl. (b) The current distribution of the open current indicates a unitary conductance increase of $\sim 0.394 \pm 0.025$ nS/channel. (c) The I-V plot recorded at 0.2mV/s indicates the voltage-induced gating at positive transmembrane potentials and demonstrates the functionality of lysenin channels in sphingomyelin-depleted conditions.

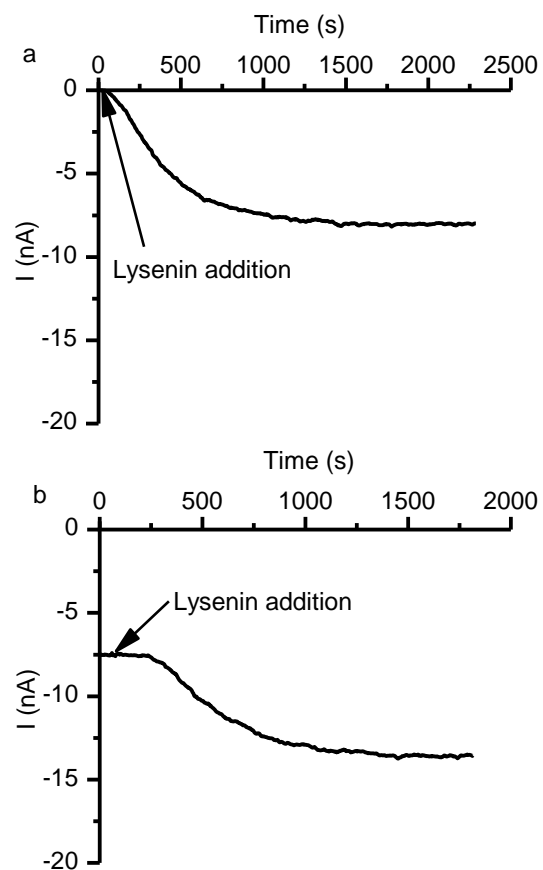


Fig. 7 Consecutive addition of lysenin for achieving increased number of inserted channels into the target lipid membrane. a) Channel insertion after addition of lysenin to a pristine membrane biased by - 60 mV is indicated by changes in ionic current. The completion of insertion is indicated by a steady state is achieved in ~ 40 minutes. b) After recording the I-V plots, a new lysenin addition promotes further insertion and leads to an increased number of channels in the membrane.

CHAPTER THREE: PURINERGIC CONTROL OF LYSENIN'S TRANSPORT AND
VOLTAGE-GATING PROPERTIES

Sheenah Bryant^{1,2}, Nisha Shrestha^{1,2}, Paul Carnig¹, Samuel Kosydar¹, Philip
Belzeski¹, Charles Hanna^{1,2}, Daniel Fologea^{1,2*}

¹Department of Physics, Boise State University, Boise, ID 83725, United States

²Biomolecular Sciences PhD Program, Boise State University, Boise, ID 83725,
United States

Corresponding Author

*Email: DanielFologea@boisestate.edu, Phone: +1 208 426 2664, Fax: +1 208
426 4330

Reprinted with permission from Copyright Clearance Center: Springer Nature,
Purinergic Signalling, Purinergic control of lysenin's transport and voltage-gating
properties, Bryant *et al*, (2016)

<https://link.springer.com/article/10.1007/s11302-016-9520-9>

https://static-content.springer.com/esm/art%3A10.1007%2Fs11302-016-9520-9/MediaObjects/11302_2016_9520_MOESM1_ESM.pdf

Abstract

Lysenin, a pore-forming protein extracted from the coelomic fluid of the earthworm *E. fetida*, manifests cytolytic activity by inserting large-conductance pores in host membranes containing sphingomyelin. In the present study, we found that adenosine phosphates control the biological activity of lysenin channels inserted into planar lipid membranes with respect to their macroscopic conductance and voltage-induced gating. Addition of ATP, ADP, or AMP decreased the macroscopic conductance of lysenin channels in a concentration-dependent manner, with ATP being the most potent inhibitor and AMP the least. ATP removal from the bulk solutions by buffer exchange quickly reinstated the macroscopic conductance and demonstrated reversibility. Single-channel experiments pointed to an inhibition mechanism that most probably relies on electrostatic binding and partial occlusion of the channel-conducting pathway, rather than ligand gating induced by the highly charged phosphates. The Hill analysis of the changes in macroscopic conduction as a function of the inhibitor concentration suggested cooperative binding as descriptive of the inhibition process. Ionic screening significantly reduced the ATP inhibitory efficacy, in support of the electrostatic binding hypothesis. In addition to conductance modulation, purinergic control over the biological activity of lysenin channels has also been observed to manifest as changes of the voltage-induced gating profile. Our analysis strongly suggests that not only the inhibitor's charge but also its ability to adopt a folded conformation may explain the differences in the observed influence of ATP, ADP, and AMP on lysenin's biological activity.

Keywords: adenosine phosphates; pore-forming toxins; lysenin; Voltage gating; Purinergic control

Introduction

Purinergic signaling, broadly defined as modulation of short- and long-term signaling functions presented by purines and pyrimidines [1, 2], is widely recognized as a fundamental mechanism of control at the molecular and cellular level in all kingdoms of life [3, 4]. Neurotransmission, secretion, transduction, cell proliferation, motility, and differentiation are typical examples of biological functions modulated by nucleotides or nucleosides acting as extracellular signaling molecules [5-11]. Burnstock's early hypothesis that ATP, the major intracellular molecule providing the energy required for multiple biochemical and biophysical processes, may actually function as an extracellular non-adrenergic and non-cholinergic signaling molecule [12, 13] was received with great skepticism [14, 15]. After several decades of extensive work, the scientific community came to the realization that ATP is widely employed as a signaling molecule in multiple biological processes in both normal and pathophysiological conditions [9, 11, 16-24]. The rapid progress in understanding and deciphering multiple molecular mechanisms of signaling revealed that ATP is a potent mediator of multiple signaling cascades, which may act through binding to, and non-hydrolytic activation of, P2X ionotropic receptors or G protein-coupled P2Y receptors [1, 3, 19, 21, 23-28]. Although multiple past studies focused on understanding the implications of ATP-controlled signaling with respect to endogenous transmembrane transporters such as ion channels [17, 19, 20, 24, 28-31], there is a recent interest in understanding how ATP controls the lytic action of pore-forming toxins (PFTs) [22, 26, 27, 32-34]. PFTs introduce unregulated conducting pathways into the host cell plasmalemma [35-39], which is expected to yield direct cytolysis. However, the generalization of direct cytolytic activity might be an

oversimplification of the lytic mechanism employed by the PFTs. Recent studies have clearly demonstrated that some PFTs may trigger an early acute release of intracellular ATP through the inserted pores, which further activates the ionotropic P2X receptors and consequently leads to later lysis via the increase of overall membrane permeability to cations such as K^+ and Ca^{2+} [22, 26, 27, 34]. This multistep mechanism is supported by studies in which PFT-mediated ATP transport across artificial vesicle membranes (which are devoid of any other channels or transporters) has been observed, whereas the direct lytic activity presented by the PFTs was minimal [22]. In addition, inhibition of cell lysis in the presence of ATP receptor antagonists demonstrated that a purinergic signaling pathway is responsible for the cell damage [26]. Nonetheless, many PFTs have a high potential to affect biological functions simply by introducing large conductance pathways within the cell membrane, thus dissipating the electrochemical gradients, which may cause serious damage and even cell death [37, 38, 40].

In this line of investigation, we asked whether or not ATP may directly interfere with the transport properties of PFTs and alter their function, without the requirement of activating ionotropic receptors. To answer this question, we focused our attention on lysenin, a 297 amino acid PFT extracted from *Eisenia foetida*, which inserts hexameric pores (~ 3 nm diameter) in artificial and natural lipid membranes containing sphingomyelin (SM) [41-45]. Several remarkable features make lysenin an excellent candidate for such studies. Lysenin's cytolytic and hemolytic activity has been extensively studied [45, 46], and its capability to tamper with the barrier function of artificial lipid bilayers is well-documented [42, 43, 47, 48]. The complete structure of the oligomeric pore inserted into membranes is not yet resolved; however, relatively recent

structural data of lysenin interacting with SM in a pre-pore state indicates the existence of a positively charged domain [49] which may promote specific electrostatic interactions with negatively charged adenosine phosphates, similar to the ionotropic P2X receptors [19, 50, 51]. In addition, unlike many other PFTs, lysenin is endowed with regulatory mechanisms by voltage and ligands [41-43, 52-54], which are in fact remarkable features of ion channels. Lysenin channels present voltage regulation manifested as voltage-induced gating at positive transmembrane voltages greater than ~ 20 mV [41, 54]. Therefore, one may expect that binding of highly charged adenosine phosphates will change the local charge distribution and influence the voltage-induced gating by overall adjustment of electrostatic interactions with the transmembrane electric fields.

Our study reports on the molecular mechanisms of interaction between lysenin channels and adenosine phosphates. The reversible inhibition in macroscopic conductance, the absence of a ligand-induced gating mechanism, the shift of the voltage-induced gating, and the correlation between the observed effects and the charge of the inhibitors led to the hypothesis of electrostatic binding as a central interaction mechanism. Our experimental results suggest that the inhibitor's ability to undergo conformational changes may modulate the interaction with lysenin channels and adjust their functionality. Although the physiological relevance of our work is obscured by the lack of information with regards to lysenin's physiological role, it is suggested that intracellular ATP may play a protective role against the lysenin's lytic action.

Materials and Methods

Reagents and Solutions

Ten milligram asolectine (Sigma Aldrich), 4 mg porcine brain SM (AvantiLipids), and 4 mg cholesterol (Sigma Aldrich) in powder form were dissolved in 200 μ L n-decane (TCI America) for lipid-membrane preparation. If not otherwise indicated in the main text, 135 mM KCl (Fisher Scientific) was used as the support electrolyte solution. Irrespective of their final concentration, all electrolyte solutions were buffered at pH 7 with 20 mM HEPES (Fisher Scientific). Ag/AgCl reference electrodes for the electrical connections with the recording device were prepared using chlorinated Ag wires of 1-mm diameter housed in fine pipette tips filled with 1 M KCl electrolyte solutions containing 1 % agarose (Fisher Scientific). A stock solution of lysenin (Sigma Aldrich) of 1 μ M final concentration was obtained by dissolving it in 100 mM KCl /50% glycerol solution. One molar stock solutions of ATP, ADP, and AMP (all from Sigma-Aldrich) were produced by dissolving the powders in deionized water. dATP was purchased as a 0.1 M stock solution from Thermo Scientific.

Bilayer Lipid Membrane Setup

The experimental setup consisted of a custom-made planar bilayer lipid membrane (BLM) chamber in vertical configuration (Supplemental Fig. 1), which comprised two polytetrafluoroethylene (PTFE) reservoirs, each capable of accommodating \sim 1 mL electrolyte solution. The two reservoirs were separated by a thin PTFE film (\sim 120- μ m thickness) in which a small central hole of \sim 60- μ m diameters was produced by an electric spark. The agarose/Ag/AgCl electrodes immersed into the electrolyte solutions were connected through flexible wires to the headstage and the

ground of the electrophysiology amplifier Axopatch 200B (Molecular Devices) for data recording and analysis in conjunction with the DigiData1440A digitizer (Molecular Devices). Full control of the recording setup, including the stimulation waveforms, was assured using the pClamp 10.2 software package (Molecular Devices). The solutions in the reservoirs were continuously mixed using a low noise bilayer stirplate (Warner Instruments) magnetic stirrer. A custom-made solution exchanger was employed in experiments requiring fast exchange of the support electrolyte. All experiments were performed at room temperature (22 ± 0.5 °C).

Experimental Protocols and Models

After a stable BLM was produced by the painting method (as indicated by capacitance and seal resistance measurement), the addition of small amounts of lysenin (0.3 nM final concentration) into the ground reservoir in voltage clamp conditions (-60 mV applied to the headstage-wired reservoir) produced a step-wise variation of the ionic current, indicative of channel insertion [42, 54]. When a steady state of the ionic current was achieved (after ~40 minutes) [54], which was indicative of insertion completion, the buffered electrolyte in the grounded reservoir was exchanged to remove the unincorporated lysenin. When required by the experiments, the insertion of only few lysenin channels was achieved by the same exchange procedure performed immediately after insertion was observed. The integrity of the inserted channels and their correct functionality was assessed by analyzing the response to positive and negative voltage stimuli [54]. The macroscopic conductance of a population of inserted channels in response to addition of adenosine phosphates was estimated from the slopes of the linear I-V curves recorded from 0 to -10 mV upon each addition [53], and the data was fitted to

the Hill equation [55, 56]. The changes in the voltage-gating profile induced by the addition of adenosine phosphates was assessed from the I-V curves recorded in response to voltage ramps ranging from -60 to 60 mV, at a rate of 0.2 mV/s [54]. The experimental open probability was fitted with the Boltzmann equation using a two-state gating model [41]. All experimental data have been analyzed by using pClamp 10.2, Origin 8.5.1 (OriginLab), and Matlab (MathWorks) software packages.

Results

ATP Reversibly Reduces the Macroscopic Conductance of Lysenin Channels Via a Non-gating Mechanism

Our first experiment aimed at demonstrating that ATP interacts with lysenin channels and alters their macroscopic conductance. After completing the insertion of lysenin channels into a planar BLM biased by -60 mV and achieving a steady state current of ~ -1.7 nA, ATP was carefully added to the reservoir on the ground side of the membrane under continuous stirring. Each addition increased the ATP concentration by 1 mM and produced a sudden decrease of the open current amplitude, indicative of concentration-dependent changes in the macroscopic conductance (Fig. 1). Similar inhibition of the ionic current has been observed when ATP was added to the headstage reservoir (Supplemental Fig. 2), pointing out ATP's ability to modulate the macroscopic conductance irrespective of the addition side. However, to mimic the presence of purines in the extracellular environment, we added the adenosine phosphates only to the ground side of the membrane.

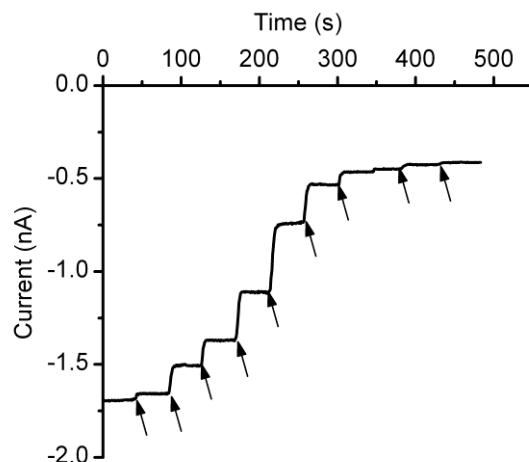


Fig. 1 ATP inhibits the macroscopic currents through lysenin channels inserted into planar BLMs. Addition of ATP to the electrolyte solutions bathing the lysenin channels yielded a significant decrease of the ionic currents in a concentration-dependent manner. The experiment was recorded at -60 mV transmembrane potential at a sampling rate of 1s, with a 1 kHz hardware filter and a 0.1 kHz software filter. Each ATP addition (indicated by *arrows*) increased the ATP concentration into the bulk by 1 mM.

The observed decrease in current may be explained by several mechanisms triggered by ATP interaction with lysenin channels, such as pore destabilization, binding and ligand-induced gating, or binding and occlusion. The interaction between lysenin and ATP may destabilize, reversibly or irreversibly, the oligomeric arrangement of the monomers composing the channel, thereby eliciting a decrease in the total macroscopic conductance. Therefore, we investigated whether or not ATP removal from the bulk solution could reinstate the conductance properties. In an experiment consisting of adding ATP (20 mM final concentration) to the ground reservoir of the BLM containing a large population of inserted lysenin channels and biased by -60 mV, a sudden drop in the open current occurred in less than 10 s (Fig. 2). Complete buffer exchange of the solution into the ground reservoir with 10 mL fresh ATP-free electrolyte reinstated the macroscopic conductance of the lysenin channels. We concluded that, irrespective of the origin of

interactions between ATP and lysenin channels, the process was reversible. The recovery in macroscopic conductance after buffer exchange suggests that the proteins were not removed from the membrane into the bulk as a result of interaction with ATP. A mechanism implying removal of channels from the membrane by ATP addition, followed by their free diffusion back into the support membrane and pore re-formation, is not supported by the fast recovery observed immediately after starting the buffer exchange procedure. Consequently, the hypothesis of an inhibition mechanism relying on strong pore destabilization after interaction with ATP was not confirmed by our experiments.

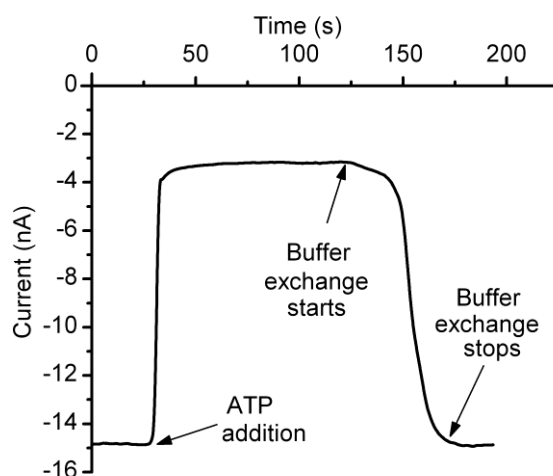


Fig. 2 Changes in macroscopic conductance induced by ATP addition are reversible. Addition of 20 mM ATP to the ground reservoir decreased the ionic current by ~80 %. Buffer exchange quickly reinstated the macroscopic conductance and demonstrated reversibility.

The next mechanism of conductance inhibition considered in our studies was ligand-induced gating. Lysenin channels have been shown to reversibly gate in a voltage-independent manner by specifically interacting with multivalent metal and organic cations [52, 53]. This ligand-induced gating is identified in single-channel experiments as sudden single-step variations of the ionic current, indicative of fast conformational

changes in response to multivalent cations [52, 53]. We therefore asked whether or not highly charged anions such as ATP might trigger a similar gating mechanism after interacting with lysenin channels. To test this, we inserted only two lysenin channels into the planar BLM by adding minute amounts of monomer (~0.3 pM final concentration) to the ground reservoir. Each of the two inserted channels indicated an open current of ~28 pA/channel at -60 mV bias potential (Fig. 3). Fast buffer exchange of the monomer-containing solution with lysenin-free electrolyte prevented further insertion. Following addition of ATP (6 mM final concentration) to the ground reservoir, fast sampling-rate recording (10 ms/sample) indicated a decrease of the open current by ~60 % in less than 20 s (Fig. 3). Unlike what has been observed for multivalent cations, i.e., gating indicated by a fast step-wise decrease of the ionic current [52, 53], ATP addition yielded a slow and monotonic variation. This suggests that ligand-induced gating is not the mechanism responsible for the observed conductance inhibition.

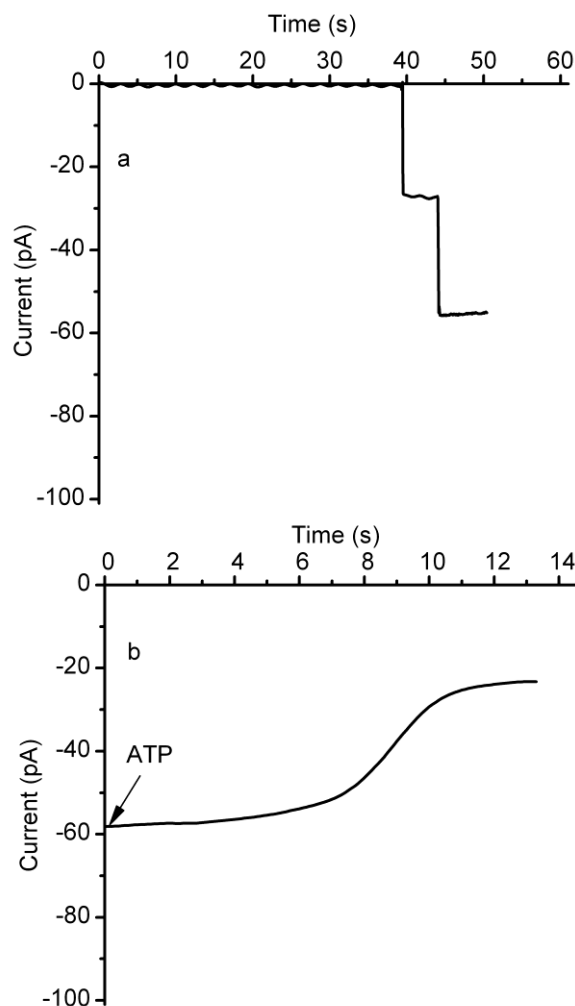


Fig. 3 The mechanism of ATP-induced conductance inhibition does not imply ligand-induced gating. a The insertion of two lysenin channels in the BLM was observed from the unitary step-wise variation of the open current produced upon each insertion. b ATP addition to the ground reservoir yielded a slow and monotonic decrease of the ionic current by ~60 %. The absence of transient changes in the open current upon ATP addition suggests that gating is not a valid mechanism for explaining ATP's inhibitory action.

ATP, ADP, and AMP Inhibit the Macroscopic Conductance of Lysin Channels In a Charge-dependent Manner by Partially Occluding the Conducting Pathway upon Cooperative Binding

ATP is a relatively voluminous molecule, with a hydrodynamic radius of ~0.55 nm [57]; therefore, its binding to the open channel may partially interrupt the current

flow. The inhibition presented by ATP, the observed reversibility, and the absence of gating support the hypothesis of an electrostatic interaction between lysenin and ATP; upon binding, ATP partially occludes the conducting pathway owing to its relatively large size. If this mechanism is correct, one may assume that other adenosine phosphates carrying less charge (e.g., ADP and AMP) may present similar yet weaker inhibitory effects. Therefore, our experiments aimed to identify the influence of the anion charge on the conducting properties by employing macroscopic conductance measurements on lysenin channels exposed to various amounts of ATP, ADP, and AMP (Fig. 4). Each conductance was estimated from the average slope of six I-V curves, recorded in response to linear voltage ramps ranging from 0 to -10 mV after inhibitor addition in three independent experiments. For ease of comparing the changes in conductance in experiments comprising different number of channels, Fig. 4 depicts the relative conductance $G_r = G/G_0$, where G_0 is the conductance measured in the absence of inhibitor, and G is the conductance measured after each inhibitor addition. The common feature identified upon closer inspection of the experimental results is that each of the inhibitors decreased the macroscopic conductance in a concentration-dependent manner, and the approach of saturation was observed irrespective of the inhibitor's chemical identity. The inhibition curves indicated that ATP was the most effective inhibitor, decreasing the conductance more than 50 % at saturation concentrations (> 15 mM). However, ADP showed a maximal decrease in conductance similar to ATP, but with a somewhat less steep inhibition curve, and a saturation concentration greater than 30 mM. Among the three inhibitors, AMP was the least potent and decreased the conductance by only ~20 %, while requiring a saturation concentration greater than 60 mM. The observed

dependency of the inhibitory effects on the anion charge supports the hypothesis that electrostatic interactions are responsible for the observed decreased in conductance, which may result from binding and partial occlusion of the channel conducting pathway.

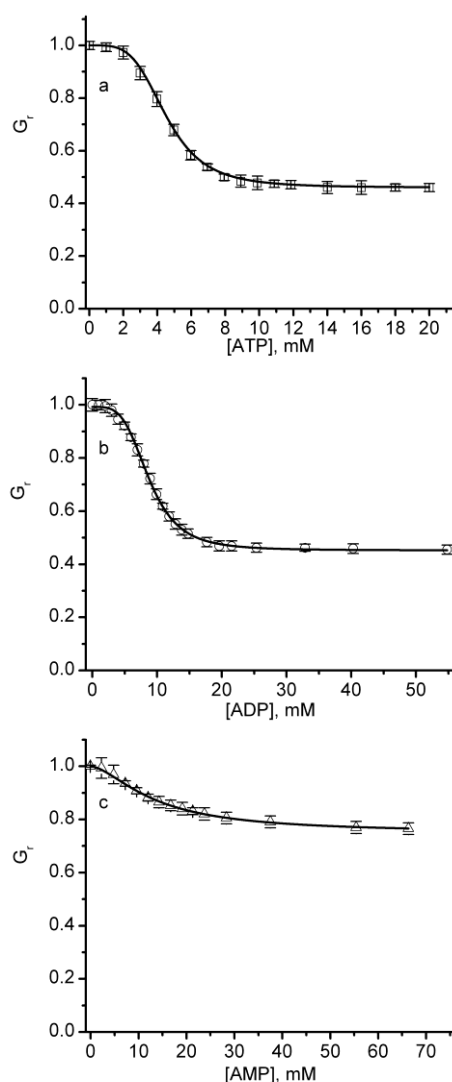


Fig. 4 Changes in relative conductance induced by the addition of ATP, ADP, or AMP. The relative macroscopic conductance G_r indicates that ATP (a) and ADP (b) were more efficient inhibitors compared to AMP (c). The relative conductance values represented by *symbols* in the plots are reported as mean \pm SD from three independent experiments. The conductance data, fitted to the Hill equation (*full line*), yielded the following parameters: (i) ATP: $IC_{50} = 4.53 \pm 0.07$ mM, and $n = 4.15 \pm 0.2$, (ii) ADP: $IC_{50} = 8.92 \pm 0.07$ mM, and $n = 3.43 \pm 0.16$, and (iii) AMP: $IC_{50} = 13.43 \pm 0.08$ mM and $n = 1.62 \pm 0.17$.

Next, we attempted to quantify the inhibitory potency of the adenosine phosphates based on a pertinent model of interaction. If lysenin channels present one or more independent binding sites, the inhibition curve may be hyperbolic in shape. However, each inhibition curve in Fig. 4 exhibits a sigmoidal response, suggesting not only the existence of multiple binding sites, but also cooperativity between binding events. Therefore, we adapted the Hill equation to describe the changes in the relative conductance G_r induced by inhibitors [55, 56]:

$$G_r = 1 - (1 - G_{min}) \frac{[x]^n}{[IC_{50}]^n + [x]^n} \quad (1)$$

where G_{min} is the relative current measured at saturation (i.e., full occupancy of the binding sites), IC_{50} is the inhibitor concentration for which the relative conductance is half-way between G_{min} and G_{max} (which is the maximal relative conductance measured in the absence of inhibitor), $[x]$ is the inhibitor concentration, and n is the Hill (cooperativity) coefficient. The direct fit of the experimental data to the Hill equation (Fig. 4) provided the following values: (i) ATP: $IC_{50} = 4.53 \pm 0.07$ mM, and $n = 4.15 \pm 0.2$; (ii) ADP: $IC_{50} = 8.92 \pm 0.07$ mM, and $n = 3.43 \pm 0.16$; and (iii) AMP: $IC_{50} = 13.43 \pm 0.08$ mM, and $n = 1.62 \pm 0.17$. Both parameters, i.e. IC_{50} and n , varied with the chemical identity of the inhibitor. IC_{50} increased (indicative of a lower binding affinity) and n decreased as the net charge of the inhibitor decreased. Among the three inhibitors, AMP demonstrated a much smaller binding affinity and a reduced cooperativity compared to the other two.

Ionic Screening Reduces ATP's Inhibition Efficiency

Electrostatic interactions between charged molecules may be significantly affected by ionic screening, which depends on the ionic strength of the bulk solutions [58]. Consequently, the electrostatic binding that leads to conductance inhibition may be adjusted by introducing additional monovalent ions into the electrolyte solutions. We chose monovalent ions because they do not interfere with the conducting properties of lysenin channels at negative transmembrane voltages [53]. We estimated the inhibitory effect of ATP by measuring the relative macroscopic conductance G_r of lysenin channels exposed to electrolyte solutions containing 50, 135, and 500 mM KCl. The inhibition plots shown in Fig. 5 clearly indicate that the higher ionic strength limited the reduction in conductance, and thus diminished the inhibition efficiency associated with ATP. At 10 mM added ATP, the ionic conductance decreased by ~72 % for 50 mM KCl, and by ~52 % for 135 mM KCl; but for the 500 mM KCl, only a modest decrease of ~12 % was recorded. The Hill analysis revealed that screening significantly modulated the ATP influence on conductance by affecting the binding affinity, as inferred from the changes to the IC_{50} . As expected, the lowest ionic concentration (50 mM KCl) elicited the lowest screening efficacy, promoted binding, and yielded the lowest IC_{50} (3.83 ± 0.05 mM). At 135 mM KCl, the IC_{50} increased to 4.36 ± 0.07 mM, indicative of more efficient screening and weaker interactions. This trend was maintained at 500 mM KCl, for which

the estimated IC_{50} was the highest (6.94 ± 0.07 mM), which correlates to the highest ionic strength and maximal screening. However, irrespective of the ionic strength, all Hill coefficient values determined from the fit (Fig. 5) were around 4.2, indicating that the cooperativity factor underwent negligible changes owing to screening. Since the anion charge alone yielded greater changes of the Hill coefficient (as shown in Fig. 2), not only charge but also other parameters related to the molecular identity and structure may be relevant for explaining the observed differences in the binding affinity of the inhibitors; we will expand upon this in the Discussion section.

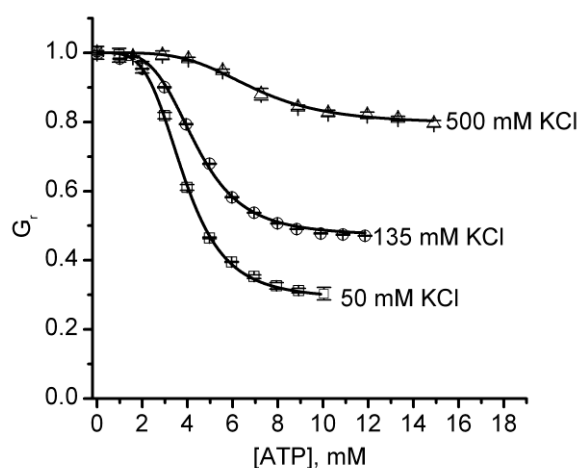


Fig. 5 Ionic screening reduces ATP inhibitory effects. The relative conductance indicates that ionic screening elicited by the addition of KCl affected the conductance changes induced by ATP addition. The lowest KCl concentration (50 mM) promoted electrostatic interactions, increased binding, and enhanced the ATP-induced inhibition. Increased KCl concentrations (135 mM and 500 mM, respectively) diminished the ATP-induced inhibition by weakening the electrostatic interactions and the binding affinity. The experimental conductance data (*symbols*) are presented as mean \pm SD from six traces recorded for each of the experiments. The average conductance data fitted to the Hill equation (*full lines*) yielded the next parameters: (i) 50 mM KCl: $IC_{50} = 3.83 \pm 0.05$ mM, $n = 4.11 \pm 0.16$; (ii) 135mM

KCl: $IC_{50} = 4.36 \pm 0.07$ mM, $n = 4.14 \pm 0.2$; and (iii) 500 mM KCl: $IC_{50} = 6.94 \pm 0.07$ mM, $n = 4.1 \pm 0.14$.

ATP and AMP Affect the Voltage-induced Gating

Lysenin channels exhibit asymmetrical voltage-induced gating at transmembrane voltages within physiological range [42, 43, 54]. Although this is an ubiquitous feature of voltage-gated ion channels [59], it is not common among PFTs. The gating mechanism is not known, but previous studies suggest that specific interactions between a charged voltage sensor domain and external electric fields may be responsible for conformational changes that lead the channels to adopt either an open or closed configuration [41, 54]. Within this two-state model, the open probability of the channels is well described by a Boltzmann distribution, which accounts for changes in free energy originating in electrostatic interactions [41, 53]. Therefore, we supposed that the binding of highly charged anions within the channel's structure can adjust the electrostatic interactions with external electric fields and consequently affect the voltage-induced gating. To demonstrate this assumption, we studied the influence of ATP and AMP (the most and the least efficient inhibitor, respectively) on the gating of lysenin channels inserted into planar membranes exposed to 50 mM KCl electrolyte solutions by analyzing the I-V curves in the range -60 to 60 mV (Fig. 6).

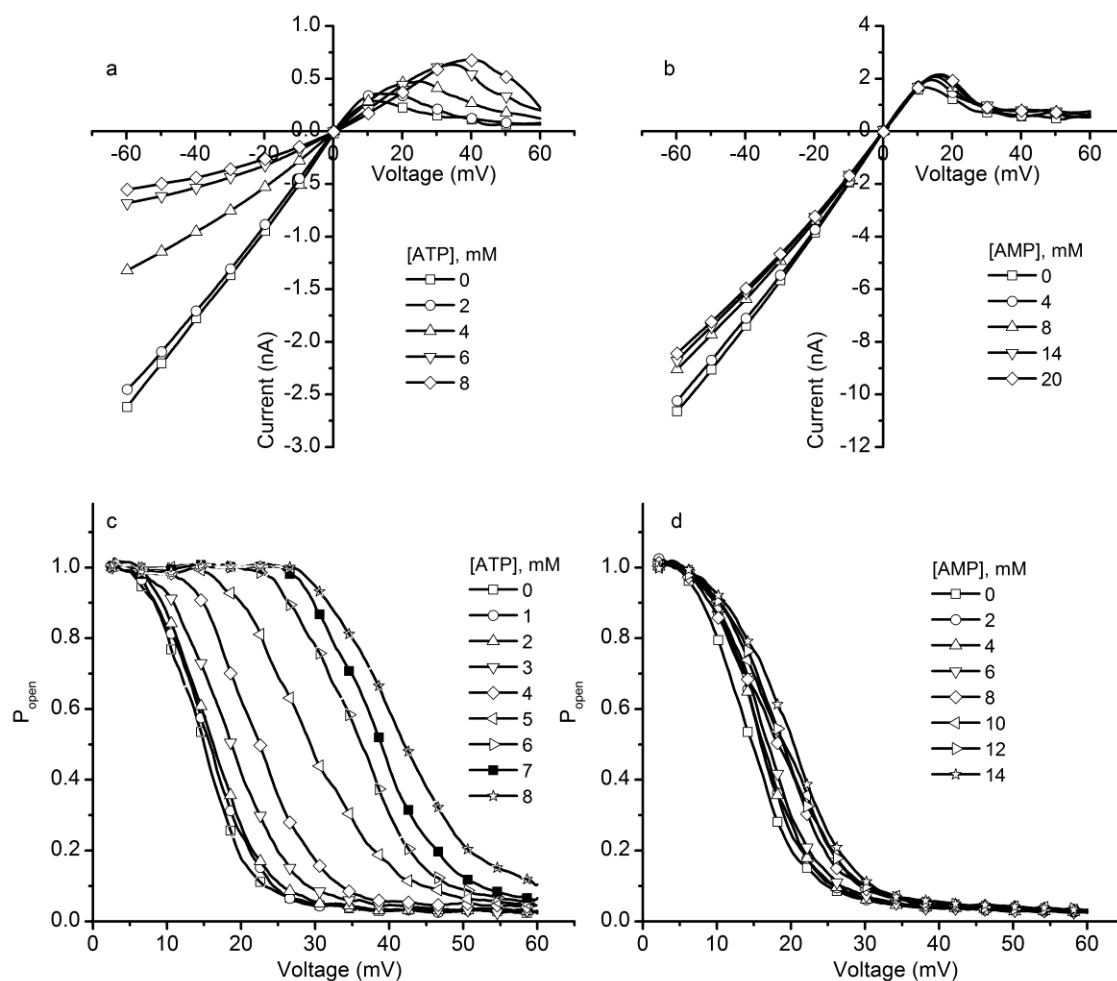


Fig. 6 ATP and AMP alter the voltage-induced gating of lysenin in a concentration-dependent manner, simultaneous with conductance inhibition. ATP addition induced a rightward shift of the voltage-induced gating, which was observed in the I-V (a) and P_{open} (c) plots. The changes induced by AMP (b I-V curves, and d P_{open}) were minimal. All data points are experimental values, with the *symbols* added solely to aid in discriminating between different experimental conditions.

In the absence of inhibitors, lysenin channels have shown the well-known response to transmembrane voltages [54], and adopted the open state at negative voltages, as indicated by the linear I-V characteristic. This ohmic behavior was preserved in the positive voltage range, up to ~ 10 mV. As the membrane depolarization advanced, lysenin channels underwent voltage-induced gating, and their closing was indicated by a significant reduction in the ionic current [54] (Fig. 6). The addition of inhibitors affected

how lysenin channels responded to transmembrane voltages, and the chemical identity of the inhibitors strongly influenced the changes. ATP addition significantly right-shifted the voltage required to achieve gating in a concentration-dependent manner (Fig. 6a). In contrast, AMP addition resulted in only a modest influence on the voltage-induced gating, and elicited only minor changes in the I-V plots in the positive voltage range (Fig. 6b). These changes were similarly reflected in the open probability plots (Fig. 6c, d), calculated for the positive voltage range by assuming a Boltzmann distribution of open states [54]. Linear fits of the I-V curves in the low positive voltage range (when all of the channels were in the open state [54]) were used to determine a theoretical maximum current I_{\max} for each voltage in the absence of channel gating, and the probability of finding a channel in the open state (P_{open}) was determined from [54, 59, 60]:

$$P_{open} = \frac{I}{I_{\max}} \quad (2)$$

where I represents the actual measured current at each voltage in the I-V curve.

The rightward shift of the open probability presented by ATP (Fig. 6c) is strong evidence of purinergic influence on channel gating; i.e., binding affects the interactions of the voltage-domain sensor with the external electric field. AMP addition yielded less significant changes in the open probability profile (Fig. 6d), which was expected since the I-V curves indicated only small changes in the voltage-induced gating in similar conditions.

We observed that besides the modulation of voltage-induced gating at positive voltages, addition of ATP and AMP affected the quasi-linear response observed in the absence of inhibitors in the negative voltage range (Fig. 6a, b). Nonetheless, the I-V characteristics maintained linearity between 0 and -10 mV in the presence of inhibitor,

while non-linearity was enhanced by membrane hyperpolarization. This observation explains why the decrease in the ionic currents measured upon ATP addition at -60 mV (see Figs. 1 and 2), was larger than the decrease in conductance estimated at saturation in otherwise similar conditions from I-V curves recorded in the range of 0 to -10 mV (as shown in Figs. 3 and 4). For this small negative voltage range, the I-V characteristics maintained linearity, and the ionic currents were not influenced by the supplementary voltage-dependent inhibition manifested at -60 mV.

dATP Inhibits the Macroscopic Conductance of Lysenin Channels

Studies presented by Hattori and Goaux on ATP binding and channel activation in P2X receptors [19] reveal structural details of the binding site, stressing the importance of hydrogen bonding in modulating the interactions between ATP and amino acids lining the binding pocket. Our experiments on lysenin included adenosine derivatives for which the number of phosphate groups varied, thus neglecting interactions presented by the base or the sugar. Therefore, we further asked whether or not changes in the chemical identity of the sugar influence the inhibitory action of the purines. In this line of inquiry, we performed an inhibition experiment by adding dATP (1 mM final concentration) to the ground side of a membrane containing lysenin channels bathed by 135 mM KCl, buffered with 20 mM HEPES and biased by -60 mV. In the presence of dATP, the macroscopic conductance of lysenin channels decreased by a significant ~75% (Fig. 7). None of the other adenosine phosphates used in our experiments demonstrated such great inhibition potency in similar experimental conditions; their inhibition efficiency at 1 mM concentration was barely observable. However, in spite of an increased inhibitory potency, the interaction with dATP was much slower than what was observed for its

counterparts. Under continuous mixing conditions, the macroscopic currents reached steady-state in a matter of seconds following ATP addition (as shown in Fig. 1, 2, and 3), while dATP addition required several hours for equilibration (Fig. 7). Furthermore, our experiments indicated a monotonic and smooth decrease of the open currents through single lysenin channels following ATP addition even at high temporal resolution (Fig. 3). In contrast, addition of dATP yielded multiple discrete changes of the open current, suggesting that lysenin channels may undergo gating at negative voltages in the presence of dATP.

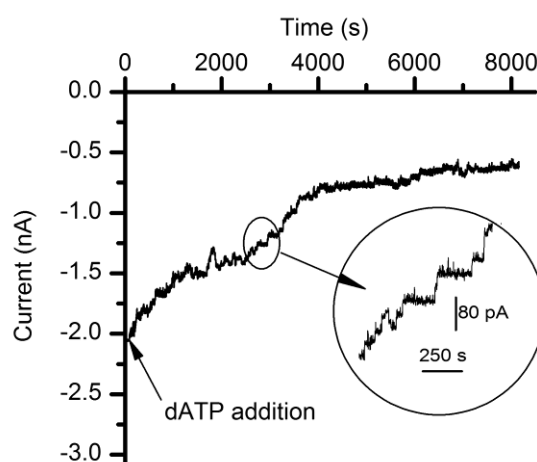


Fig. 7 dATP inhibits the macroscopic currents through lysenin channels inserted into planar BLMs. Addition of 1 mM dATP to the electrolyte solutions bathing the lysenin channels yielded a significant yet slow decrease of the ionic currents. The *inset* shows step-wise variations of the open current, suggesting a possible gating mechanism. The experiment was recorded at -60 mV transmembrane potential at a sampling rate of 1s, with a 1 kHz hardware filter and a 0.1 kHz software filter.

Discussion

Intricate interactions between lysenin channels and adenosine phosphates were manifested as changes of both macroscopic conductance and voltage-induced gating. The experimental evidence presented by our work suggests a mechanism of interaction driven primarily by electrostatic attraction between inhibitors and positive charges, delineating

multiple binding sites within the channel's structure. Although multivalent cations interacting with lysenin channels induce conformational changes upon binding to negatively charged binding sites [53], an eventual gating mechanism triggered by the addition of large anions was not supported by our experimental data. The observed inhibition in conductance induced by ATP was quickly reversed by buffer exchange, which was indicative of the absence of permanent changes to the channel's structure induced by the interactions. The existence of multiple binding sites within a channel's structure was suggested by the excellent fit of the inhibition curves with the Hill equation, accounting for positive cooperativity. The IC_{50} 's estimated for ATP, ADP, and AMP from the Hill fit correlated the binding affinities to the net charge of the inhibitors. ATP showed the most prominent influence on the macroscopic conductance, while AMP had a much lower influence on both the conductance and voltage-induced gating, which may be explained in part by its smaller charge. The hypothesis of electrostatic interactions was further sustained by the analysis of lysenin response to ATP with varying ionic strength of the electrolyte solutions bathing the channels by the addition of monovalent salts. The addition of KCl promoted screening and weakened the electrostatic interactions; consequently, screening diminished the ATP inhibition potency, as indicated by the significant increase of the IC_{50} upon salt addition. However, the increased ionic strength did not affect the cooperativity coefficient, which maintained a value of ~ 4.2 irrespective of the ionic strength. The inhibition curves recorded for ATP, ADP, and AMP in identical salt conditions clearly indicated different values of the cooperativity coefficients and the IC_{50} s, which we initially assumed to reflect solely the different net charge of the inhibitors. However, besides charge, the size of the inhibitors may vary

with the additional phosphate groups. Given the large size of adenosine, the relative size variation with the number of phosphate groups may be considered less significant.

Therefore, the ionic current decrease would be expected to be similar upon individual binding of either of the charged phosphates. As depicted in Fig. 4, ATP and ADP yielded similar decrease in conductance at saturation, but ADP showed a slightly lower binding affinity. In contrast, AMP showed a much lower binding affinity and elicited only a modest decrease in conductance at saturation. This apparent inconsistency may be explained by considering eventual changes in the inhibitor's shape induced by polyphosphate binding to specific sites, which was irrefutably demonstrated for P2X ionotropic receptors [19]. Inspection of the electronic density maps derived from Δ P2X4-C-ATP co-crystals reveal a unique binding motif favoring extensive hydrophilic interactions with β -phosphates and γ -phosphates of the U-shaped ATP molecule [19, 50]. Therefore, besides the inhibitor's charge, its ability to fold may also play an essential role in determining the binding affinity and cooperativity. This observation may explain why AMP, which has limited folding capabilities [19] presented such distinct behavior in terms of inhibition efficiency when compared to either ATP or ADP.

The inhibitory effect presented by dATP adds another layer of intricacy to the interactions between adenosine phosphates and lysenin channels. Structurally, ATP and dATP are similar and the net charge distribution generated by the phosphate groups at identical pH is expected to be the same. The major structural difference between the two molecules is the presence of a hydroxyl group at the 2' carbon position of the ribose, which presents potential for supplementary hydrogen bonding. If this extra hydrogen bonding is part of the interaction mechanism, one would expect a stronger interaction

between lysenin and ATP and therefore a stronger inhibitory effect. However, our results indicated a greater yet slower inhibition presented by dATP. To reconcile this apparent discrepancy, a closer inspection of the evolution of the macroscopic currents following dATP addition may offer a plausible answer. In the presence of dATP, the changes of the ionic current were more discrete, and the step-wise variation suggested gating as part of the inhibitory mechanism. Although many of the sudden changes in current were much larger than what would be expected from the gating of a single channel, it is possible for multiple channels to undergo gating within the large sampling time interval used for data recording (1 s). The greater inhibitory efficiency observed for dATP could be due to a concerted mechanism implying both occlusion and gating, without implying an interaction with the binding site that is stronger than ATP. However, the lack of structural details of the lysenin oligomeric pore prevents any clear elucidation of the potential role of hydrogen bonding in modulating the purine's binding ability and the channel's conductance.

In addition to macroscopic conductance, the voltage-induced gating was affected by addition of inhibitors in a charge- and concentration-dependent manner. AMP induced insignificant changes in the voltage-gating profile. In contrast, ATP showed a more prominent influence on the voltage response, which may be explained by its increased charge and improved folding capability. The changes in the voltage gating profile suggest an altered kinetics and/or equilibrium of the conformational transitions. Our analysis tacitly assumed that the open probability was estimated from open currents measured at equilibrium, and it is well-known that lysenin channels respond slowly to changes in the transmembrane voltage [54]. In the absence of adenosine phosphates from bulk, the low

voltage rate (0.2 mV/s) used to plot the I-V curves and to estimate the open probabilities suffices for approximating each experimental point as descriptive of a truly steady state [54]. However, this assumption may not be true for the experiments comprising ATP addition, which may change the kinetics and increase the time required for the channels to adjust their conformation in response to changes of the transmembrane voltage. Whatever the case, the experimental results indicate alterations of channel functionality induced by ATP addition.

Our studies support the concept of purinergic control over the biological activity of exogenous transmembrane transporters. Adenosine phosphates interfered with the functionality of lysenin channels and promoted changes in their macroscopic conductance and voltage-induced gating. The use of lysenin channels inserted into artificial membrane systems begs fundamental questions regarding the potential physiological relevance of the findings. Answering those questions is not a trivial task since the physiological role of lysenin itself in its native environment is still obscure. As a matter of fact, lysenin is not even a transmembrane protein in *E. fetida*. Nonetheless, potential physiological clues may be inferred from the well documented biological activity of lysenin channels inserted into natural or artificial membranes. Lysenin acts as a PFT when interacting with membranes containing SM and presents strong cytolytic and hemolytic activity. This fundamental physiological aspect is common to other PFTs presenting high structural similarities to lysenin [61]. Our experiments comprised inhibitor addition to the ground side of the membranes, which mimics the extracellular environment. The *in vivo* concentration of extracellular ATP is much smaller than what has been used in our work to induce observable changes in the transport properties of lysenin channels [57, 62].

However, we observed a similar decrease of the ionic currents when ATP was added to the headstage side (Supplemental Fig. 2). Since lysenin resembles a cytolytic toxin, and the average amount of intracellular ATP is within the range for which sustained conductance inhibition was observed in our experiments [57, 62], we conclude that intracellular ATP could play a protective role of limiting the lytic activity of toxins. While the inhibitory effect of dATP was even more pronounced than the one of ATP, this potency may not translate into a protective role since the intracellular or extracellular dATP concentration is usually in the μM range [63]. In addition to the lytic activity, lysenin shares fundamental features of ion channels, such as voltage-induced gating. The binding of adenosine phosphates to the lysenin channel tampered with the electrostatic interactions responsible for gating. Such alterations in functionality could prove pivotal for understanding the molecular mechanisms determining the biological activity of ion channels *in vivo*. While a limited number of ion channels present specific receptors for purines within their structure, many others may present charged domains acting as non-specific binding sites for adenosine phosphates. Changes in local distribution of the electric field induced by electrostatic binding of purines or pyrimidines may modulate the response of ion channels to electric or chemical stimuli, thereby affecting their biological activity. In this respect, current work is underway to broaden the pharmacological perspective of our findings by considering metabolically stable analogs and polyphosphates acting as ecto-nucleosidases capable of controlling the flow of ions and molecules through cell membranes.

Acknowledgments

Research reported in this publication was partially supported by the National Science Foundation under Award Number 1554166, the National Institute of General Medical Sciences of the National Institutes of Health under Award Number P20GM109095, Sigma Xi Grants-in-Aid of Research G20141015697430, and the National Aeronautics and Space Administration under Grant Number NNX15AU64H. The content is solely the responsibility of the authors and does not necessarily represent the official views of the granting agencies.

Conflict of Interest: The authors declare that they have no conflict of interest.

References

1. Burnstock G (2007) Purine and pyrimidine receptors. *Cell Mol Life Sci* 64 (12):1471-1483
2. Burnstock G (2011) Introductory overview of purinergic signalling. *Front Biosci* 3:896-900
3. Burnstock G, Verkhratsky A (2009) Evolutionary origins of the purinergic signalling system. *Acta Physiol* 195 (4):415-447
4. Chatterjee C, Sparks DL (2014) P2X receptors regulate adenosine diphosphate release from hepatic cells. *Purinerg Signal* 10:587-593
5. Burnstock G (2015) An introduction to the roles of purinergic signalling in neurodegeneration, neuroprotection and neuroregeneration. *Neuropharmacology*. doi:10.1016/j.neuropharm.2015.05.031
6. Menendez-Mendez A, Diaz-Hernandez JI, Miras-Portugal MT (2015) The vesicular nucleotide transporter (VNUT) is involved in the extracellular ATP effect on neuronal differentiation. *Purinerg Signal* 11 (2):239-249

7. Rampon C, Gauron C, Meda F, Volovitch M, Vríz S (2014) Adenosine enhances progenitor cell recruitment and nerve growth via its A₂B receptor during adult fin regeneration. *Purinerg Signal* 10 (4):595-602
8. Shatarat A, Dunn WR, Ralevic V (2014) Raised tone reveals ATP as a sympathetic neurotransmitter in the porcine mesenteric arterial bed. *Purinerg Signal* 10 (4):639-649
9. Burnstock G (2006) Pathophysiology and therapeutic potential of purinergic signaling. *Pharmacol Rev* 58 (1):58-86
10. Burnstock G (2015) Blood cells: an historical account of the roles of purinergic signalling. *Purinerg Signal* 11(4):411-434
11. Hofer M, Pospisil M, Dusek L, Hoferova Z, Komurkova D (2014) Lack of adenosine A₃ receptors causes defects in mouse peripheral blood parameters. *Purinerg Signal* 10 (3):509-514
12. Burnstock G (1972) Purinergic nerves. *Pharmacol Rev* 24:509-581
13. Burnstock G, G. C, D. S, A. S (1970) Evidence that adenosine triphosphate or a related nucleotide is the transmitter substance released by non-adrenergic inhibitory nerves in the gut. *Brazilian Journal of Pharmacology* 40:668-688
14. Burnstock G (2009) Purinergic signalling: past, present and future. *Braz J Med Biol Res* 42:3-8
15. Burnstock G (2012) Purinergic signalling: its unpopular beginning, its acceptance and its exciting future. *Bioessays* 34:218-225
16. Adinolfi E (2013) New intriguing roles of ATP and its receptors in promoting tumor metastasis. *Purinerg Signal* 9 (4):487-490
17. Beall C, Watterson KR, McCrimmon RJ, Ashford ML (2013) AMPK modulates glucose-sensing in insulin-secreting cells by altered phosphotransfer to K_{ATP} channels. *J Bioenerg Biomembr* 45 (3):229-241
18. Haanes KA, Kowal JM, Arpino G, Lange SC, Moriyama Y, Pedersen PA, Novak I (2014) Role of vesicular nucleotide transporter VNUT (SLC17A9) in release of

- ATP from AR42J cells and mouse pancreatic acinar cells. *Purinerg Signal* 10 (3):431-440
19. Hattori M, Gouaux E (2012) Molecular mechanism of ATP binding and ion channel activation in P2X receptors. *Nature* 485 (7397):207-212
 20. Housley GD, Morton-Jones R, Vlajkovic SM, Telang RS, Paramanathasivam V, Tadros SF, Wong AC, Froud KE, Cederholm JM, Sivakumaran Y, Snguanwongchai P, Khakh BS, Cockayne DA, Thorne PR, Ryan AF (2013) ATP-gated ion channels mediate adaptation to elevated sound levels. *P Natl Acad Sci USA* 110 (18):7494-7499
 21. Morrow GB, Nicholas RA, Kennedy C (2014) UTP is not a biased agonist at human P2Y₁₁ receptors. *Purinerg Signal* 10 (4):581-585
 22. Skals M, Bjaelde RG, Reinholdt J, Poulsen K, Vad BS, Otzen DE, Leipziger J, Praetorius HA (2014) Bacterial RTX toxins allow acute ATP release from human erythrocytes directly through the toxin pore. *J Biol Chem* 289 (27):19098-19109
 23. Takai E, Tsukimoto M, Harada H, Kojima S (2014) Autocrine signaling via release of ATP and activation of P2X₇ receptor influences motile activity of human lung cancer cells. *Purinerg Signal* 10 (3):487-497
 24. Vial C, Roberts JA, Evans RJ (2004) Molecular properties of ATP-gated P2X receptor ion channels. *Trends in Pharmacological Sciences* 25 (9):487-493
 25. Feng JF, Gao XF, Pu YY, Burnstock G, Xiang Z, He C (2015) P2X₇ receptors and Fyn kinase mediate ATP-induced oligodendrocyte progenitor cell migration. *Purinerg Signal* 11 (3):361-369
 26. Skals M, Jorgensen NR, Leipziger J, Praetorius HA (2009) α -Hemolysin from *Escherichia coli* uses endogenous amplification through P2X receptor activation to induce hemolysis. *P Natl Acad Sci USA* 106 (10):4030-4035
 27. Skals M, Leipziger J, Praetorius HA (2011) Haemolysis induced by α -toxin from *Staphylococcus aureus* requires P2X receptor activation. *Pflug Arch Eur J Phy* 462 (5):669-679

28. Stelmashenko O, Compan V, Browne LE, North RA (2014) Ectodomain movements of an ATP-gated ion channel (P2X2 receptor) probed by disulfide locking. *J Biol Chem* 289 (14):9909-9917
29. Hwang TC, Kirk KL (2013) The CFTR ion channel: gating, regulation, and anion permeation. *Cold Spring Harbor Perspectives in Medicine* 3 (1):a009498. doi: 10.1101/cshperspect.a009498
30. Quinton PM, Reddy MM (1992) Control of CFTR chloride conductance by ATP levels through non-hydrolytic binding. *Nature* 360 (6399):79-81
31. Rorsman P, Ramracheya R, Rorsman NJ, Zhang Q (2014) ATP-regulated potassium channels and voltage-gated calcium channels in pancreatic alpha and beta cells: similar functions but reciprocal effects on secretion. *Diabetologia* 57 (9):1749-1761
32. Larsen CK, Skals M, Wang T, Cheema MU, Leipziger J, Praetorius HA (2011) Python erythrocytes are resistant to α -hemolysin from *Escherichia coli*. *J Membrane Biol* 244 (3):131-140
33. Masin J, Fiser R, Linhartova I, Osicka R, Bumba L, Hewlett EL, Benz R, Sebo P (2013) Differences in purinergic amplification of osmotic cell lysis by the pore-forming RTX toxins *Bordetella pertussis* CyaA and *Actinobacillus pleuropneumoniae* ApxIA: the role of pore size. *Infect Immun* 81 (12):4571-4582
34. Skals M, Jensen UB, Ousingsawat J, Kunzelmann K, Leipziger J, Praetorius HA (2010) *Escherichia coli* α -hemolysin triggers shrinkage of erythrocytes via $K_{Ca3.1}$ and TMEM16A channels with subsequent phosphatidylserine exposure. *J Biol Chem* 285 (20):15557-15565
35. Aroian R, Goot FGvd (2007) Pore forming toxins and cellular non-immune defences. *Curr Opin Microbiol* 10:57-61
36. Bashford CL (2001) Pore-forming toxins: attack and defence at the cell surface. *Cell Mol Biol Lett* 6 (2A):328-333
37. Gilbert RJ (2002) Pore-forming toxins. *Cell Mol Life Sci* 59:832-844

38. Gonzalez MR, Bischofberger M, Pernot L, van der Goot FG, Freche B (2008) Bacterial pore-forming toxins: The (w)hole story? *Cell Mol Life Sci* 65:493-507
39. Parker MW, Feil SC (2005) Pore-forming protein toxins: from structure to function. *Prog Biophys Mol Bio* 88:91-142
40. Reig N, van der Goot FG (2006) About lipids and toxins. *FEBS Lett* 580:5572-5579
41. Fologea D, Krueger E, Lee R, Naglak M, Mazur Y, Henry R, Salamo G (2010) Controlled gating of lysenin pores. *Biophys Chem* 146:25-29
42. Ide T, Aoki T, Takeuchi Y, Yanagida T (2006) Lysenin forms a voltage-dependent channel in artificial lipid bilayer membranes. *Biochem Bioph Res Co* 346:288-292
43. Kwiatkowska K, Hordejuk R, Szymczyk P, Kulma M, Abdel-Shakor A-B, Plucienniczak A, Dolowy K, Szewczyk A, Sobota A (2007) Lysenin-His, a sphingomyelin-recognizing toxin, requires tryptophan 20 for cation-selective channel assembly but not for membrane binding. *Mol Membr Biol* 24 (2):121-134
44. Shakor A-BA, Czurylo EA, Sobota A (2003) Lysenin, a unique sphingomyelin-binding protein. *FEBS Lett* 542:1-6
45. Yamaji-Hasegawa A, Makino A, Baba T, Senoh Y, Kimura-Suda H, Sato S, Terada N, Ohno S, Kiyokawa E, Umeda M, Kobayashi T (2003) Oligomerization and pore formation of a sphingomyelin-specific toxin, lysenin. *J Biol Chem* 278 (25):22762-22770
46. Bruhn H, Winkelmann J, Andersen C, Andra J, Leippe M (2006) Dissection of the mechanisms of cytolytic and antibacterial activity of lysenin, a defence protein of the annelid *Eisenia fetida*. *Dev Comp Immunol* 30:597-606
47. Fologea D, Krueger E, Rossland S, Bryant S, Foss W, Clark T (2013) Cationic polymers inhibit the conductance of lysenin channels. *The Scientific World Journal* 2013, Article ID 316758. doi: 10.1155/2013/316758

48. Krueger E, Al Faouri R, Fologea D, Henry R, Straub D, Salamo G (2013) A model for the hysteresis observed in gating of lysenin channels. *Biophys Chem* 184:126-130
49. De Colibus L, Sonnen AFP, Morris KJ, Siebert AC, Abrusci P, Plitzko J, Hodnik V, Leippe M, Volpi E, Anderluh G, Gilbert RJC (2012) Structures of lysenin reveal a shared evolutionary origin for pore-forming proteins and its mode of sphingomyelin recognition. *Structure* 20:1498-1507
50. Chataigneau T, Lemoine D, Grutter T (2013) Exploring the ATP-binding site of P2X receptors. *Frontiers in Cellular Neuroscience* 7 (Article 273). doi:10.3389/fncel.2013.00273
51. Ennion S, Hagan S, Evans RJ (2000) The role of positively charged amino acids in ATP recognition by human P2X₁ receptors. *J Biol Chem* 275 (38):29361-29367
52. Fologea D, Al Faori R, Krueger E, Mazur YI, Kern M, Williams M, Mortazavi A, Henry R, Salamo GJ (2011) Potential analytical applications of lysenin channels for detection of multivalent ions. *Anal Bioanal Chem* 401:1871-1879
53. Fologea D, Krueger E, Al Faori R, Lee R, Mazur YI, Henry R, Arnold M, Salamo GJ (2010) Multivalent ions control the transport through lysenin channels. *Biophys Chem* 152 (1-3):40-45
54. Fologea D, Krueger E, Mazur YI, Stith C, Okuyama Y, Henry R, Salamo GJ (2011) Bi-stability, hysteresis, and memory of voltage-gated lysenin channels. *BBA-Biomembranes* 1808:2933-2939
55. Lee BH, Zheng J (2015) Proton block of proton-activated TRPV1 current. *J Gen Physiol* 146 (2):147-159
56. Tantama M, Licht S (2008) Use of calculated cation- π binding energies to predict relative strengths of nicotinic acetylcholine receptor agonists. *ACS Chem Biol* 3 (11):693-702
57. Sabirov RZ, Okada Y (2004) Wide nanoscopic pore of maxi-anion channel suits its function as an ATP-conductive pathway. *Biophys J* 87 (3):1672-1685

58. Block BM, Stacey WC, Jones SW (1998) Surface charge and lanthanum block of calcium current in bullfrog sympathetic neurons. *Biophys J* 74:2278-2284
59. Bezanilla F (2005) Voltage-gated ion channels. *IEEE T Nanobiosci* 4 (1):34-48
60. Tao X, Lee A, Limapichat W, Dougherty DA, MacKinnon R (2010) A gating charge transfer center in voltage sensors. *Science* 328:67-73
61. Shogomori H, Kobayashi T (2008) Lysenin: A sphingomyelin specific pore-forming toxin. *BBA-Gen Subjects* 1780 (3):612-618
62. Schwiebert EM, Zsembery A (2003) Extracellular ATP as a signaling molecule for epithelial cells. *BBA-Biomembranes* 1615 (1-2):7-32
63. Traut TW (1994) Physiological concentrations of purines and pyrimidines. *Mol Cell Biochem* 140 (1):1-22

Electronic Supplementary Material

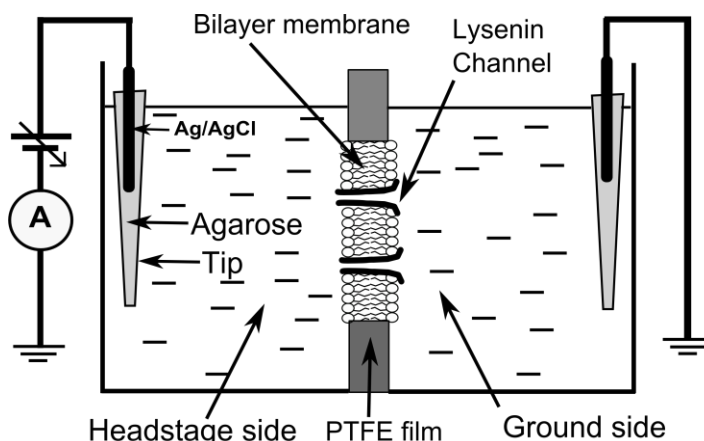


Fig. 8 The experimental setup consisted of a custom-made planar bilayer lipid membrane chamber, which was comprised of two PTFE reservoirs, each capable of accommodating ~1 mL electrolyte solution. The two reservoirs were separated by a thin PTFE film (~120 μm thickness) in which a small central hole of ~60 μm diameter was produced by an electric spark. The agarose/Ag/AgCl electrodes immersed into the electrolyte solutions were connected through flexible wires to the electrophysiology amplifier.

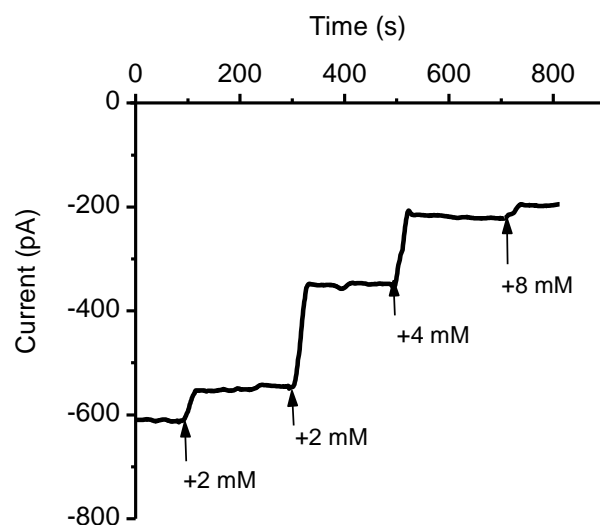


Fig. 9 ATP inhibits the macroscopic currents through lysenin channels inserted into planar lipid membranes irrespective of the addition side. Addition of ATP to the headstage-wired solution yielded a significant decrease of the ionic currents in a concentration-dependent manner, similar to what was observed after ATP addition to the ground side (see the main text). The experiment was recorded at -60 mV transmembrane potential at a sampling rate of 1s, with a 1 kHz hardware filter and a 0.1 kHz software filter. Each ATP addition (indicated by arrows) increased the ATP concentration by the amount indicated in the figure.

CHAPTER FOUR: INSIGHTS INTO THE VOLTAGE REGULATION MECHANISM
OF THE PORE-FORMING TOXIN LYSENIN

Sheenah Lynn Bryant ^{1,2}, Tyler Clark ¹, Christopher Alex Thomas ¹, Kaitlyn
Summer Ware ¹, Andrew Bogard ^{1,2}, Colleen Calzacorta ¹, Daniel Prather ¹ and Daniel
Fologea ^{1,2,*}

¹Department of Physics, Boise State University, Boise, ID 83725, USA;
sheenahbryant@boisestate.edu (S.L.B.); tylerpatrickclark@gmail.com (T.C.);
christopherthomas908@boisestate.edu (C.A.T); kware@u.boisestate.edu (K.S.W.);
andybogard@boisestate.edu (A.B.);
colleenpoulton@u.boisestate.edu (C.C.); danielprather@u.boisestate.edu (D.P.)

²Biomolecular Sciences Graduate Program, Boise State University, Boise, ID
83725, USA

Correspondence:

*DanielFologea@boisestate.edu; Tel.: +1-208-426-2664

Reprinted with permission from Copyright Clearance Center: Springer Nature,
Toxins, Insights into the voltage regulation mechanism of the pore-forming toxin lysenin,
Bryant *et al.*, (2018)

<https://www.mdpi.com/2072-6651/10/8/334>

Abstract

Lysenin, a pore-forming toxin (PFT) extracted from *Eisenia fetida*, inserts voltage-regulated channels into artificial lipid membranes containing sphingomyelin. The voltage-induced gating leads to a strong static hysteresis in conductance, which endows lysenin with molecular memory capabilities. To explain this history-dependent behavior, we hypothesized a gating mechanism that implies the movement of a voltage domain sensor from an aqueous environment into the hydrophobic core of the membrane under the influence of an external electric field. In this work, we employed electrophysiology approaches to investigate the effects of ionic screening elicited by metal cations on the voltage-induced gating and hysteresis in conductance of lysenin channels exposed to oscillatory voltage stimuli. Our experimental data show that screening of the voltage sensor domain strongly affects the voltage regulation only during inactivation (channel closing). In contrast, channel reactivation (reopening) presents a more stable, almost invariant voltage dependency. Additionally, in the presence of anionic Adenosine 5'-triphosphate (ATP), which binds at a different site in the channel's structure and occludes the conducting pathway, both inactivation and reactivation pathways are significantly affected. Therefore, the movement of the voltage domain sensor into a physically different environment that precludes electrostatically bound ions may be an integral part of the gating mechanism.

Keywords: lysenin; pore forming toxins; voltage gating; hysteresis; electrostatic screening

Key Contribution: This study investigates the voltage regulation of the pore forming toxin lysenin and proposes a gating mechanism that implies the movement of a voltage domain sensor from an aqueous environment into the hydrophobic core of the membrane upon voltage-induced conformational changes.

Introduction

Lysenin, a pore forming toxin (PFT) found in the coelomic fluid of the red earthworm *E. fetida*, induces cytolysis and hemolysis of cells that contain sphingomyelin in their plasmalemma [1–5]. Electrophysiology [2,6,7] and atomic force microscopy [8–10] investigations of lysenin inserted into artificial membrane systems have shown that this lytic activity stems from self-insertion of large conducting pores in the target membrane. The physiological role of lysenin is still obscure; nonetheless, lysenin channels possess a great variety of intricate biophysical properties which are commonly shared with ion channels, including large transport rate and selectivity [2,7]. Additionally, lysenin is endowed with unique regulatory mechanisms that set it apart from other PFTs. For example, when reconstituted in artificial membrane systems, lysenin channels show reversible ligand-gating induced by multivalent cations [11,12]. Remarkably, the ligand-induced gating is influenced by the charge density of the ligands; small and highly charged ions (e.g., trivalent metal cations) bind the channel protein at a specific site and induce conformational changes that switch the channel's conductance between open (fully conducting) and closed (non-conducting), while divalent or voluminous polycations force the channel into a sub-conducting state [11,12]. The macroscopic conductance of the channels is also reversibly modulated by purines (e.g., adenosine phosphates), for which the mechanism of conductance reduction stems from anions binding to a specific site inside the channel's lumen and impeding the ionic flow [13]. This mechanism of channel occlusion is fundamentally different from ligand-induced gating, which employs a cation-binding site to induce conformational changes.

The most striking feature of lysenin channels is their unique voltage regulation, which has been extensively explored in multiple studies [2,6,7,14,15]. Voltage regulation is a fundamental feature of many PFTs, which generally present symmetrical voltage gating at large transmembrane potentials [16]. In contrast, lysenin channels displays asymmetrical voltage induced gating, which occurs at low transmembrane voltages [6,7] and resembles a basic feature of voltage-gated ion channels. Specifically, lysenin channels are in a high-conductance state (open) for a large range of negative voltages and at low positive voltages. At transmembrane potentials exceeding ~ 10 – 20 mV, the lysenin channels transition to a closed conformation characterized by negligible conductance [6,17].

For a population of lysenin channels, the open-close transition is described by a Boltzmann distribution within a two-state model for which the transition is relatively slow, being characterized by a relaxation time of several seconds [17]. The slow response to applied voltages creates premises for dynamic hysteresis in conductance which occur when applying variable voltages that change too fast to be followed by conformational changes of the channels [18]. This non-equilibrium leads to distinct pathways for channel inactivation (channel closing induced by increasing, ascending voltage ramps) and reactivation (channel reopening during decreasing, descending voltage ramps). Dynamic conductance hysteresis, which may be a source of molecular memory, is a fundamental feature of voltage-gated ion channels exposed to oscillatory voltages for which the period of the stimulus is comparable to the relaxation time [18]. However, this phenomenon fails to account for the behavior of lysenin. Lysenin presents a large, static hysteresis in conductance [14,17], which is not common among ion channels or pore forming proteins.

While dynamic hysteresis vanishes when the period of the voltage stimulus greatly exceeds the characteristic relaxation time (i.e., when the channels are at equilibrium at any given time during voltage stimulation), lysenin channels retain conductance hysteresis over voltage ramps lasting several hours [17], much larger than their relaxation time.

This unusual feature may be related to the mechanism by which lysenin channels respond to voltage stimuli. In experiments investigating the effects of temperature on lysenin gating [17], it has been found that higher temperatures elicit a strong shift of the voltage-induced gating during ascending voltage ramps. In contrast, temperature has negligible influence on channel reactivation (descending voltage ramps) and the open probability (P_{open}) is invariant. This stable reactivation pathway leads to a static hysteresis [17], which could be better understood by gaining more insights into the gating mechanism. This may be possible by considering recent structural data of the lysenin channels [19–21], which in conjunction with novel explorations may shed more light on lysenin's intricate voltage-induced gating and molecular memory.

It has been suggested that lysenin channels alter their conformation by the movement of a gate coupled to a charged voltage domain sensor when under the influence of an external electric field [6], which is functionally similar to many voltage-gated ion channels [22–28]. Structural data reveals the presence of hinge-like, flexible structures essential for pore formation [19–21] which may allow the elusive voltage domain sensor to move. Since both ionic strength and pH strongly modulate the voltage-induced gating of lysenin channels [6], it is natural to assume that the charged voltage domain sensor is exposed to the bulk ionic solution at rest (the state in which all the channels are open at

zero transmembrane potential), and screened. To explain the invariant reactivation pathway, we hypothesized that conformational changes, leading to channel closing, move the voltage domain sensor into an environment for which novel physical properties influence how the channels will further respond to voltage stimuli, such as the hydrophobic core of the membrane. Irrespective of different nomenclatures used to define the protein domains, available X-ray and Cryo-EM structural data [19,21] show a mushroom-shaped channel comprising a head and a β -barrel long pore (stem). One may surmise that the voltage domain sensor could be located in the head region since those domains are more prone to movement. In addition, the same structural data indicates the presence of multiple charged sites capable of binding both anions and cations, and lysenin presents such capabilities [11–13,29].

The present work was undertaken to produce evidence for the hypothesis that the voltage domain sensor moves into a physically different environment during gating. Our investigations considered electrostatic screening elicited by monovalent and multivalent metal cations acting as counterions for the voltage domain sensor. A simple two-state gating model that assumes a Boltzmann distribution of the states [6,30–32] allowed us to estimate the midway voltage of activation ($V_{0.5}$, the voltage at which the P_{open} equals 0.5) and the number n of elementary gating charges in various experimental conditions comprising electrostatic screening induced by counterions. Our results show that electrostatic screening has a major influence on channel inactivation, while the reactivation pathway is basically invariant. However, investigations conducted by employing ATP, which modulate the macroscopic conductance by binding to the channel lumen and partially occluding the conducting pathway [13], show a quantitatively and

qualitatively different influence on voltage-induced gating, in support of the hypothesized gating mechanism.

Results and Discussions

2.1. Monovalent Metal Cations Modulate the Voltage-Induced Gating of Lysenin Channels During Inactivation, while Minimally Influencing the Reactivation Pathway

The macroscopic ionic currents through a large population of lysenin channels, which were inserted into the bilayer membrane and exposed to increasing monovalent ion concentrations, underwent visible changes with regards to their magnitude and voltage required to initiate the open-close transitions during ascending voltage ramps (channel closing, or inactivation, Figure 1a), as our group reported in a previous study [6].

Addition of KCl yielded larger slopes of the linear portion of the current–voltage (I–V) curves recorded at low voltages (i.e., a larger macroscopic conductance, equal to I/V), which follows the increase of the support electrolyte’s ionic conductivity. In addition, we observed a significant shift in the voltage required to initiate voltage-induced gating, which was also dependent on the ionic concentration of the bulk [6]. This shift suggests that the voltage domain sensor of the channel was exposed to the external ionic solution and addition of counterions enhanced electrostatic screening and reduced the gating charge. Consequently, larger transmembrane voltages and electric fields were required to actuate the gate and close the channel. In contrast, the ionic currents recorded for descending voltage ramps (channel reopening, or reactivation, after voltage-induced closing) show both a different qualitative and quantitative response to monovalent ion addition (Figure 1b). To facilitate direct comparison with the ionic currents recorded during ascending ramps, an identical range for the y axis was used to plot the I–V

characteristic corresponding to descending voltage ramps. For identical ionic concentrations, the maximal currents recorded during the descending ramps are clearly smaller than what was recorded for the ascending ramps, demonstrating the previously observed hysteresis in conductance [14,17]. In brief, for the same transmembrane voltage, the macroscopic current may have different values depending on the channel's history (previously open, or previously closed, respectively). Nonetheless, when the decreasing transmembrane voltages approached ~ 10 mV, the channels fully reopened and their initial conductance was fully reinstated; as inferred from the I–V plots recorded at low transmembrane voltages for all ionic concentrations and ramp directions, the currents and the slopes of the I–V plots at low transmembrane potentials were identical for the two cases, indicating full channel reopening. However, unlike what was observed for ascending voltage ramps, monovalent cation addition did not significantly alter the voltage at which the close-open transition occurred during descending ramps, irrespective of the ionic concentration.

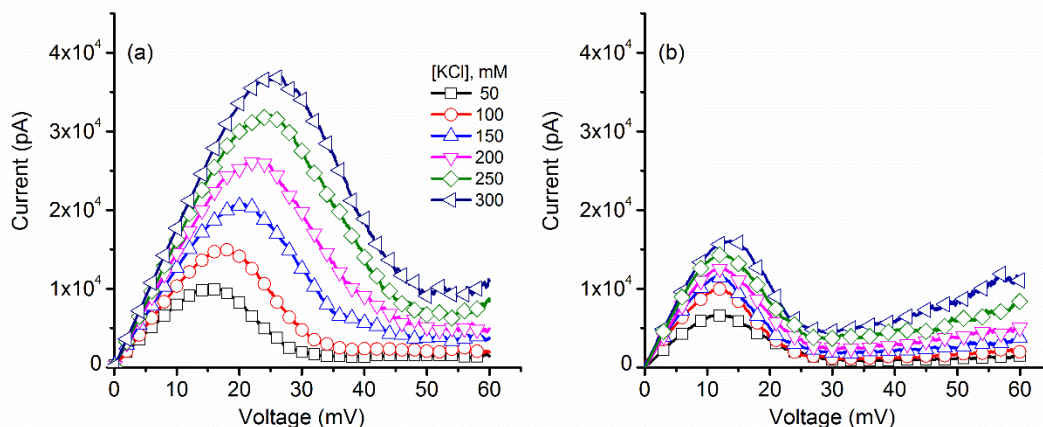


Figure 1. Effects of KCl addition on the I–V characteristics of a population of lysenin channels. (a) The I–V plots recorded during ascending voltage ramps indicated changes of the macroscopic conductance (I/V) and voltage required to initiate gating. (b) The I–V plots corresponding to descending voltage ramps showed similar changes in the macroscopic conductance of open channels but less dependence of the close-open transition on the ionic concentration, along with hysteresis in macroscopic conductance. Each trace in the panels represents a single, typical run for each particular concentration. All the points in the plots are experimental points; the symbols have been added as a visual aid to discriminate between ionic concentrations.

These differences in response to applied voltages, ramp direction, and ionic conditions were also observed in the experimental P_{open} plots (Figure 2), constructed as described in the Materials and Methods section. The very low-voltage experimental points presented large deviations of the P_{open} (due to the very low currents and large noise, which may imply division by near zero numbers), and these points were not represented in the plots. KCl addition yielded a significant rightward shift of the P_{open} for ascending voltage ramps (Figure 2a), while only minor changes were observed for the descending voltage ramps (Figure 2b). These results show a steady, almost invariant channel reactivation pathway, resembling what our group has reported in experiments exploring the effects of temperature on lysenin channel voltage-induced gating [17].

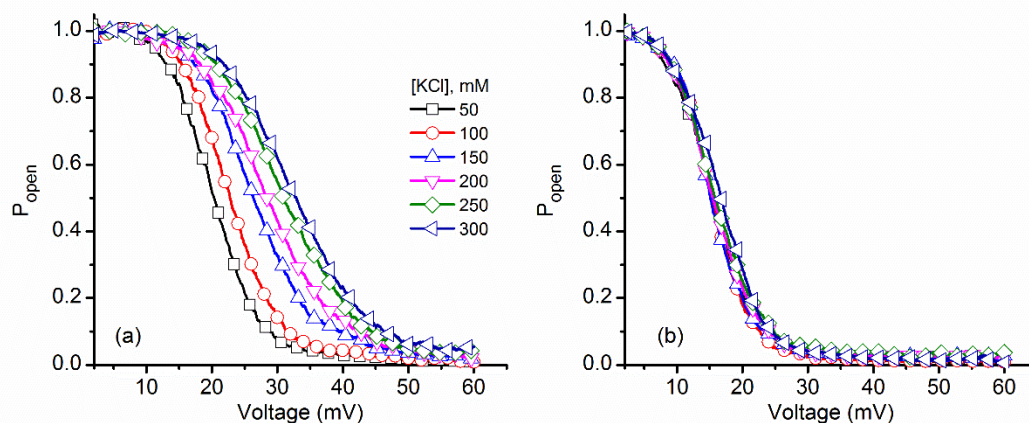


Figure 2. KCl influence on lysenin channels' experimental open probability. (a) The open probability of lysenin channels as a function of voltage underwent a substantial rightward shift for the ascending voltage ramps as the KCl concentration increased. (b) In contrast, negligible changes of the open probability occurred during channel reactivation (descending voltage ramps), irrespective of the bulk KCl concentration. Each plot represents a typical curve of the experimental open probability calculated for each particular concentration. All the points in the plots are experimental points, with the symbols added to allow identification of the ionic conditions.

For both ramps, we estimated the midway voltage of activation, $V_{0.5}$, from the P_{open} plots [31,33]. Figure 3a shows that $V_{0.5}$ increased monotonically from ~ 20 mV to ~ 35 mV upon KCl addition during ascending voltage ramps. As we already surmised from the P_{open} plots, only negligible changes of $V_{0.5}$ were observed for the descending voltage ramps. The $V_{0.5}$ values were next introduced into the Boltzmann distribution equation (see Materials and Methods: Equation (2)) to calculate the number of elementary gating charges n (depicted in Figure 3b).

As predicted from the channel inactivation P_{open} plots, monovalent ion addition led to major variation of the gating charge, which decreased with increasing ionic strength from $\sim 7.5 e$ to $\sim 4.5 e$; the non-linear decrease resembles an exponential decay, in accordance with surface screening [34]. However, the descending voltage ramps yielded a much

smaller variation of the gating charge, and were slightly greater (up to $\sim 8 e$) for all experimental ionic strengths.

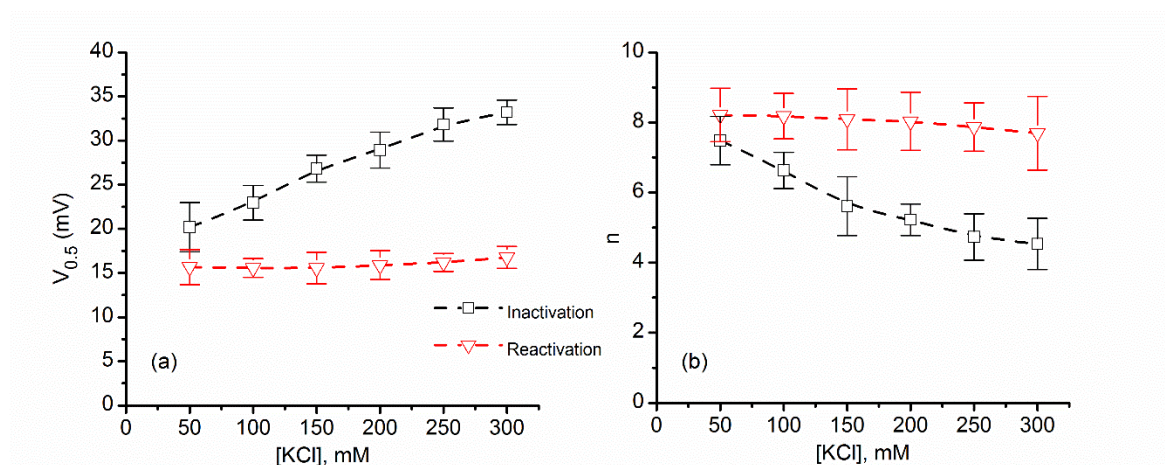


Figure 3. Variation of the midway voltage of activation $V_{0.5}$ and number of elementary gating charges n as a function of KCl concentration. (a) The experimental values of $V_{0.5}$ calculated for ascending voltage ramps presented a significant increase with added KCl, while only a weak influence was encountered for descending voltage ramps. (b) The values of n calculated from the fit of the Boltzmann distribution equation, for each KCl concentration, suggested strong electrostatic screening of the voltage domain sensor for channel inactivation; only minor changes were estimated for channel reactivation. Each experimental point is represented as mean \pm SD from three independent experiments.

These intricate results show that the history of channel conformation (i.e., closed or open state) influences its further response to applied voltages, which is the essence of molecular memory [17]. This may be realized by dynamic changes in the energy landscape elicited upon conformational changes. The more stable, almost invariant reactivation pathway may provide some clues for understanding the mechanism of the gating process. The strong influence of ionic strength on the gating charge estimated for the inactivation pathway, together with the minimal influence observed during reactivation, suggests that the voltage domain sensor may be exposed to very different environmental conditions during transitions. For a channel in the open state, the voltage

domain sensor appears to be exposed to the external electrolyte solution. Therefore, KCl addition promoted electrostatic screening of the gating charge, which led to the rightward shift of the P_{open} during the ascending voltage ramps in a concentration-dependent manner. Channel closure is accompanied by conformational changes and movement of the voltage domain sensor that acts on the gate. This process may result in positioning of the voltage domain sensor into a low polarity environment (i.e., the hydrophobic core of the membrane), from which both water and bound counterions are excluded by the large Born energy penalty [35–38]. Therefore, irrespective of the ionic strength, the voltage domain sensor will be mostly stripped of electrostatically bound counterions upon gating. Consequently, after channel closing, the voltage domain sensor is characterized by a larger gating charge less influenced by the ionic strength of the bulk solution, which may explain the more stable reopening (reactivation) pathway. This proposed mechanism is well-established for ion channels, for which the movement of a charged voltage domain sensor into the hydrophobic core of the bilayer has been reported [39–43]. Therefore, the “paddle in oil” concept, which consists of large movements of the voltage domain sensor into the hydrophobic core of the membrane [41], is accepted as a valid model of ion channel gating.

2.2. Multivalent Metal Cations Influence the Voltage Regulation of Lysenin Channels Similarly to Monovalent Ions

Electrostatic screening is dependent on ionic strength, which increases with the second power of the electrovalence [44,45], and thus one may expect an even greater influence on the channel’s response upon exposure to multivalent ions. However, our group has reported that multivalent ions induce channel closure by a ligand-induced

gating mechanism [11,12], which may introduce roadblocks for such investigations. For example, trivalent metal cations (especially lanthanides) reversibly close lysenin channels and annihilate their macroscopic conductance at $\sim 100 \mu\text{M}$ bulk concentration [11,12]. Although μmolar addition of La^{3+} may elicit only minor changes of the macroscopic conductance, such small concentrations may not sufficiently screen a gating charge which is simultaneously exposed to substantially larger concentrations of monovalent ions in the support electrolyte. However, it appears that the binding of multivalent ions is more specific and much stronger than monovalent ions [11,12]. This may aid in achieving significant changes of the gating charge without major changes of the macroscopic conductance (owing to significant ligand-induced gating), even upon simultaneous exposure to relatively high concentrations of monovalent ions. Therefore, we investigated the effects of La^{3+} ions on the voltage gating of lysenin channels while using the same experimental approaches adopted for KCl. Addition of small amounts of La^{3+} (no more than $2 \mu\text{L}$ of various stock LaCl_3 solutions with concentration in the range 0.1 mM – 1 mM for each addition) to the bulk electrolyte (1 mL of 100 mM KCl) to achieve target La^{3+} concentrations (up to $1.4 \mu\text{M}$) elicited great changes in the I–V characteristics plotted for ascending voltage ramps (Figure 4a). As we observed that, for the case of KCl, La^{3+} addition required greater transmembrane voltages to initiate voltage-induced gating. For all the La^{3+} concentrations used in these experiments, almost identical slopes of the I–V curves at low transmembrane potentials (the linear, ohmic portion of the curves) indicated that La^{3+} addition elicited negligible changes with respect to the solution conductivity or ligand-induced gating. Comparative analysis of the I–V curves (Figure 4) revealed that, similar to KCl, the voltage required for reopening the channels

during descending voltage ramps was smaller than what was required for closing, and that the reopening occurred at similar voltages irrespective of the amount of added La^{3+} .

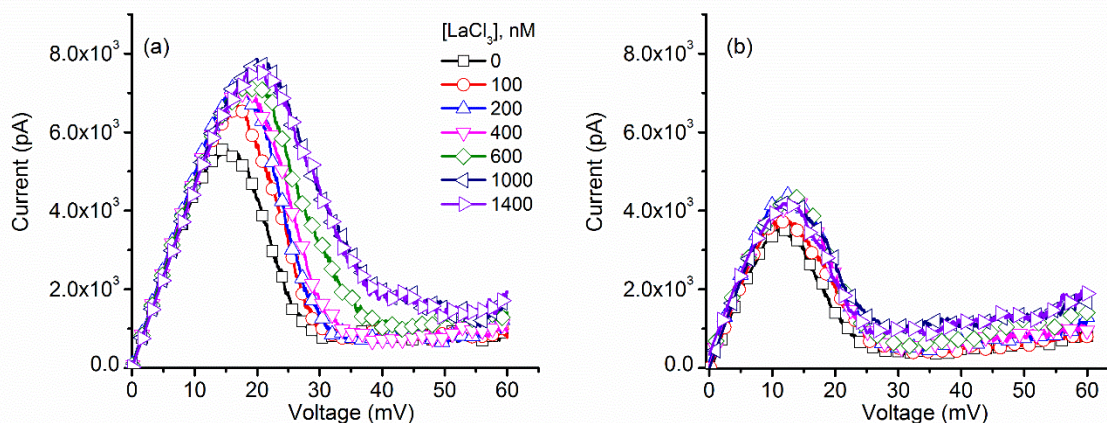


Figure 4. LaCl_3 influence on the I–V characteristics of lysenin channels. (a) The I–V plots recorded for ascending voltage ramps indicated LaCl_3 induced changes of the voltage required to initiate gating. (b) The I–V plots corresponding to descending voltage ramps indicated a minimal influence from the multivalent cations. Each trace in the plots for both panels represents experimental points, with the symbols added as a visual aid.

These features were also observed in the experimental P_{open} plots constructed for both ascending and descending voltage ramps recorded upon La^{3+} addition (Figure 5). The multivalent metal cations induced a significant rightward shift of the P_{open} for ascending voltage ramps, while the effects presented by the same ions on the P_{open} corresponding to descending voltage ramps were minimal. Therefore, we concluded that the reactivation pathway suffered little influence from the multivalent ions and maintained invariance. In addition, these experimental data show that the influence of La^{3+} manifests even in the presence of much larger concentrations of monovalent ions in the bulk solution, suggesting a greater affinity for their binding sites. We concluded that both monovalent and multivalent cations may compete for the same binding sites since

counterion binding is greatly diminished in the presence of very large concentrations of monovalent cations [13].

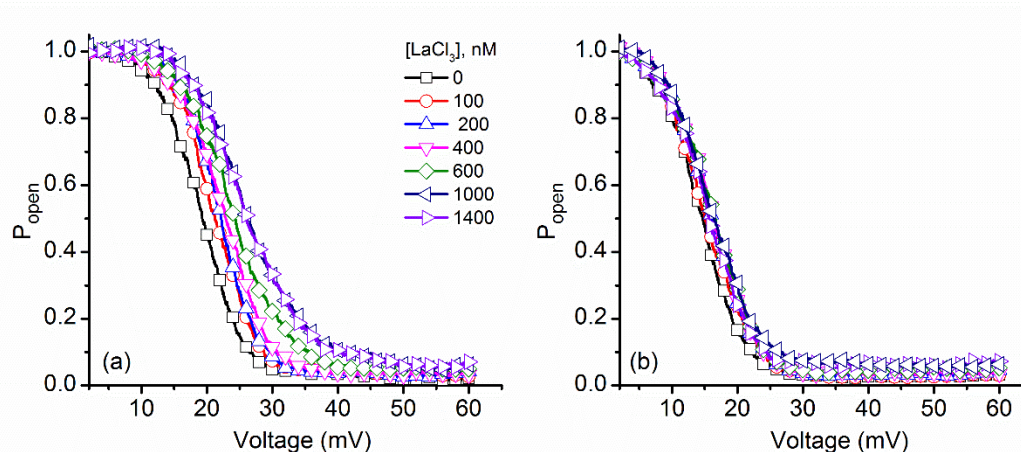


Figure 5. Changes of the experimental open probability (P_{open}) of lysenin channels induced by addition of LaCl_3 . (a) The voltage-dependent open probability of the lysenin channels shifted substantially rightward for the ascending voltage ramps as the LaCl_3 concentration increased. (b) Conversely, and as with addition of KCl , minor changes were observed during descending voltage ramps. Each trace was constructed from experimental points, with the symbols added for better discrimination between ionic conditions.

The experimental $V_{0.5}$ (Figure 6a) and n (Figure 6b) estimated from the best fit of the P_{open} curves for ascending voltage ramps increased significantly (from ~ 18 mV to ~ 26 mV) upon sub- μM La^{3+} addition, showing great screening effectiveness compared to KCl . Such a result was expected, based on the assumption that both monovalent and multivalent cations elicit ionic screening. Nonetheless, steadier values of $V_{0.5}$ and n were obtained during descending voltage ramps, similar to KCl . This constitutes supplementary evidence for a gating mechanism that implies the movement of the voltage domain sensor into a more hydrophobic environment and supports the hypothesis that multivalent and monovalent cations act similarly, but with different affinities with respect to electrostatic binding to the voltage domain sensor.

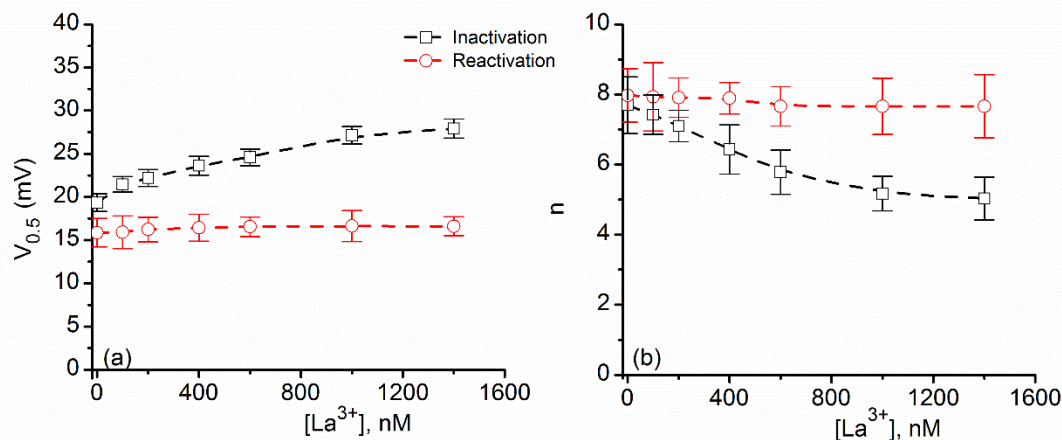


Figure 6. The dependence of $V_{0.5}$ and n on the bulk LaCl_3 concentration. (a) Addition of LaCl_3 induced significant increases of the $V_{0.5}$ calculated for ascending voltage ramps, while having yielded little change for the descending voltage ramps. (b) The total number of elementary charges indicated effective electrostatic screening of the voltage domain sensor upon addition of LaCl_3 during channel inactivation, while insignificant changes occurred during reactivation. Each experimental point is represented as mean \pm SD from three independent experiments.

2.3. ATP Binding to Lysenin Channels Modulates the Voltage-Induced Gating and Affects Both the Inactivation and Reactivation Pathways

The above experiments comprised addition of cations capable of electrostatic interactions with the voltage domain sensor, hence eliciting ionic screening of the gating charge. However, lysenin channels are also capable of interacting with large anions, such as adenosine phosphates, whose interaction manifests as changes in the macroscopic conductance in a concentration dependent manner [13]. Unlike multivalent cations, which most probably bind to a negatively charged site on the voltage domain sensor, purines most likely bind a positively-charged region in channel lumen and elicit physical occlusion of the conducting pathway. Moreover, the binding of purines is a cooperative process, and is most prominent for the highly charged ATP [13]. Therefore, we questioned whether ATP binding to a different site may have a similar influence on the

voltage gating profile of lysenin channels, which would challenge the movement of the voltage domain sensor into a more hydrophobic environment as a valid hypothesis.

To answer these questions, we investigated the effects of ATP addition on the lysenin channel voltage-induced gating in similar experiments comprised of ascending and descending voltage ramps. The experimental I–V plots (Figure 7) show that ATP addition to the 135 mM KCl bulk slightly decreased the macroscopic conductance of the open channels in a concentration dependent manner [13], as indicated by the reduced slopes of the linear portions of the I–V curves at low voltages. ATP addition induced a significant shift of the voltage required to close the channels during ascending voltage ramps, similar to monovalent and multivalent metal cations. The response to voltage in the presence of ATP recorded for descending voltage ramps (Figure 7b) was fundamentally different. The hysteresis in conductance remained, and manifested as a different, history-dependent macroscopic current recorded at identical transmembrane voltages. However, the reactivation pathway in the presence of ATP was not invariant, as concluded from the changes observed in the I–V plots.

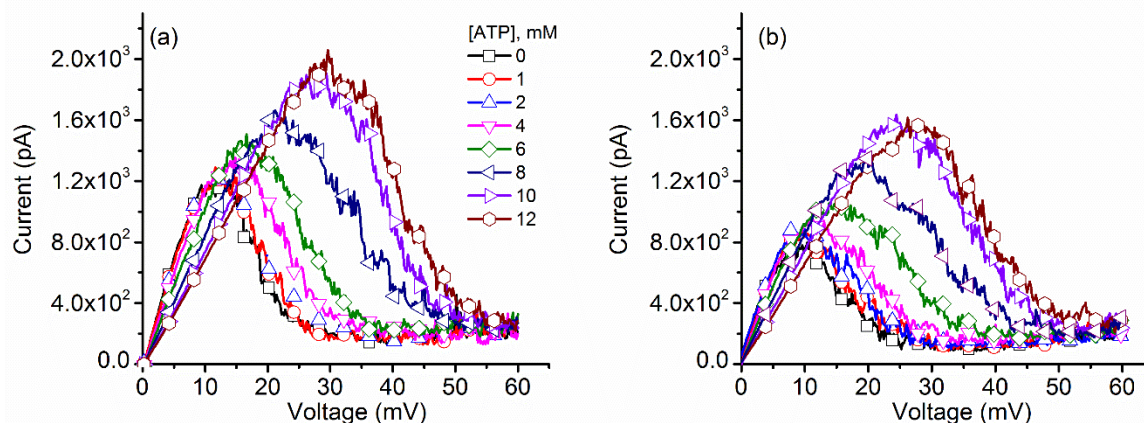


Figure 7. ATP affects the I–V characteristics of lysenin channels in a concentration dependent manner. (a) The I–V plots recorded during ascending voltage ramps showed that ATP addition modulated the macroscopic conductance and voltage-induced gating of lysenin channels. (b) Opposite to metal cations, ATP induced similar significant changes during descending voltage ramps. Each trace in the panels of the plots represents experimental points, and the symbols have been added to allow easy identification of experimental concentrations.

These features are better observed in the experimental P_{open} curves (Figure 8), which were devoid of any influence from the changes in the macroscopic conductance of open channels. Channel inactivation during ascending voltage ramps show a strong rightward shift with ATP addition (Figure 8a), similar to what was observed for both monovalent and multivalent cations. What is striking is that the P_{open} for descending voltage ramps presented a significant concentration-dependent rightward shift (Figure 8b), which is very different from the invariant curves recorded for metal cation addition. Moreover, both I–V and P_{open} plots suggested that a maximal influence of ATP manifests in the 4 mM–10 mM concentration range, while outside this range the induced changes were smaller. This is consistent with the cooperative binding of ATP to lysenin channels, as described in a previous report [13].

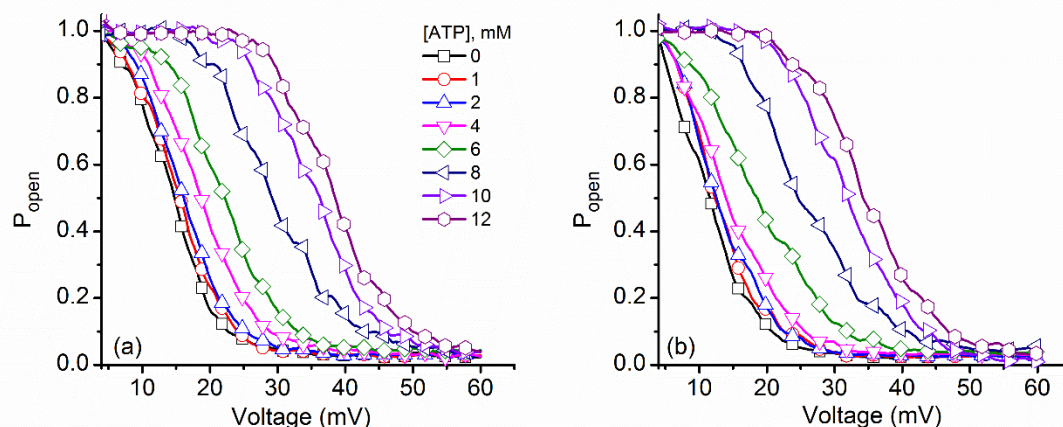


Figure 8. Increased ATP concentration shifted the voltage-dependent open probability of lysenin channels. Addition of ATP induced a rightward shift of the experimental open probability during both (a) ascending and (b) descending voltage ramps. Each plot represents a typical curve of the experimental open probability calculated for each particular concentration. All the points in the plots are experimental points, and the symbols have been added to allow easy identification of the ATP concentrations. For representation, the P_{open} curves have been smoothed with the Savitsky–Golay protocol (23 smoothing points).

Differences between metal cations and ATP were also observed in the estimated $V_{0.5}$ and n calculated at different concentrations (Figure 9). Both $V_{0.5}$ and n followed similar patterns of change with ATP concentration, as expected from the summary analysis of the P_{open} and I – V plots. Also, the particular sigmoidal shape of the plots is in agreement with the cooperative binding of ATP to lysenin [13]. Interestingly, the $V_{0.5}$ value measured at 0 mM ATP (i.e., ~12 mV) was the smallest recorded from all the experiments described in this work. This may be explained by considering the consistently lower number of channels inserted in the membrane for the ATP experiments; previous studies reported that crowding in the membrane plane (achievable at large channel densities) may influence the voltage gating of lysenin channels [15]. In the case of the ATP experiments, a different lysenin batch was used, which consistently provided a lower number of inserted channels that gated at lower transmembrane voltages.

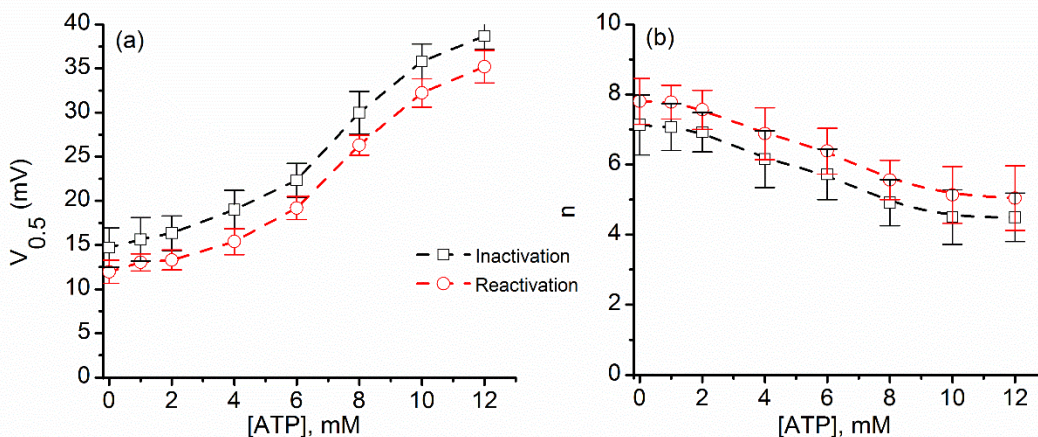


Figure 9. ATP addition alters $V_{0.5}$ and n for both inactivation and reactivation voltage ramps. For the ascending and descending voltage ramps, both $V_{0.5}$ (a) and n (b) varied with the concentration of ATP. Each experimental point is represented as mean \pm SD from three independent experiments.

We presented evidence in support of the hypothesis that the voltage domain sensor of the lysenin channel moves into a different physical environment upon voltage-induced gating. Based on earlier evidence presented for ion channels, we assumed that the gating charge, exposed to the aqueous environment at rest, may penetrate deep into the membrane and exclude the bound ions. Before closing, the voltage domain sensor is electrostatically screened by cations; therefore, ionic strengths significantly modulate the voltage-induced gating. Channel reopening after closing comprises a voltage domain sensor which is minimally screened and results in a more stable reactivation pathway. From investigating the influence of ATP on voltage gating, we concluded that anions act in a very different manner than cations because they do not bind to the same sites of the channel. The cations bind to the voltage domain sensor, which then undergoes conformational changes and penetrates into a more hydrophobic environment from which water and ions are excluded. For ATP, which binds a different site, the influence on the voltage induced gating may be explained by long range electrostatic interactions between

the bound anions and the voltage domain sensor, which may manifest even when the voltage domain sensor is in a nonpolar environment. The proposed gating mechanism is supported by experimental data but we may not overlook some experimental and theoretical limitations. In this work, we consistently used a reasonably-long period for the driving voltage stimulus (20 min), which is much larger than the characteristic relaxation time of lysenin channels (seconds). However, addition of cations or anions may substantially change the relaxation time, and therefore the I - V and P_{open} plots may not represent true steady states. Nonetheless, in such situations, the channels that closed at lower voltages resided for longer times in the closed state, yet the reactivation pathway was invariant. Also, the Boltzmann distribution considered in this work (and similar approaches [31]) did not account for dynamic changes of the energy landscape during gating. In spite of these limitations, both the similarities and differences between the voltage-induced gating of lysenin channels exposed to cations and anions support a model in which the voltage domain sensor moves into the membrane, and may explain the persistent hysteresis in conductance.

Materials and Methods

3.1. Bilayer Lipid Formation, Channel Insertion, and Ionic Addition

The vertical bilayer membrane chamber consisted of two polytetrafluoroethylene (PTFE) reservoirs (~1 mL volume each) separated by a thin PTFE film in which a small hole (~ 70 μm diameter) was pierced by an electric spark. The reservoirs were filled with electrolyte solutions (50 mM KCl, if not otherwise noted, buffered with 20 mM HEPES, pH 7.2) and connected to the Axopatch 200B electrophysiology amplifier (Molecular Devices, San Jose, CA, USA) via Ag/AgCl electrodes. The analog signal of the amplifier

was further digitized and recorded with the DigiData 1440A digitizer controlled by the pClamp 10.6.2.2 software package (Molecular Devices, San Jose, CA, USA). The bilayer was produced using a mixture of 1 mg asolectin (Sigma-Aldrich, St. Louis, MO, USA), 0.4 mg cholesterol (Sigma-Aldrich, St. Louis, MO, USA), and 0.5 mg sphingomyelin (Avanti Polar Lipids Inc., Alabaster, AL, USA) in 100 μ L n-decane (TCI America, Portland, OR, USA). The bilayer integrity was verified by both capacitance and conductance measurements. Channel insertion was performed by addition of small amounts of lysenin (0.3 pM final concentration, Sigma-Aldrich, St. Louis, MO, USA) to the ground reservoir under continuous stirring with a low noise magnetic stirrer (Warner Instrument, Hamden, CT, USA). Individual channel insertion was monitored by observing the discrete, step-wise changes of the ionic current through the membrane biased by -60 mV transmembrane potentials [7]. After completion of insertion, observed as a steady value of the ionic current, the free lysenin was removed by flushing the ground reservoir with fresh buffered electrolyte. Lysenin gating at positive potentials was observed from I–V plots recorded in the range 0 mV: +60 mV by exposing the channel-containing membrane to voltage ramps created with the digitizer. We observed that different batches of lysenin presented slight differences with respect to voltage-induced gating (i.e., variations of the voltage required to initiate gating), therefore we used identical batches of lysenin for each independent experiment focused on investigating the influence of a particular ion on the gating profile.

Stock solutions of KCl (Fisher Scientific, Pittsburgh, PA, USA), LaCl₃ (Alpha Aesar, Tewksbury, MA, USA), and ATP (Sigma-Aldrich, St. Louis, MO, USA) were prepared by dissolving the powders in 20 mM HEPES (pH 7.2). To achieve the target

concentrations in the bulk, corresponding amounts of stock solutions were added to both reservoirs under continuous stirring. This procedure was repeated for all target concentrations achieved for the experiments.

3.2. Data Collection, Analysis, and Mathematical Modelling

For each ionic concentration, the voltage-induced gating of lysenin channels was investigated by recording the ionic currents in response to linear, triangle-shaped voltage ramps. The ramps were created with the pClamp 10.6.2.2 software package (Molecular Devices, San Jose, CA, USA) and delivered to the electrophysiology amplifier via one of the digitizer's outputs. Each voltage ramp stimulus had a period of 20 min (10 min for ascending, and 10 min for descending) in the range 0 mV: +60 mV, at a sampling rate of minimum 1 s, with a 1 kHz hardware filter. Each recording was saved as a separate file and further analyzed with Origin 8.5.1 (OriginLab, Northampton, MA, USA), pClamp 10.6.2.2 (Molecular Devices, San Jose, CA, USA) and Mathematica 10.4 (Wolfram Research, Champaign, IL, USA).

For analysis and modelling, we considered that the voltage-induced gating of lysenin channels is described by a two-state model [6]:



Within this model, the open probability P_{open} of the channels in response to applied voltages is described by the Boltzmann distribution [31,46]:

$$P_{open} = \frac{1}{1 + e^{\frac{-neF(V_{0.5}-V)}{RT}}} \quad (2)$$

Where n is the total number of elementary gating charges e of the voltage domain sensor ($e = 1.6 \times 10^{-19}$ C), $V_{0.5}$ is the midway voltage of activation (the voltage at which $P_{open} =$

0.5), V is the applied voltage, R is the universal gas constant (8.34 J/K), F is Faraday's number ($F = 96485.33$ C/mol), and T is the absolute temperature ($T = 295$ K).

Within the two-state model, the experimental open probability for each applied voltage was derived from [23,32,47]:

$$P_{open} = \frac{I}{I_{max}} \quad (3)$$

where I is the ionic current measured for a particular voltage, and I_{max} is the ionic current that would be recorded at the same voltage if all the channels were open. For each particular voltage, I_{max} was estimated from a straight line constructed by fitting the linear portion of each I - V curve recorded at low transmembrane voltages (when all the channels are open).

The midway voltage of activation was experimentally determined from the P_{open} , plotted for each of the ionic conditions, and further used in the theoretical model to determine n . Since even a closed lysenin channel may present a small leakage current [6,17], this was corrected in the experimental P_{open} only for the two highest KCl concentrations used in our experiment, which presented visible leakages. No other correction was performed for experimental data. All graphs have been prepared using the Origin 8.5.1 software.

Acknowledgements

Author Contributions: Conceptualization, S.L.B and D.F.; Methodology, S.L.B., C.A.T, and D.F.; Software, T.C., K.S.W, and D.F.; All the authors contributed to data recording, analysis, interpretation, and manuscript preparation.

Funding: This research was funded by National Science Foundation (NSF, USA) grant number 1554166 and National Aeronautics and Space Administration (NASA, USA) grant number NNX15AU64H.

Conflicts of Interest: The authors declare no conflict of interest. The funders had no role in the design of the study; in the collection, analyses, or interpretation of data; in the writing of the manuscript, and in the decision to publish the results.

References

1. Bruhn, H.; Winkelmann, J.; Andersen, C.; Andra, J.; Leippe, M. Dissection of the mechanisms of cytolytic and antibacterial activity of lysenin, a defense protein of the annelid *Eisenia fetida*. *Dev. Comp. Immunol.* **2006**, *30*, 597–606.
2. Kwiatkowska, K.; Hordejuk, R.; Szymczyk, P.; Kulma, M.; Abdel-Shakor, A.-B.; Plucienniczak, A.; Dolowy, K.; Szewczyk, A.; Sobota, A. Lysenin-His, a sphingomyelin-recognizing toxin, requires tryptophan 20 for cation-selective channel assembly but not for membrane binding. *Mol. Membr. Biol.* **2007**, *24*, 121–134.
3. Shakor, A.-B.A.; Czurylo, E.A.; Sobota, A. Lysenin, a unique sphingomyelin-binding protein. *FEBS Lett.* **2003**, *542*, 1–6.
4. Shogomori, H.; Kobayashi, T. Lysenin: A sphingomyelin specific pore-forming toxin. *Biochim. Biophys. Acta* **2008**, *1780*, 612–618.
5. Yamaji-Hasegawa, A.; Makino, A.; Baba, T.; Senoh, Y.; Kimura-Suda, H.; Sato, S.B.; Terada, N.; Ohno, S.; Kiyokawa, E.; Umeda, M.; et al. Oligomerization and pore formation of a sphingomyelin-specific toxin, lysenin. *J. Biol. Chem.* **2003**, *278*, 22762–22770.
6. Fologea, D.; Krueger, E.; Lee, R.; Naglak, M.; Mazur, Y.; Henry, R.; Salamo, G. Controlled gating of lysenin pores. *Biophys. Chem.* **2010**, *146*, 25–29.

7. Ide, T.; Aoki, T.; Takeuchi, Y.; Yanagida, T. Lysenin forms a voltage-dependent channel in artificial lipid bilayer membranes. *Biochem. Biophys. Res. Commun.* **2006**, *346*, 288–292.
8. Yilmaz, N.; Kobayashi, T. Visualization of lipid membrane reorganization induced by a pore-forming toxin using high-speed atomic force microscopy. *ACS Nano* **2015**, *9*, 7960–7967.
9. Yilmaz, N.; Yamada, T.; Greimel, P.; Uchihashi, T.; Ando, T.; Kobayashi, T. Real-time visualization of assembling of a sphingomyelin-specific toxin on planar lipid membranes. *Biophys. J.* **2013**, *105*, 1397–1405.
10. Yilmaz, N.; Yamaji-Hasegawa, A.; Hullin-Matsuda, F.; Kobayashi, T. Molecular mechanisms of action of sphingomyelin-specific pore-forming toxin, lysenin. *Semin. Cell Dev. Biol.* **2018**, *73*, 188–198.
11. Fologea, D.; Al Faori, R.; Krueger, E.; Mazur, Y.I.; Kern, M.; Williams, M.; Mortazavi, A.; Henry, R.; Salamo, G.J. Potential analytical applications of lysenin channels for detection of multivalent ions. *Anal. Bioanal. Chem.* **2011**, *401*, 1871–1879.
12. Fologea, D.; Krueger, E.; Al Faori, R.; Lee, R.; Mazur, Y.I.; Henry, R.; Arnold, M.; Salamo, G.J. Multivalent ions control the transport through lysenin channels. *Biophys. Chem.* **2010**, *152*, 40–45.
13. Bryant, S.; Shrestha, N.; Carnig, P.; Kosydar, S.; Belzeski, P.; Hanna, C.; Fologea, D. Purinergic control of lysenin's transport and voltage-gating properties. *Purinerg. Signal.* **2016**, *12*, 1–11.
14. Krueger, E.; Al Faouri, R.; Fologea, D.; Henry, R.; Straub, D.; Salamo, G. A model for the hysteresis observed in gating of lysenin channels. *Biophys. Chem.* **2013**, *184*, 126–130.
15. Krueger, E.; Bryant, S.; Shrestha, N.; Clark, T.; Hanna, C.; Pink, D.; Fologea, D. Intramembrane congestion effects on lysenin channel voltage-induced gating. *Eur. Biophys. J.* **2016**, *45*, 187–194.

16. Bainbridge, G.; Gokce, I.; Lakey, J.H. Voltage gating is a fundamental feature of porin and toxin β -barrel membrane channels. *FEBS Lett.* **1998**, *431*, 305–308.
17. Fologea, D.; Krueger, E.; Mazur, Y.I.; Stith, C.; Okuyama, Y.; Henry, R.; Salamo, G.J. Bi-stability, hysteresis, and memory of voltage-gated lysenin channels. *Biochim. Biophys. Acta-Biomembr.* **2011**, *1808*, 2933–2939.
18. Pustovoit, M.A.; Berezhkovskii, A.M.; Bezrukov, S.M. Analytical theory of hysteresis in ion channels: Two state model. *J. Chem. Phys.* **2006**, *125*, 194907.
19. Bokori-Brown, M.; Martin, T.G.; Naylor, C.E.; Basak, A.K.; Titball, R.W.; Savva, C.G. Cryo-EM structure of lysenin pore elucidates membrane insertion by an aerolysin family protein. *Nat. Commun.* **2016**, *7*, 11293.
20. De Colibus, L.; Sonnen, A.F.; Morris, K.J.; Siebert, C.A.; Abrusci, P.; Plitzko, J.; Hodnik, V.; Leippe, M.; Volpi, E.; Anderluh, G.; et al. Structures of lysenin reveal a shared evolutionary origin for pore-forming proteins and its mode of sphingomyelin recognition. *Structure* **2012**, *20*, 1498–1507.
21. Podobnik, M.; Savory, P.; Rojko, N.; Kisovec, M.; Wood, N.; Hambley, R.; Pugh, J.; Wallace, E.J.; McNeill, L.; Bruce, M.; et al. Crystal structure of an invertebrate cytolysin pore reveals unique properties and mechanism of assembly. *Nat. Commun.* **2016**, *7*, doi:11598. 10.1038/ncomms11598.
22. Andersen, O.S.; Ingolfsson, H.I.; Lundbaek, J.A. Ion channels. *Wiley Encycl. Chem. Biol.* 2008, Volume 2, 419-436.
23. Bezanilla, F. The voltage sensor in voltage-dependent ion channels. *Physiol. Rev.* **2000**, *80*, 555–592.
24. Bezanilla, F. Voltage-gated ion channels. *IEEE T. Nanobiosci.* **2005**, *4*, 34–48.
25. Bezanilla, F. How membrane proteins sense voltage. *Nat. Rev. Mol. Cell Biol.* **2008**, *9*, 323–331.
26. Bezanilla, F. Ion channels: From conductance to structure. *Neuron* **2008**, *60*, 456–468.

27. Gonzalez, C.; Morera, F.J.; Rosenmann, E.; Alvarez, O.; Latorre, R. S3b amino acid residues do not shuttle across the bilayer in voltage-dependent shaker K⁺ channels. *Proc. Nat. Acad. Sci. USA* **2005**, *102*, 5020–5025.
28. Swartz, K.J. Sensing voltage across lipid membranes. *Nature* **2008**, *456*, 891–897.
29. Bryant, S.L.; Eixenberger, J.E.; Rosslund, S.; Apsley, H.; Hoffmann, C.; Shrestha, N.; McHugh, M.; Punnoose, A.; Fologea, D. ZnO nanoparticles modulate the ionic transport and voltage regulation of lysenin nanochannels. *J. Nanobiotechnol.* **2017**, *15*, 90. doi:10.1186/s12951-017-0327-9.
30. Islas, L.D.; Sigworth, F.J. Electrostatics and the gating pore of Shaker potassium channels. *J. Gen. Physiol.* **2001**, *117*, 69–89.
31. Rappaport, S.M.; Tejjido, O.; Hoogerheide, D.P.; Rostovtseva, T.K.; Berezhkovskii, A.M.; Bezrukov, S.M. Conductance hysteresis in the voltage-dependent anion channel. *Eur. Biophys. J.* **2015**, *44*, 465–472.
32. Xu, Y.P.; Shin, H.G.; Szep, S.; Lu, Z. Physical determinants of strong voltage sensitivity of K⁺ channel block. *Nat. Struct. Mol. Biol.* **2009**, *16*, 1252–1258.
33. Correa, A.M.; Bezanilla, F.; Latorre, R. Gating kinetics of batrachotoxin-modified Na⁺ channels in the squid giant axon-voltage and temperature effects. *Biophys. J.* **1992**, *61*, 1332–1352.
34. Block, B.M.; Stacey, W.C.; Jones, S.W. Surface charge and lanthanum block of calcium current in bullfrog sympathetic neurons. *Biophys. J.* **1998**, *74*, 2278–2284.
35. Bostrom, M.; Ninham, B.W. Energy of an ion crossing a low dielectric membrane: The role of dispersion self-free energy. *Biophys. Chem.* **2005**, *114*, 95–101.
36. Cherstvy, A.G. Electrostatic screening and energy barriers of ions in low-dielectric membranes. *J. Phys. Chem. B* **2006**, *110*, 14503–14506.
37. Glaeser, R.M.; Jap, B.K. The Born energy problem in bacteriorhodopsin. *Biophys. J.* **1984**, *45*, 95–97.

38. Parsegian, A. Energy of an ion crossing a low dielectric membrane: Solutions to four relevant electrostatic problems. *Nature* **1969**, *221*, 844–846.
39. Jiang, Y.X.; Lee, A.; Chen, J.Y.; Ruta, V.; Cadene, M.; Chait, B.T.; MacKinnon, R. X-ray structure of a voltage-dependent K⁺ channel. *Nature* **2003**, *423*, 33–41.
40. Jiang, Y.X.; Ruta, V.; Chen, J.Y.; Lee, A.; MacKinnon, R. The principle of gating charge movement in a voltage-dependent K⁺ channel. *Nature* **2003**, *423*, 42–48.
41. Lee, A.G. Ion channels: A paddle in oil. *Nature* **2006**, *444*, 697–697.
42. Schmidt, D.; Jiang, Q.X.; MacKinnon, R. Phospholipids and the origin of cationic gating charges in voltage sensors. *Nature* **2006**, *444*, 775–779.
43. Sigworth, F.J. Structural biology: Life's transistors. *Nature* **2003**, *423*, 21–22.
44. Debye, V.P.; Huckel, E. Zur theorie der elektrolyte. *Phys. Chem.* **1923**, *24*, 185–206.
45. Solomon, T. The definition and unit of ionic strength. *J. Chem. Educ.* **2001**, *78*, 1691–1692.
46. Latorre, R.; Vargas, G.; Orta, G.; Brauchi, S. Voltage and temperature gating of thermoTRP channels. In *TRP Ion Channel Function in Sensory Transduction and Cellular Signaling Cascades*, Liedte, W.B., Heller, S., Eds.; CRC Press/Taylor & Francis: Boca Raton, FL, USA, 2007; Chapter 21, 287–302.
47. Tao, X.; Lee, A.; Limapichat, W.; Dougherty, D.A.; MacKinnon, R. A gating charge transfer center in voltage sensors. *Science* **2010**, *328*, 67–73.